8-2018

Evaluation and Development of CPT Based Pile Design in Nebraska Soils

Alex Silvey
University of Nebraska - Lincoln, a.silvey34@gmail.com

EVALUATION AND DEVELOPMENT

OF CPT BASED PILE DESIGN IN NEBRASKA SOILS

by

Alex Silvey

A THESIS

Presented to the Faculty of

The Graduate College at the University of Nebraska

In Partial Fulfillment of Requirements

For the Degree of Master of Science

Major: Civil Engineering

Under the Supervision of Professor Chung Rak Song

Lincoln, Nebraska

August, 2018

EVALUATION AND DEVELOPMENT OF CPT BASED PILE DESIGN IN NEBRASKA SOILS

Alex Silvey, M.S.

University of Nebraska, 2018

Advisor: Chung Rak Song

Cone penetration testing (CPT) is a well established geotechnical subsurface investigation technique commonly used for site characterization and soil classification. The CPT gives real time end resistance, side friction, and pore pressure readings. Axially loaded piles also share these two resistance mechanisms, suggesting the cone can be considered similar to a miniature pile. This study focused on evaluating eight CPT methods prediction of pile bearing capacity. The Nebraska Department of Roads (NDOR) conducts dynamic load tests (PDA) of driven pile to verify pile capacity for bridge foundations. 91 comparisons of CPT logs and PDA data were evaluated. CPT prediction methods were assessed based on prediction ratio and statistical performance. Controlling bearing mechanism was identified as a key influence in method accuracy. Subsequently, piles were identified as end bearing or skin friction pile for further method analysis. The CPT methods were calibrated to maximize accuracy for Nebraska's regional soil conditions. A numeric modeling study was also conducted to investigate cone vs. pile behavior. The study found cone influence depth for end resistance about 10D, while pile influence depth ranged from 1-3 times the diameter. Relative sensitivity to over and underlying soft/hard layers was also identified. Most importantly, computational modeling confirmed *qb/qc* factors in accordance with or slightly higher than the empirical methods. Bearing capacity was most accurately predicted by modified Prince & Wardle

method for end bearing pile, while a modified Philipponnat's method gave the best prediction for friction pile. CPT based pile design developed by the study offers a more robust design approach to accompany modern soil investigation techniques.

ACKNOWLEDGEMENTS

I am very grateful for where I am and for the opportunities I have been presented, and there are many people to thank for helping me get to where I am today. Without the support and encouragement from those who surround me, I wouldn't be able to achieve what I have.

Primary funding for this project was provide under NTRC project SG-18 by the Nebraska Department of Roads. I am especially appreciative of the opportunity to work with NDOR, who has always been a leader in continually furthering Nebraska's engineers & infrastructure.

I would specifically like to thank a few people who have been influential throughout the duration of this project. First, I would like to thank Dr. Chung Song. I am thankful for the opportunity to work with him on this project and learn from his guidance. He saw a path for me from the very beginning of graduate school, even when I was at times unsure myself. Dr. Song's mentorship has pushed me to expand my horizons and become a better engineer. His expertise has always offered a practical perspective that has been invaluable to me in my time as a student.

For all of the late nights spent developing the project and assistance with numeric modeling, I have my friend and fellow graduate student Binyam Bekele to thank. Binyam was always there when the project seemed to stall to trade ideas with and develop a plan to move forward. His expertise continually relied upon.

I would like to thank my coworkers in the geotechnical section at NDOR for support and flexibility the last two years. Without the knowledge and skills from analysis to field operations that they have taught me, I would not have been prepared to complete this research.

Finally, I have my parents and brother for their unwavering support throughout my academic pursuits. You are the ones who have pushed me to accomplish the highest goals. Thank you for instilling my work ethic, and even more for always being so unselfish towards me.

TABLE OF CONTENTS

LIST OF FIGURES

LIST OF TABLES

CHAPTER 1 INTRODUCTION

1.1 Background

The cone penetration test (CPT) is a widely used in situ test for geotechnical investigation of subsurface soil conditions. The test provides stratification information, soil identification, and estimates physical properties such as strength of the soil. When the cone penetrometer is advanced into the ground, tip resistance and sleeve friction parameters are measured. Further capabilities of the testing device have been developed over the years and subsequently incorporated into the device in either the form of direct measurement or derived correlations from existing measurements. Cone penetration testing is economical sounding method that offers continuous and reliable profile data. CPT is a valuable tool for geotechnical work and becomes even more powerful when combined with traditional field and lab test regiments.

Deep foundations are chosen in structural applications when bearing cannot be achieved in shallow soil strata required by spread footing designs. In Nebraska, deep foundations are the most common choice of foundation type used by NDOR (Nebraska Department of Roads) for bridges. The deep foundation transmits the load to deep strata obtaining higher bearing capacity and often helps minimize settlement of the structure. Pile foundations are the most common deep foundation option, installed by either driven or cast in place methods. NDOR predominantly uses steel HP piles, steel pipe piles, precast prestressed square concrete piles and bored cast in place drilled shafts.

1.2 Cone Penetration Test (CPT)

The cone penetration test has gained popularity as quick and reliable soil exploration test that provides soundings of subsurface conditions. The CPT device consists of a conical tip advanced by cylindrical drilling rods. Some type of hydraulic pushing mechanism pushes the probe into the ground at a constant rate, and the required forces to advance the cone are measured. The force measurements collected during testing include cone tip resistance (q_c) and the sleeve friction (f_s) along the shaft (sleeve) of the penetrometer. Figure 1.1 is a schematic of the CPT probe and Figure 1.2 shows NDOR's drill rig used as hydraulic push and retraction platform for CPT testing. The cone itself can vary in projected surface area ranging from 2 cm^2 to 40 cm^2, but all sharing the 60° apex angle of the original cone developed by Dutch scientists. The most common cones found in practice are the 10 cm^2 and 15 cm^2 variants. NDOR use the 10 cm^2 cone for its CPT testing. Newer iterations of the electric CPT have added further sensor capabilities such a pore pressure measurement, also referred to as the piezocone or CPTu. Other possible sensors include temperature, geophones, and electric resistivity making the CPT an extremely versatile testing device for numerous in situ applications.

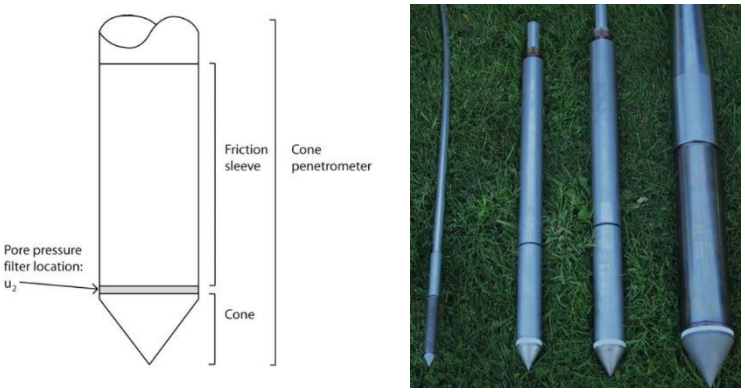

Fig. 1.1 CPT diagram and cone sizes (Cabal & Robertson, 2010)

Fig. 1.2 NDOR CPT Platform

Limitations of CPT are dependent on two primary factors: 1) the nature of the soil where the probe is advanced 2) The hydraulic capacity of the pushing mechanism. CPT testing is ideal for soft fine-grained soils. Granular materials such as dense sands or coarse gravels often cannot be penetrated using this test. Pushing capacity requires a static reaction force greater than the resistance experience by the cone to continue advancement. This can be achieved by static weight of heavy (excess of 20 ton) equipment, or by advancing anchors into the ground to supplement machine weight. Provided optimal conditions, CPT soundings can be advance in excess of 150 ft. The cone is advanced at a standard penetration rate of 2 cm/sec, with reading intervals maintained in the range of 20 mm to 200 mm.

1.3 Pile Foundations

Pile foundations are among the most common deep foundation types. Like all deep foundations, piles transfer the majority of a structural load from the surface to deeper strata where higher bearing capacities can be obtained. In the case of bridges, pile foundations also may reduce risk from impacts such as scour at water crossings. Piling, if installed to sufficient depth, can survive a scour event and still provided superstructure support, where a shallow foundation may not be suitable for such situations. Piles are classified by properties including material, displacement style, load support condition, and method of installation. Table 1.1 below presents typical classification for pile foundations. The displacement and load transfer behavior of piling is dependent on subsurface conditions, the geometry of the pile, and ultimately the interaction between these factors.

Table 1.1 Classification of pile foundations

Classification as per:	Classified as:
Nature of load transfer or support	1. Side friction
	2. End-bearing
Displacement properties	1. Full displacement
	2. Partial displacement
	3. Non-displacement
Material composition	1. Steel
	2. Concrete
	3. Timber
	4. Composite
Method of Installation	1. Driven
	2. Drilled & cast in place

Axial load capacity of piles can be assessed by a derivation from the general bearing capacity equation shown below.

$$Q_u = Q_p + Q_s = q_p A_p + f_s A_s \quad (1)$$

where Q_u = ultimate pile capacity (unit of force), Q_p = end-bearing capacity (unit of force), Q_s = skin or shaft friction capacity (unit of force), q_p = unit tip resistance (unit of stress), f_s = unit skin friction (unit of stress), A_p = area of pile tip, and A_s = area of pile shaft. Ultimate axial load capacity can be directly measured in during or after installation using static, statnamic, or dynamic load testing programs. Analytical techniques based on shear strength of soils, or in situ tests such SPT N-values, and CPT results can also provide basis for ultimate capacity design or analysis.

1.4 Overview & Objectives

Cone penetration testing has been used by NDOR personnel for geotechnical investigation and site characterizations alongside traditional exploration and sampling methods such as SPT and undisturbed sampling since the early 2000s. CPT applications have included investigation and design related to MSE walls, slope investigations, and various shallow foundation applications. Use of CPT for bridge foundation investigation has been fairly limited primarily because the department's hydraulic pushing platforms were unable to advance the cone to the necessary depths of deep bridge foundations, often in excess of 70 ft. Recently, larger capacity push platforms have made obtaining the required depths possible. NDOR geotechnical engineers realize the potential advantage of

CPT testing and design for deep foundation applications. This project aims to advance pile design practice in Nebraska, founded in more modern in situ testing regiments.

The CPT cone can be considered as a small-scale pile. The point resistance (q_c) and the sleeve friction (f_s) are similar to the end bearing (Q_p) and skin friction (Q_s) portions of resistance contributing a pile's bearing capacity. This close relationship lends itself to applying CPT test data for axial pile capacity prediction. The CPT sounding gives a continuous profile of the subsurface, providing detailed information of soil properties along the entire shaft of a pile. More traditional in situ test methods such as the standard penetration test (SPT) collect samples at discrete intervals, typically every 5 ft.

This project will focus on the use of CPT data for the computation of bearing capacity for axially loaded pile in Nebraskan soils. Project objectives are outlined below:

a) Conduct literature review on existing methods of direct pile bearing capacity prediction using CPT data.
b) Collect information on in-service bridge foundation piles in Nebraska and analyze load test data/installation records to determine accurate bearing capacity.
c) Compare CPT bearing capacity methods to and load test data
d) Find appropriate factors to correlate measured CPT cone tip resistance/sleeve friction with end bearing/skin friction resistance specific to regional soil conditions in Nebraska.
e) Implement Nebraska specific factors into CPT based pile bearing capacity prediction methods.

CHAPTER 2 LITERATURE REVIEW

2.1 General

Bearing capacity prediction is a common application of in-situ tests; the CPT offers capability for this application. The physics of the cone penetration and driven pile have similarities, leading to this correlation. The continuous profile obtained from CPT testing yields much more detailed information for the design of pile foundation capacity compared to traditional discrete sampling such as the standard penetration test. Pile bearing behavior depends on the type of pile installed and the nature of the soil strata encountered. The axial capacity prediction methods presented below use a variety of correlation factors to compare the end bearing and sleeve friction from the cone to associated bearing mechanisms of pile foundations. Literature review was conducted for direct capacity prediction methods used by other department of transportation agencies.

2.2 Aoki & De Alencar (1975) Method

Aoki and De Alencar suggested the following relationship for the prediction of unit end bearing capacity (q_t) of piles from CPT data.

$$q_t = \frac{q_{ca}}{F_b} \tag{2}$$

Where q_{ca} = average cone tip resistance around the pile toe, F_b = empirical factor depending on the type of pile, given in Table 2.1. The authors similarly proposed the following for unit skin friction capacity (f).

$$f = q_{cs}\frac{\alpha}{F_s} \tag{3}$$

Where q_{cs} = average cone tip resistance for each soil layer along the shaft of the pile, F_s = empirical factor that depends on the type of pile, also given in Table 2.1, and finally α_s = empirical factor dependent on soil type, presented in Table 2.2.

Table 2.1 Factors Fb and Fs for different pile types

Pile type	Fb	Fs
Bored	3.5	7.0
Franki	2.5	5.0
Steel	1.75	3.5
Precast concrete	1.75	3.5

Table 2.2 Factor α_s for different soil types

Soil type	α_s (%)	Soil type	α_s (%)	Soil type	α_s (%)
Sand	1.4	Sandy silt	2.2	Sandy clay	2.4
Silty sand	2.0	Sandy silt w/ clay	2.8	Sandy clay w/ silt	2.8
Silty sand w/ clay	2.4	Silt	3.0	Silty clay w/ sand	3.0
Clayey sand w/ silt	2.8	Clayey silt w/ sand	3.0	Silty clay	4.0
Clayey sand	3.0	Clayey silt	3.4	Clay	6.0

2.3 Bustamante and Gianeselli (1982) Method (LCPC/LCP Method)

The Laboratoire Central des Ponts et Chausees or French method (known as LCPC) was proposed by Bustamante and Gianeselli based on the analysis of nearly 200 pile load tests, including several pile types and founded in various subsurface strata conditions. This method uses only cone tip resistance (q_c) to predict both unit end bearing and unit skin friction of axially loaded pile. The sleeve friction (f_s) data obtained from the CPT is not considered for this analysis. This method considers pile type and installation method adjustments for capacity prediction. Unit end bearing resistance is predicted by the following equation:

$$q_p = K_c q_{ca} \tag{4}$$

Where K_c = empirical end bearing coefficient from Table 2.3 depending on installation method and soil conditions, and q_{ca} = equivalent average cone tip resistance obtained from the procedure shown if Figure 2.1.

Unit skin friction is estimated from the following equation:

$$f = \frac{q_c}{\alpha_{LCPC}} \tag{5}$$

Where α_{LCPC} =side friction coefficient from Table 2.4.

The procedure for equivalent average cone tip resistance is outlined below in combination with Figure 2.1.

1. Compute mean value of q_c (termed q_{ca}) over a distance a = 1.5*D above and below the pile tip, where D is pile diameter.

2. Eliminate q_c values outside the range: $1.3q'_{ca}$ to $.7q'_{ca}$ over the averaging section +/- *a* from the pile tip.

3. Calculate equivalent cone tip resistance q_{ca}, by calculating the new mean value over the same distance from the reduced data from the previous step.

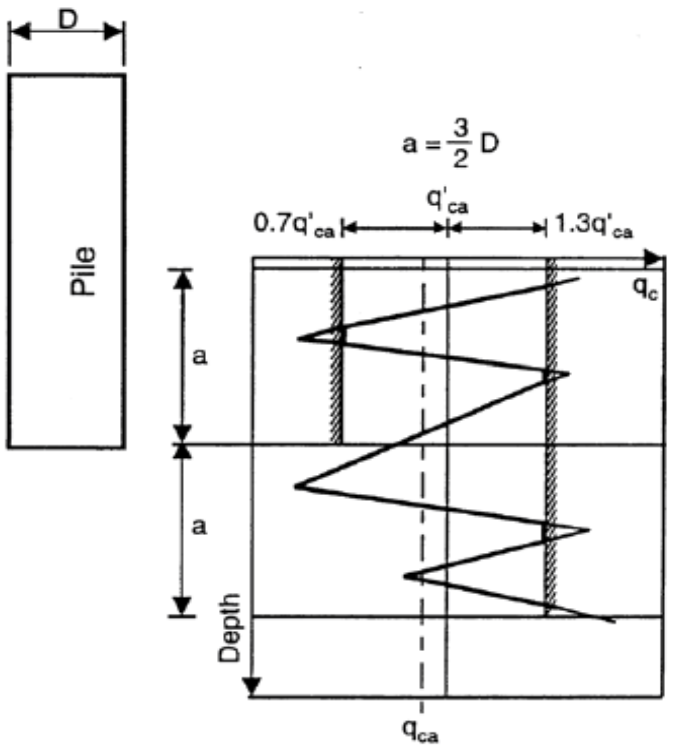

Fig. 2.1 Procedure for calculation of q_{ca} (after Bustamante and Gianeselli 1982)

Table 2.3 End-bearing coefficients, K_c

Nature of soil	q_c (MPa)	Factors K_c	
		Group I	Group II
Soft clay and mud	<1	0.4	0.5
Moderately compacted clay	1 to 5	0.35	0.45
Silt and loose sand	≤ 5	0.4	0.5
Compacted to stiff clay and compacted silt	>5	0.45	0.55
Soft chalk	≤ 5	0.2	0.3
Moderately compacted sand and gravel	5 to 12	0.4	0.5
Weathered to fragmented chalk	>5	0.2	0.4
Compacted to very compact sand and gravel	>12	0.3	0.4

Group I: plain bored piles; mud bored piles; micro piles (grouted under low pressure); cased bored piles; hollow auger bored piles; piers; barrettes.
Group II: cast screwed piles; driven precast piles; prestressed tubular piles; driven cast piles; jacked metal piles; micro piles (small diameter piles grouted under high pressure with diameter < 250 mm); driven grouted piles (low pressure grouting); driven metal piles; driven rammed piles; jacket concrete piles; high pressure grouted piles of large diameter.

Table 2.4 Friction coefficients, α_{LCPC}

Nature of soil	q_c (MPa)	Category									
		Coefficients, α				Maximum limit of f (MPa)					
		I		II		I		II		III	
		A	B	A	B	A	B	A	B	A	B
Soft clay and mud	< 5	30	90	90	30	0.015	0.015	0.015	0.015	0.035	
Moderately compact clay	1 to 5	40	80	40	80	0.035	0.035	0.035	0.035	0.08	≥ 0.12
						(0.08)	(0.08)	(0.08)			
Silt and loose sand	≤ 5	60	150	60	120	0.035	0.035	0.035	0.035	0.08	-
Compact to stiff clay and compact silt	> 5	60	120	60	120	0.035	0.035	0.035	0.035	0.08	≥ 0.20
						(0.08)	(0.08)	(0.08)			
Soft chalk	≤ 5	100	120	100	12	0.035	0.035	0.035	0.035	0.08	-
Moderately compact sand and gravel	5 to 12	100	200	100	200	0.08	0.035	0.08	0.08	0.12	≥ 0.20
						(0.12)	(0.08)	(0.12)			
Weathered to fragmented chalk	> 5	60	80	60	80	0.12	0.08	0.12	0.12	0.15	≥ 0.20
						(0.15)	(0.12)	(0.15)			
Compact to very compact sand and gravel	> 12	150	300	150	200	0.12	0.08	0.12	0.12	0.15	≥ 0.20
						(0.15)	(0.12)	(0.15)			

Category-IA: plain bored piles; mud bored piles; hollow auger bored piles; micropiles (grouted under low pressure); cast screwed piles; piers; barrettes.
Category-IB: cased bored piles; driven cast piles.
Category-IIA: driven precast piles; prestressed tubular piles; jacket concrete piles.
Category-IIB: driven metal piles; jacked metal piles.
Category-IIIA: driven grouted piles; driven rammed piles.
Category-IIIB: high pressure grouted piles of large diameter >250 mm; micropiles (grouted under high pressure).
Note: maximum limit unit skin friction f: bracket values apply to careful execution and minimum disturbance of soil due to construction

2.4 de Ruiter and Beringen (1979) Method

This procedure, also known as the European method, was developed based CPT and pile information studied in the North Sea. End bearing and skin friction determination is further differentiated by sandy or clayey conditions encountered in the subsurface. Individual discussions follow on end bearing and side friction resistance prediction methods based on the predominant soil classification.

Clayey soils

End bearing resistance is computed in clays by first finding the undrained shear strength (S_u) from the cone tip resistance per equation 6 then applying a bearing factor as shown below in equation 7.

$$S_u = \frac{q_c}{N_k} \tag{6}$$

$$q_p = N_c S_u \tag{7}$$

Where q_c = average cone tip resistance around the pile tip by Schmertmann method, N_k = cone factor, ranging from 15 to 20, adjusted for local conditions. The term q_p = unit end bearing resistance and N_c = bearing capacity factor, typical taken as N_c = 9 for this method. Shaft resistance in cohesive material is given by the following relationship.

$$f_s = \beta S_u \tag{8}$$

Where f_s = unit skin friction, β is an adhesion factor taken as β = 1 for normally consolidated soils and β = .5 for overconsolidated soils. Undrained shear strength is determined by the same method presented above for end bearing (equation 6)

Sandy soils

In sand, end bearing is evaluated in similar fashion to the Schmertmann method. Unit skin friction is determined by the comparison of following, selecting the minimum value:

$$f_s = \min \begin{bmatrix} f_s(CPT) \\ \frac{q_c}{300}(compression) \\ \frac{q_c}{400}(tension) \\ 1.2\ \text{TSF} \end{bmatrix} \quad (9)$$

The authors also stated upper bound values of 150 TSF and 1.2 TSF for q_t and f_s respectively.

2.5 Penpile (1978) Method

The Penpile method was developed for Mississippi DOT by Crisby et al. The following relationships predict unit end bearing and skin friction based on the tip resistance and sleeve friction respectively. The two following equations for end bearing are dependent on tip embedment in clayey or sandy soil.

$$q_p = 0.25 q_c \quad \text{(clay)} \quad (10)$$

$$q_p = 0.125 q_c \quad \text{(sand)} \quad (11)$$

Where q_c = average of 3 cone tip resistances near pile tip. Pile skin friction is subsequently determined by the following procedure:

$$f = \frac{f_s}{1.5 + 0.1 f_s} \tag{12}$$

Where f_s = is sleeve friction from the CPT, with the relationship only valid in the units of pounds per square inch (psi).

2.6 Philipponnat (1980) Method

Philipponnat proposed the following equation to estimate the unit end bearing of pile:

$$q_t = k_b q_{ca} \tag{13}$$

Where k_b = factor considering soil type, given in Table 2.5 and q_{ca} is average cone tip resistance detailed below:

$$q_{ca} = \frac{q_{ca\,(A)} + q_{ca\,(B)}}{2} \tag{14}$$

where $q_{ca}(A)$ and $q_{ca}(B)$ are average cone tip resistances over the distance 3B (B = pile diameter) above and below the pile tip respectively. The author recommends inspection of this range and removal of extreme spikes in tip resistance prior to averaging over this interval.

Table 2.5 Bearing capacity factors (k_b)

Soil type	k_b
Gravel	0.35
Sand	0.40
Silt	0.45
Clay	0.50

Unit skin friction is calculated by the following relationship using tip resistance values from the CPT:

$$f = \frac{\alpha_s}{F_s} q_{cs} \tag{15}$$

Where α_s depends on the pile type. For driven precast concrete piles α_s = 1.25. The factor F_s is related to soil type and presented in Table 2.6. The term q_{cs} = average cone tip resistance along the pile shaft.

Table 2.6 Empirical factor (F_s)

Soil type	F_s
Clay and calcareous clay	50
Silt, sandy clay, and clayey sand	60
Loose sand	100
Medium dense sand	150
Dense sand and gravel	200

2.7 Prince & Wardle (1982) Method

Prince and Wardle developed a method to estimate capacity from CPT data based on analysis of load tested piles installed in stiff clay (London clay). The unit end bearing capacity is predicted by the following relationship:

$$q_p = k_b q_c \tag{16}$$

Where k_b is a factor based only pile installation method. For driven piles, k_b =.35 and k_b =.30 for jacked piles. Similarly, unit skin fiction is computed from sleeve friction data using the following equation:

$$f = k_s f_s \tag{17}$$

Where again k_s is a factor which depends on the pile installation method. For driven piles, k_s = .53, for jacked piles, k_s = .62 and for bored piles, k_s = .49. Upper limits of q_p and f were imposed per this method. These values are 150 TSF and .12 TSF for unit end bearing and skin friction respectively.

2.8 Schmertmann (1978) Method

Schmertmann outlined a procedure for unit end bearing based on Begemann's method and two separate methods for side friction prediction in clays and sands respectively. Considerations are given for pile types and installation methods by Schmertmann.

End-bearing Determination

Unit end bearing is determined by evaluating a failure zone above and below the pile tip. The following equation is given for end bearing.

$$q_p = \frac{q_{c1} + q_{c2}}{2} \leq 15\,\text{MPa} \tag{18}$$

Where q_p = end bearing resistance, q_{c1} = average cone tip resistances of zones ranging from *0.7D to 4D* below the pile tip, q_{c2} = average cone tip resistances over a distance *8D* above the pile tip. More details are given on this procedure in Figure 2.2.

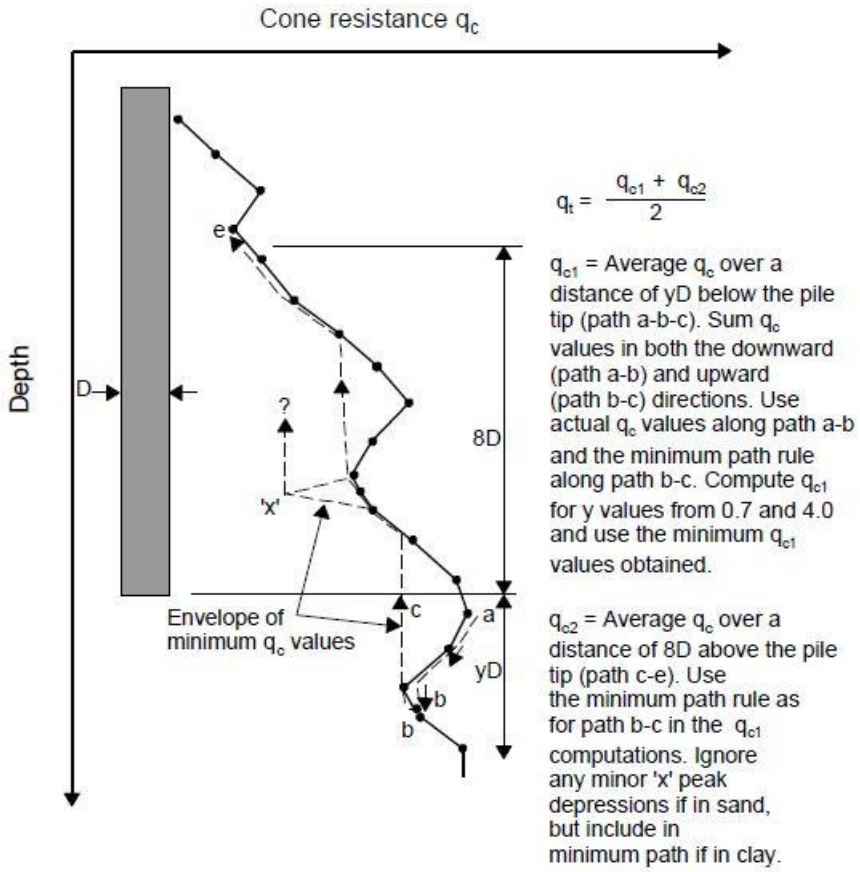

Fig. 2.2 Procedure for calculation of qt by Schmertmann method

This method also indicates that additional evaluation of soil strata in the zone defined by 4D to 10D below the pile tip. The failure surface of the soil surrounding the pile may extend into this region, thus if weaker strata exists, reductions should be considered by the designer. Schmertmann gave an upper bound for q_c at 300 TSF. Separate discussions are conducted for skin friction determination based on soil type, the processes are presented below.

Sandy Soils

Calculating the skin friction in sand is based on Nottingham's 1975 procedure which considers cone sleeve friction, the equation follows.

$$F_s = K\left[\sum_{y=0}^{8D}\frac{y}{8D} f_s A'_s + \sum_{y=8D}^{L} f_s A'_s\right] \quad (19)$$

Where F_s = ultimate skin friction resistance, K = sand correction factor-based pile depth to width ratio, determined from Figure 2.3. y = depth of f_s considered, D = pile width/diameter, L = pile length, and A'_s = soil-pile contact area. An upper bound of 1.2 TSF is recommended for sleeve friction.

Clay Soils

In cohesive soils, Schmertmann developed a simple relationship based on the CPT sleeve friction with an adjustment factor for pile type shown below.

$$F_s = \alpha_c f_s A_s \quad (20)$$

Where F_s = ultimate skin friction resistance, α_c = ratio of pile to penetrometer sleeve friction, A_s = pile-soil contact area. α_c can be obtained from Figure 2.4 shown below.

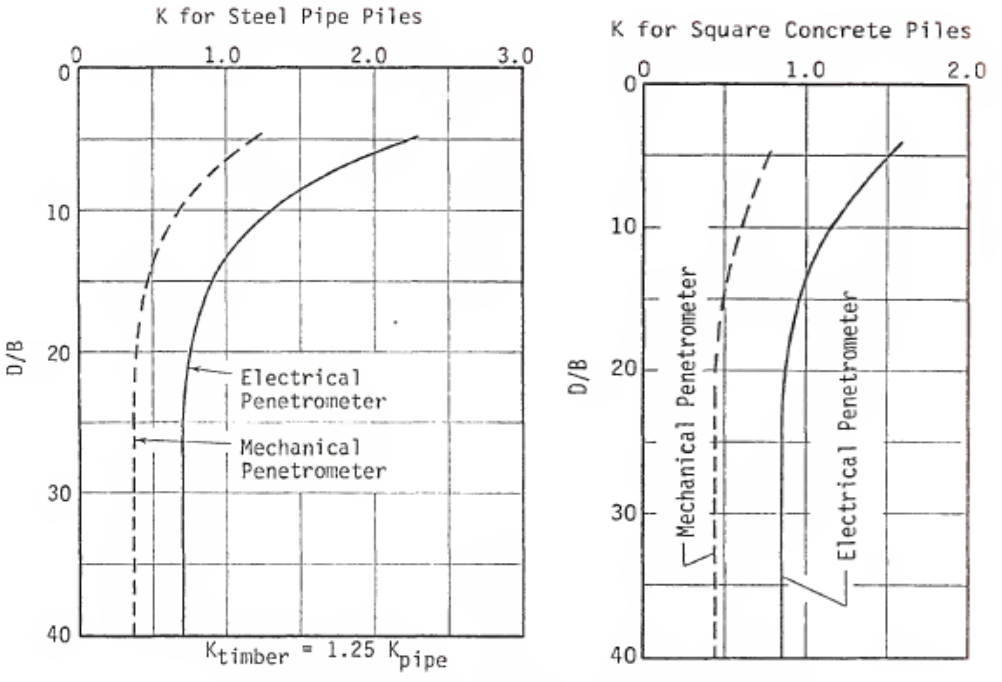

Fig. 2.3 *K*, Design curves for pile side friction in sand (after Nottingham 1975)

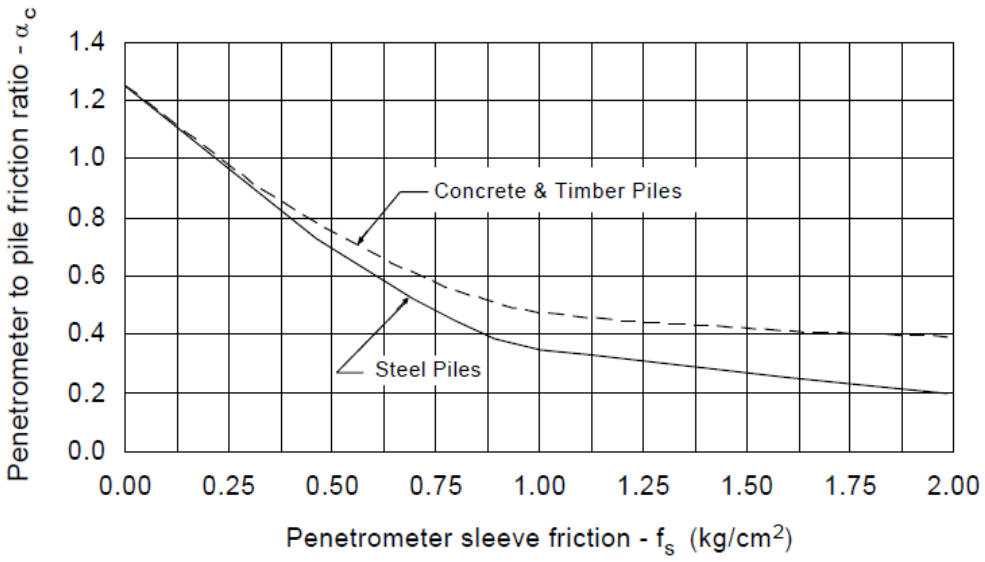

Fig. 2.4 αc, Design curves for pile side friction in clay (Schmertmann 1978)

The author recommended a 25% reduction of skin friction for bored or cast in place piling compared to driven piles. HP piles can be considered with a rectangular cross section simulating plugging effects.

2.9 Tumay & Fakhroo (1982) Method

This method was developed primarily for piles installed in cohesive soil conditions. Unit end bearing is computed by a process very similar to the Schmertmann method shown below.

$$q_t = \frac{q_{c1} + q_{c2}}{4} + \frac{q_a}{2} \tag{21}$$

Where q_{c1} = average q_c values 4D below the pile tip, q_{c2} = average minimum q_c values 4D below the pile tip, and q_a = average minimum values ranging 8D above the pile tip.

The authors proposed the following relationship for unit skin friction prediction.

$$f = mf_{sa} \tag{22}$$

Where f_{sa} = average local friction in TSF, and m = an adhesion factor given in terms of f_{sa} by:

$$m = 0.5 + 9.5e^{-9 f_{sa}} \tag{23}$$

f_{sa} is defined by the equation below:

$$f_{sa} = \frac{F_t}{L} \tag{24}$$

Where F_t = total CPT friction for pile embedment and L = pile length.

CHAPTER 3 METHODOLOGY

3.1 Method Overview

The objective of this project is to evaluate CPT based pile bearing prediction methods for driven pile in Nebraska. The CPT bearing capacity methods discussed previously use different approaches to determine end bearing and skin friction capacity of piles, and each of these methods presumably have strengths and limitations related to pile type and soil conditions. Nebraska has a wide range of geologic conditions across the state, ranging from wind deposited silts and sands to highly overconsolidated glacially impacted materials. Additionally, some parts of the state have shallow formations of rock or rock like intermediate geo-materials (IGMs) such as shale which offer quality bearing strata for driven pile foundations. This study collected data from NDOR at bridge locations that had the following records: 1) driven pile records 2) dynamic load test data 3) boring information 4) CPT records. These records were then used to evaluate in place bearing capacity of installed bridge foundation piles, which could further be statistically compared to CPT prediction output. The following sections provide further information on site selection and data sampling.

3.2 Site Selection

The primary objective of project site selection for this research project was to obtain data representative of the majority of Nebraska soil conditions encountered during bridge foundation design and installation. During discussion with the advisory committee, a focus was placed on selecting sites that represented soil conditions where NDOR recognized potential for CPT subsurface investigation in future bridge foundation work. Two primary factors drove the projects selected for further evaluation. First, not all

soil conditions in Nebraska are conducive to CPT investigation. In particular, sites with significant strata (> 10 ft) of dense sands and gravels at shallow elevations are difficult for the pushed cone to penetrate. This is a well-known limitation of the CPT test, and other traditional boring techniques are typically used for geotechnical investigation. Due to this, most projects selected had predominately softer, fine grained material throughout the profile. This is not to say that granular material conditions were not evaluated in any capacity, rather sites with 60+ ft of dense/highly angular sand and gravel typically found in the western part of the state were avoided.

Second the availability of load test data was a significant factor in the site choice for this project. NDOR selectively preforms dynamic load tests on structures of high value or high load capacity. Other structures are selected based on cost/benefit, limited geotechnical investigation, and concern for site variability. The objective of PDA dynamic load testing is to verify in place pile capacities are meeting design capacity, and occasionally provided project specific pile driving adjustments.

Initial site selection consisted of 34 bridge projects consisting of 48 bridge structures. Each structure was further investigated to find substructure elements (e.g. Abutment #1, Pier #2) with existing PDA records and corresponding CPT logs. In some instances, bridges with dynamic load tests for all four substructures were compared to only two existing CPT logs. Two borings or CPT investigations is common for NDOR bridge replacement projects evaluated by the geotechnical section. Some projects had quality load test data but had been built prior to widespread CPT use by the department

on bridge. As a result, NDOR staff conducted new CPTs at these sites where subsurface conditions were favorable to advancing the cone to adequate depths.

Final project selection for further study included 17 projects consisting of 20 bridges. Table 3.1, presents the project and structure information of those projects studied for this research. Figure 3.1 below is a map of Nebraska with locations of the selected projects and associated interstate, state highway, or county bridge classification. Further information related to substructure and specific piling information will be discussed later.

Table 3.1 CPT Project information

PN	CN	SN	PN	CN	SN
34-6(133)	12425	C05501305P	80-9(865)	12492	S080 40436
		S034 31644	80-9(838)	12465	S080 41341
		S034 31644	159-7(106)	12381a	S159 01373
77-2(1025)	11801	S077 09368	85-2(111)	22203	S085 0042
80-2(106)	51459B	S080 08295L	7066(43)	12785	C006602905
80-9(865)	12492	S080 40436	80-9(811)	21929	S080 43555
180-9(519)	11347	S180 00205	80-9(828)	12455	S080 42094
77-3(128)	22265	S077 11185	80-9(801)	21867	S080 44207
75-2(167)	21849e	S034 38219	15-3(115)	32132	S015 13411
81-2(1035)	42050A	S081 08578	80-9(830)	12457	S080 41856

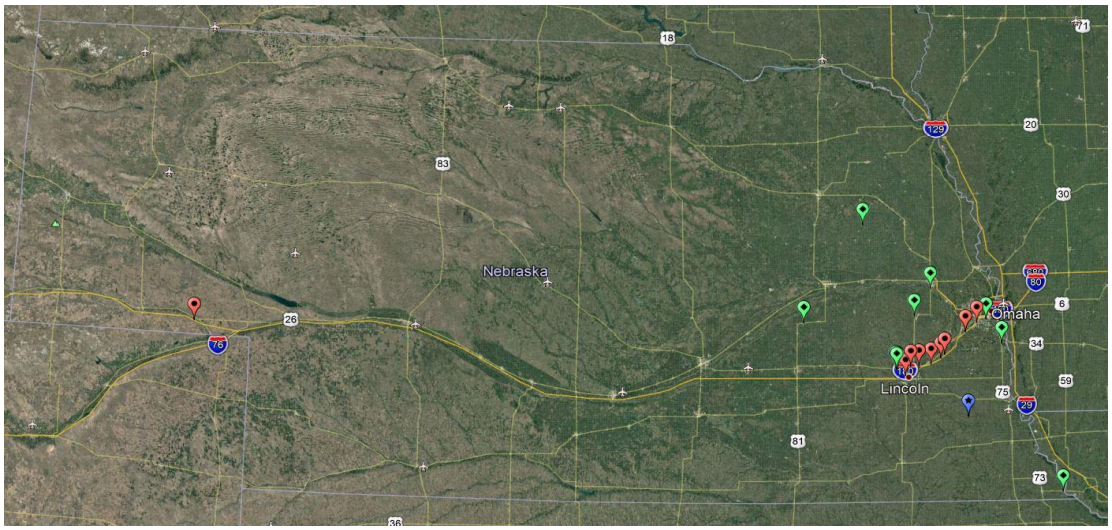

Fig. 3.1 Site map of selected CPT/PDA bridge sites

3.3 In Place Pile Capacity

NDOR's LRFD pile driving equation was also considered in addition to dynamic load test results. Equation 25, is the equation used for official pile capacity verified and reported by department field personnel. The equation has been well verified and represents a Nebraska specific capacity determination design engineers have confidence in. Driving equation results are typically found to be slightly conservative compared to PDA/CAPWAP analysis results, as reported by NDOR geotechnical staff.

$$\varphi Q_u = \frac{4E}{s+.5} \tag{25}$$

Where ϕ = resistance factor, ϕ =.7, E = hammer energy defined by E = W*H, where W is the ram weight of the hammer in kips, H is the fall of the ram in feet, and finally s = pile set (distance the pile moves when struck) in inches/blow.

3.4 Pile Type

Pile type can be generally classified as end bearing or skin friction piling. NDOR policy typically specifies steel HP pile for end bearing controlled designs, and steel pipe piles or precast prestressed concrete piles in the case of side friction dominant designs. HP piles most commonly used by the state are HP10x42, HP12x53, and HP14x89 sizes. Steel pipe piles are almost all 12.75" O.D. with 3/8in wall thickness and welded plate bottoms. Prestressed concrete pile used by the state can be square, circular, or hexagonal with 28-day strength ranging from 4000-5000psi. In this study HP piles, pipe piles and square concrete piles were evaluated. CPT bearing design methods used allowed for pile shape and type considerations. This project analyzed 33 pipe piles, 40 HP piles, and 5 concrete piles. After initial analysis, pile type was considered for variations in dynamic

load test results versus predicted CPT capacity. Individual pile "sizes" were considered, but analysis ultimately led to the classification of pile type the predominant bearing resistance condition, end bearing or side friction. Thus, pile classification for bearing evaluation and statistical analysis grouped all HP piles as end bearing, and pipe piles and concrete piles as friction piles in accordance with NDOR practice.

3.5 CPT Data

CPT data collected was collected and output in digital form directly from the logging software. The software logs depth, tip resistance (q_c), sleeve friction (f_s), and pore pressure (u_2) real time while the cone is advanced. Information is then saved to the log file which can be exported in [.csv] format. A report is generated containing the measured information discussed above as well as important project information. An example of raw CPT output is shown below in Figure 3.2, from project 80-9(811).

	A	B	C	D	E	F	G	H	I	J	K	L	M	N	O	P	Q	R	S	T	U	V	W
1	H [m]	qc [MPa]	fs [MPa]	u2 [MPa]	Incl. [°]	v [cm/s]	Rf [%]	Uo [MPa]	qt [MPa]	ft [MPa]	sigmaVo [	sigma'Vo [	qt-sigmaV	Qt []	Fr []	Bq []	Rf(qc) [%]	Uh [MPa]	Rfd []	soil []	L [m]	D [m]	UW [kN/m^3]
2	0	0	0	0.0006	1.9	0	100	0	0	0	0	0	0	10	100	6	100	0	0	1	0	0	12.5
3	0.02	0.139	0.0001	0	0.6	0	0.072	0	0.139	0	0	0	0.139	396.429	0.072	0	0.072	0	0	1	0.02	0.02	17.5
4	0.04	0.471	0.0001	-0.0002	0.6	0	0.042	0	0.471	0	0.001	0.001	0.47	671.383	0.043	-0.0004	0.042	0	0	1	0.04	0.04	17.5
5	0.06	0.913	0.0001	0.0007	0.6	18	0.022	0	0.914	0	0.001	0.001	0.912	869.011	0.022	0.0008	0.022	0	0	6	0.06	0.06	17.5
6	0.08	1.154	0.0001	0.0036	0.6	19	0.017	0	1.154	0	0.001	0.001	1.153	817.635	0.017	0.0031	0.017	0	0	6	0.08	0.08	18
7	0.1	1.028	0.0001	0.0023	0.5	19	0.019	0	1.028	0	0.002	0.002	1.027	580.055	0.019	0.0022	0.019	0	0.024	6	0.1	0.1	18
8	0.12	0.959	0.0001	0.0044	0.4	20	0.021	0	0.96	0	0.002	0.002	0.958	451.879	0.021	0.0046	0.021	0	0.021	6	0.12	0.12	17.5
9	0.14	0.98	0.0001	0.005	0.4	20	0.02	0	0.981	0	0.002	0.002	0.979	394.565	0.02	0.0051	0.02	0	0.019	6	0.14	0.14	18
10	0.16	1.057	0.0001	0.0055	0.4	21	0.019	0	1.058	0	0.003	0.003	1.055	371.493	0.019	0.0052	0.019	0	0.018	6	0.16	0.16	18
11	0.18	1.123	0.0001	0.0063	0.4	20	0.018	0	1.124	0	0.003	0.003	1.121	350.253	0.018	0.0056	0.018	0	0.017	6	0.18	0.18	18
12	0.2	1.183	0.0001	0.0066	0.4	21	0.017	0	1.184	0	0.004	0.004	1.18	331.488	0.017	0.0056	0.017	0	0.017	6	0.2	0.2	18
13	0.22	1.23	0.0001	0.0062	0.4	20	0.016	0	1.231	0	0.004	0.004	1.228	313.156	0.016	0.0051	0.016	0	0.016	6	0.22	0.22	18
14	0.24	1.314	0.0001	0.0063	0.4	20	0.015	0	1.315	0	0.004	0.004	1.31	306.151	0.015	0.0048	0.015	0	0.016	6	0.24	0.24	18
15	0.26	1.34	0.0001	0.0061	0.5	20	0.015	0	1.341	0	0.005	0.005	1.336	287.96	0.015	0.0046	0.015	0	0.015	6	0.26	0.26	18
16	0.28	1.375	0.0001	0.0052	0.5	20	0.015	0	1.376	0	0.005	0.005	1.371	274.166	0.015	0.0038	0.015	0	0.015	6	0.28	0.28	18
17	0.3	1.381	0.0001	0.0052	0.6	19	0.014	0	1.382	0	0.005	0.005	1.377	256.879	0.015	0.0038	0.014	0	0.015	6	0.3	0.3	18
18	0.32	1.407	0.0001	0.0044	0.6	21	0.014	0	1.407	0	0.006	0.006	1.402	245.032	0.014	0.0031	0.014	0	0.014	6	0.32	0.32	18
19	0.34	1.424	0.0001	0.0038	0.6	20	0.014	0	1.424	0	0.006	0.006	1.418	233.278	0.014	0.0027	0.014	0	0.014	6	0.34	0.34	18
20	0.36	1.425	0.0001	0.0033	0.6	20	0.007	0	1.425	0	0.006	0.006	1.419	220.309	0.007	0.0023	0.007	0	0.007	6	0.36	0.36	18
21	0.38	1.46	0.0001	0.0021	0.6	19	0.007	0	1.46	0	0.007	0.007	1.454	213.755	0.007	0.0014	0.007	0	0.007	6	0.38	0.38	18
22	0.4	1.53	0.0001	0.0016	0.6	0	0.013	0	1.531	0	0.007	0.007	1.523	212.481	0.013	0.0011	0.013	0	0.013	6	0.4	0.4	18.5
23	0.42	1.559	0.005	-0.001	0.5	19	0.34	0	1.559	0.005	0.008	0.008	1.552	206.057	0.342	-0.0006	0.34	0	0.349	6	0.42	0.42	18
24	0.44	1.549	0.011	-0.0018	0.4	18	0.736	0	1.549	0.011	0.008	0.008	1.541	195.339	0.74	-0.0012	0.736	0	0.741	6	0.44	0.44	18
25	0.46	1.558	0.018	-0.0029	0.4	18	1.155	0	1.558	0.018	0.008	0.008	1.55	187.841	1.162	-0.0019	1.155	0	1.156	5	0.46	0.46	18
26	0.48	1.569	0.029	-0.0045	0.4	20	1.868	0	1.569	0.029	0.009	0.009	1.56	181.181	1.878	-0.0029	1.867	0	1.86	5	0.48	0.48	18
27	0.5	1.595	0.034	-0.0058	0.4	20	2.159	0	1.594	0.034	0.009	0.009	1.585	176.667	2.171	-0.0037	2.157	0	2.168	5	0.5	0.5	18
28	0.52	1.629	0.04	-0.007	0.4	20	2.445	0	1.628	0.04	0.009	0.009	1.618	173.467	2.459	-0.0043	2.443	0	2.502	5	0.52	0.52	18
29	0.54	1.627	0.045	-0.0074	0.6	19	2.755	0	1.626	0.045	0.01	0.01	1.616	166.793	2.772	-0.0046	2.753	0	2.815	5	0.54	0.54	18
30	0.56	1.627	0.052	-0.0086	0.6	21	3.174	0	1.626	0.052	0.01	0.01	1.616	160.764	3.194	-0.0053	3.171	0	3.241	4	0.56	0.56	18
31	0.58	1.621	0.054	-0.0091	0.6	19	3.322	0	1.619	0.054	0.01	0.01	1.609	154.557	3.344	-0.0057	3.319	0	3.389	4	0.58	0.58	18
32	0.6	1.586	0.055	-0.0101	0.4	20	3.477	0	1.585	0.055	0.011	0.011	1.574	146.148	3.501	-0.0064	3.473	0	3.487	4	0.6	0.6	18
33	0.62	1.574	0.056	-0.0104	0.4	20	3.543	0	1.572	0.056	0.011	0.011	1.561	140.252	3.568	-0.0067	3.539	0	3.551	4	0.62	0.62	18
34	0.64	1.567	0.056	-0.0121	0.6	19	3.558	0	1.566	0.056	0.011	0.011	1.554	135.254	3.584	-0.0078	3.553	0	3.588	4	0.64	0.64	18
35	0.66	1.557	0.052	-0.013	0.6	20	3.352	0	1.555	0.052	0.012	0.012	1.543	130.183	3.377	-0.0084	3.347	0	3.398	4	0.66	0.66	18

Fig. 3.2 Raw CPT output in [.csv] format

Penetration of the cone was conducted at the standard 2 cm/s. Groundwater table elevation is determined graphically from the distribution of u_2 pore pressures measured by the PCPT probe. CPT analysis software preforms soil classification. NDOR typically uses the Robertson 1986 method, which was also adopted for use in this project. Soil classification analysis is typically set a 0.1ft intervals by the NDOR geotechnical section. This classification was taken directly from the output file for use in pile capacity methods where required. Standard zero-spike data correction was conducted by the CPT analysis software to correct for false responses during rod addition.

3.6 Dynamic Load Test Data

Pile load tests can be generally classified into three methods based on the loading mechanism and behavior:

1) Static Load Test
2) Dynamic Load Test
3) Statnamic Load Test

The state of Nebraska uses dynamic load testing to verify bearing capacity of driven deep foundations across the state. One of the first and most widely used systems is the Pile Driving Analyzer (PDA) manufactured and supported by Pile Dynamics Inc.

Dynamic load testing was first used by NDOR in the early 2000s on test piles for select projects, and use has continued to present day. This provided a large quantity of records for driven pile foundations. For the purposes of this research, dynamic load test data for the entire length of the pile was desirable. Many times though, department use of the pile analyzer is for final drive capacity verification, or for set up factor determination.

Consequently, some of the available data was eliminated, not because it was unusable in all cases, but rather complete driving records allowed for more complete analysis and comparison to CPT methods. The dynamic load test data comprises of two components. First, the raw wave signal data is recorded for each hammer blow. The PDA unit records this information to the log. A real time capacity is provided to the engineer; however, these are only estimates and are not considered accurate for capacity verification. An example of the real time PDA data collection compiled into the log file is shown in Figure 3.3.

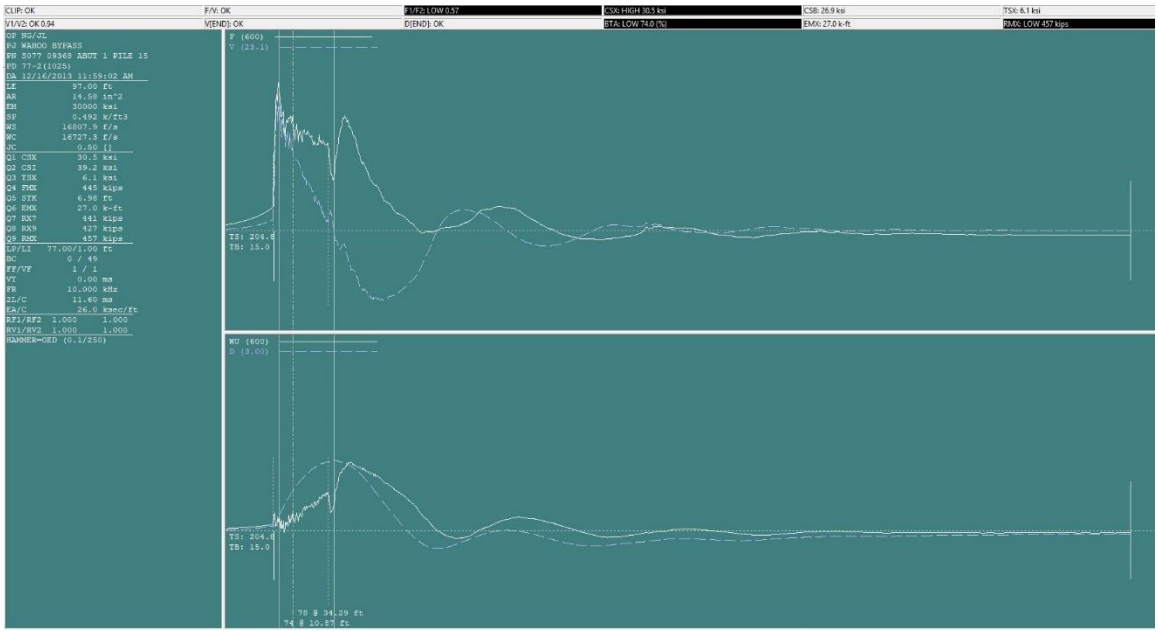

Fig. 3.3 PDA log file example

The second component of the dynamic load test requires further analysis of the raw data. This is performed by CAPWAP software, which uses a wave signal matching technique to refine an accurate capacity. Blows are analyzed individually, which means the load test data can be calculated at any desired depth from a complete log, but the data is discrete and computationally speaking time consuming. Figure 3.4 is an example of the

CAPWAP analysis. Most importantly from this analysis, the load test data gives an accurate ultimate axial capacity and additionally end bearing and skin friction distributions that could be compared to CPT data.

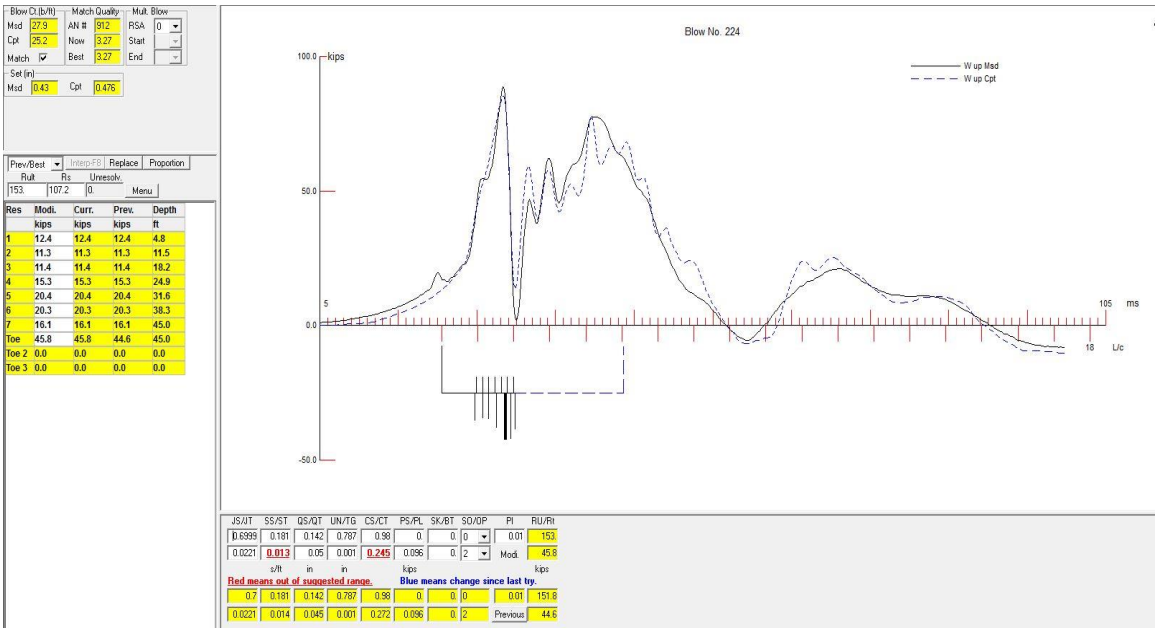

Fig. 3.4 CAPWAP analysis output

For this project the objective to sample load test data at periodic intervals of pile installation length for complete driving records, focusing on the last 10-15 ft of the embedment length. The rational being, that these conditions represent near design bearing conditions such as embedment length and firmer soil strata. For some comparisons, incomplete PDA records or CPT penetration refusal limited the range of pile embedment lengths that could be further analyzed with CAPWAP. Finally, department driving records were also acquired for PDA/CPT comparison. These records allowed for verification of pile penetration length, measured “set”, and “hammer fall” at 5 ft intervals on test piles to be compared with dynamic load test records.

3.7 CPT Based Bearing Prediction

The core task of this project was to implement CPT based bearing capacity design methods for axially load piles. Due to the repetitive nature and computational effort required, functions for each of the eight discussed methods was coded in a combination of Microsoft Excel and RStudio suites. Numerical and graphical output is also from Excel. These methods were selected due to widespread availability and ease of use. Additionally, by providing bearing computation along the entire CPT profile rather than for discrete elevations used in analysis, the CPT methods can be developed as a design tool for NDOR geotechnical engineers designing pile. This continuous bearing vs depth style is consistent with current commercial pile design software. Furthermore, multiple comparisons could be conducted at desired embedment locations.

CHAPTER 4 PILE ANALYSIS

4.1 CPT Profile

CPT data was provided in raw format from field collection and needed to be processed prior to bearing capacity prediction. Section 3.5 details standard methods that were applied to each profile. In addition, the CPT profile was compared alongside boring logs where available for soil strata verification. Elevation data in relation to bridge substructure elements needed to be calculated for most projects. Figure 4.1 contains boring log information from bridge plans. Figure 4.2 is a processed CPT graphic ready for further bearing analysis.

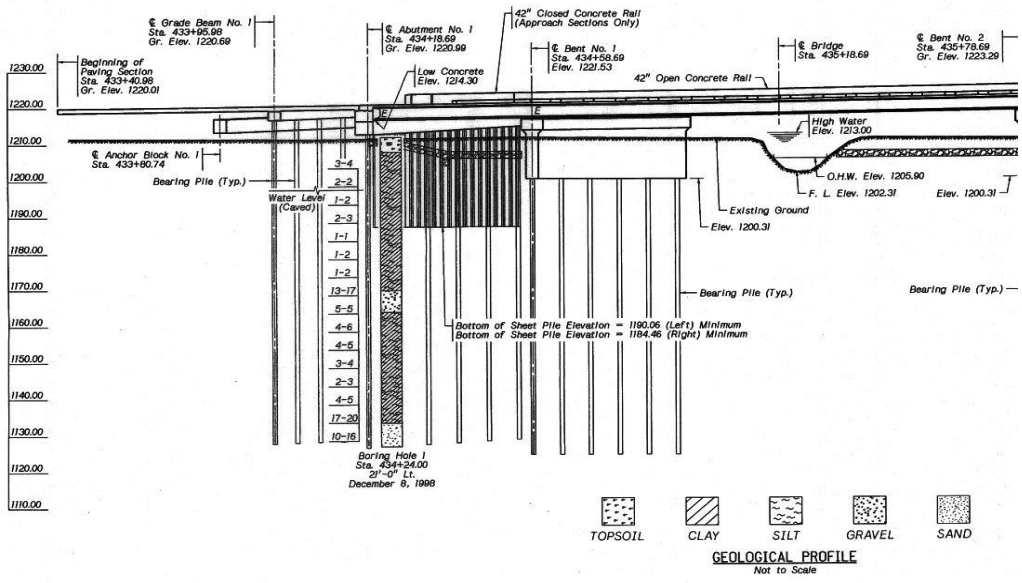

Fig. 4.1 Example of boring log information from bridge plans

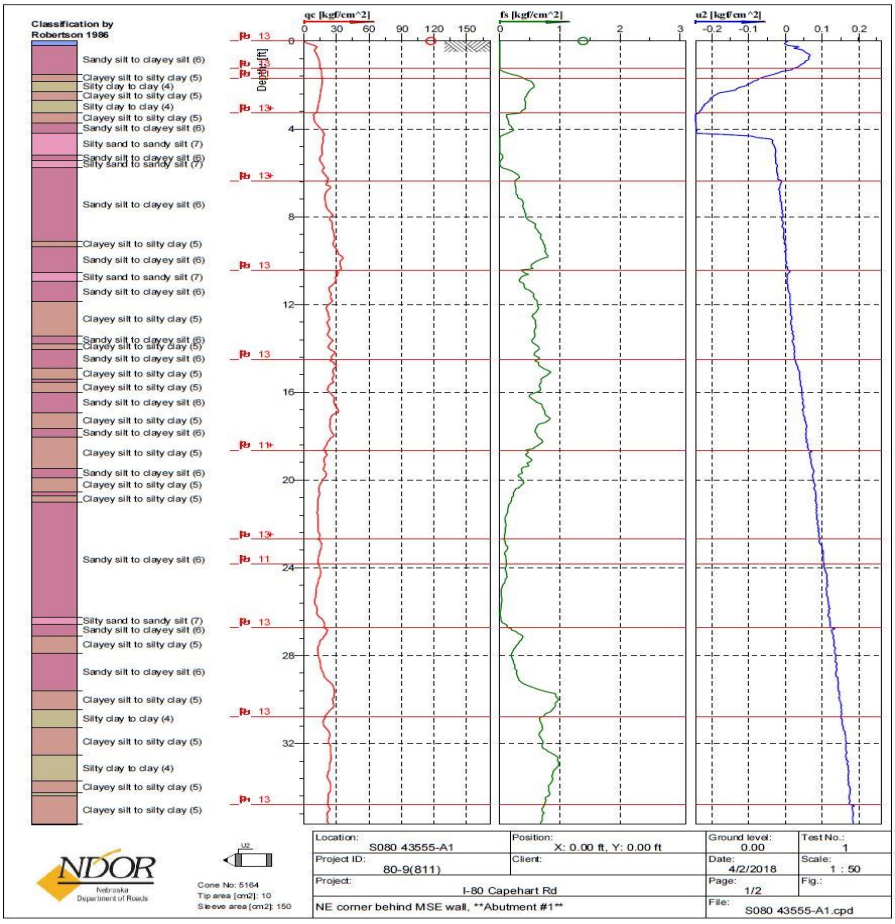

Fig. 4.2 Example of Cone Penetration (CPT) Log

4.2 CPT Bearing Capacity

Bearing capacity was calculated by eight known CPT based methods investigated in chapter 2. These methods were Aoki & DeAlencar, LCPC, European, Penpile, Philipponnat, Prince & Wardle, Schmertmann, and finally Tumay & Fakhroo. Each CPT profile was evaluated over the entire length of the log. End bearing capacity was predicted at each CPT log interval (approximately .75”). Similarly, unit skin friction was calculated at each depth, then accumulated down the profile. Finally, a summation of resistances was gathered for ultimate bearing capacity prediction at every logged depth. The figures below are an example of the resultant output including the numerical

capacities and graphics comparing end bearing, skin friction, and total capacity for all eight prediction methods.

	Penpile			Philipponnat			Prince & Wardle			LCPC			Aoki			Schmertmann			European			Tumay		
H [ft]	Qp [kip]	Qs [kip]	Q [kip]	Qp [kip]	Qs [kip]	Q [kip]	Qp [kip]	Qs [kip]	Q [kip]	Qp [kip]	Qs [kip]	Q [kip]	Qp [kip]	Qs [kip]	Q [kip]	Qp [kip]	Qs [kip]	Q [kip]	Qp [kip]	Qs [kip]	Q [kip]	Qp [kip]	Qs [kip]	Q [kip]
12.99213	2.00	33.70	35.70	5.56	47.48	53.04	3.01	46.46	49.47	15.70	16.17	31.87	8.18	33.16	41.34	4.35	23.08	27.44	2.61	40.08	42.69	8.39	26.18	34.57
13.05774	1.98	33.70	35.68	5.48	47.57	53.06	3.01	46.47	49.47	15.68	16.23	31.91	8.30	33.20	41.50	4.54	23.09	27.63	2.72	40.15	42.87	8.54	26.31	34.85
13.12336	1.96	33.72	35.68	5.41	47.66	53.07	3.01	46.48	49.48	15.65	16.30	31.95	8.44	33.25	41.69	4.51	23.10	27.61	2.71	40.21	42.92	8.70	26.45	35.14
13.18898	3.89	33.73	37.62	5.98	47.76	53.74	3.01	46.49	49.50	15.62	16.37	31.99	8.60	33.29	41.89	4.67	23.12	27.78	2.80	40.28	43.08	8.88	26.58	35.46
13.25459	3.85	33.76	37.61	5.92	47.86	53.79	3.36	46.51	49.88	15.60	16.44	32.03	8.79	33.34	42.13	4.76	23.14	27.90	2.86	40.35	43.21	9.09	26.71	35.80
13.32021	3.82	33.79	37.62	5.88	47.97	53.85	3.71	46.54	50.25	15.57	16.50	32.08	8.99	33.39	42.38	4.85	23.17	28.02	2.91	40.43	43.34	9.31	26.85	36.16
13.38583	3.80	33.83	37.63	5.84	48.10	53.93	4.07	46.57	50.64	15.55	16.57	32.12	9.18	33.44	42.63	5.01	23.21	28.22	3.01	40.52	43.53	9.55	26.98	36.52
13.45144	3.78	33.88	37.65	5.79	48.22	54.02	4.25	46.61	50.86	15.52	16.64	32.16	9.36	33.50	42.86	3.43	23.25	26.68	2.06	40.62	42.68	9.76	27.11	36.87
13.51706	3.76	33.92	37.68	5.76	48.36	54.12	4.42	46.65	51.07	15.50	16.71	32.20	9.51	33.57	43.08	3.74	23.29	27.03	2.25	40.72	42.96	9.92	27.24	37.17
13.58268	3.76	33.97	37.73	5.74	48.49	54.23	4.60	46.69	51.29	15.47	16.77	32.24	9.64	33.63	43.27	4.06	23.33	27.39	2.43	40.82	43.25	10.07	27.38	37.45
13.64829	3.76	34.02	37.78	5.72	48.63	54.35	4.60	46.73	51.33	15.45	16.84	32.29	9.75	33.70	43.46	4.34	23.38	27.71	2.60	40.92	43.52	10.23	27.51	37.74
13.71391	3.76	34.07	37.83	5.70	48.77	54.47	4.78	46.78	51.55	15.42	16.91	32.33	9.86	33.77	43.63	4.60	23.42	28.02	2.76	41.02	43.78	10.36	27.64	38.00
13.77953	3.77	34.12	37.89	5.69	48.92	54.61	4.95	46.82	51.77	15.40	16.98	32.37	9.95	33.85	43.79	4.90	23.47	28.37	2.94	41.13	44.07	10.46	27.77	38.23
13.84514	3.77	34.17	37.94	5.69	49.07	54.76	5.13	46.87	52.00	15.37	17.04	32.42	10.00	33.92	43.93	5.19	23.52	28.71	3.12	41.25	44.36	10.43	27.90	38.34
13.91076	3.76	34.23	37.99	5.70	49.22	54.93	5.31	46.92	52.23	15.35	17.11	32.46	10.05	34.00	44.05	5.49	23.57	29.06	3.30	41.36	44.66	10.53	28.04	38.56
13.97638	3.76	34.30	38.05	5.73	49.37	55.10	5.13	46.98	52.10	15.32	17.18	32.50	10.09	34.08	44.17	5.47	23.63	29.09	3.28	41.48	44.76	10.61	28.17	38.78
14.04199	3.75	34.37	38.12	5.75	49.52	55.27	4.95	47.04	51.99	15.30	17.25	32.55	10.13	34.15	44.29	5.72	23.69	29.41	3.43	41.59	45.02	10.72	28.30	39.03
14.10761	3.75	34.44	38.19	5.78	49.67	55.45	5.13	47.11	52.23	15.28	17.31	32.59	10.18	34.23	44.41	5.87	23.76	29.64	3.52	41.70	45.22	10.85	28.43	39.28
14.17323	3.74	34.52	38.27	5.82	49.81	55.63	4.95	47.18	52.13	15.25	17.38	32.63	10.21	34.30	44.50	6.00	23.84	29.84	3.60	41.81	45.41	10.77	28.56	39.34
14.23885	3.74	34.61	38.35	5.86	49.96	55.82	4.78	47.27	52.04	15.23	17.45	32.68	10.23	34.36	44.59	6.23	23.93	30.16	3.74	41.91	45.65	10.76	28.70	39.46
14.30446	3.73	34.71	38.44	5.92	50.12	56.03	4.95	47.36	52.31	15.21	17.52	32.72	10.26	34.44	44.69	3.83	24.01	27.85	2.30	42.02	44.32	10.86	28.83	39.69
14.37008	3.73	34.80	38.53	5.98	50.28	56.26	5.48	47.44	52.93	15.18	17.56	32.75	10.28	34.52	44.80	4.46	24.10	28.57	2.68	42.14	44.82	10.97	28.96	39.93
14.4357	3.73	34.89	38.62	6.05	50.46	56.51	6.19	47.53	53.72	15.16	17.61	32.77	10.29	34.61	44.90	5.10	24.19	29.29	3.06	42.28	45.34	11.09	29.09	40.18
14.50131	3.72	34.99	38.71	6.15	50.63	56.78	6.01	47.62	53.63	15.14	17.66	32.80	10.29	34.70	44.99	5.67	24.28	29.94	3.40	42.41	45.81	11.19	29.22	40.41
14.56693	3.71	35.09	38.80	6.26	50.81	57.07	5.84	47.71	53.55	15.12	17.73	32.84	10.29	34.79	45.07	6.19	24.37	30.56	3.71	42.54	46.25	11.29	29.35	40.64
14.63255	3.70	35.19	38.89	6.39	50.98	57.36	5.84	47.81	53.64	15.10	17.79	32.89	10.29	34.87	45.16	6.78	24.45	31.23	4.07	42.67	46.74	11.38	29.48	40.87
14.69816	3.70	35.29	38.98	6.52	51.14	57.66	5.66	47.90	53.56	15.07	17.86	32.93	10.29	34.96	45.24	7.36	24.54	31.90	4.42	42.79	47.21	11.48	29.62	41.09
14.76378	3.69	35.39	39.08	6.65	51.30	57.95	5.66	47.99	53.65	15.05	17.93	32.98	10.27	35.03	45.30	7.95	24.63	32.57	4.77	42.92	47.69	11.12	29.75	40.86
14.8294	3.69	35.49	39.18	6.76	51.38	58.14	5.31	48.09	53.40	15.04	18.00	33.03	10.28	35.10	45.39	7.83	24.71	32.55	4.70	43.04	47.74	11.20	29.88	41.08
14.89501	3.69	35.60	39.29	7.22	51.52	58.74	4.95	48.20	53.15	15.02	18.06	33.08	10.31	35.17	45.48	8.30	24.82	33.11	4.98	43.15	48.12	11.27	30.01	41.28
14.96063	3.69	35.71	39.40	7.33	51.61	58.94	4.78	48.30	53.08	15.01	18.13	33.14	10.34	35.22	45.55	8.56	24.92	33.48	5.14	43.25	48.39	11.36	30.14	41.50
15.02625	3.69	35.81	39.50	7.43	51.64	59.06	0.36	48.40	48.75	14.99	18.20	33.19	10.38	35.26	45.64	5.64	24.99	30.64	3.39	43.26	46.65	8.32	30.27	38.59
15.09186	3.68	35.91	39.59	7.14	51.75	58.88	5.31	48.49	53.80	14.98	18.27	33.24	10.52	35.31	45.83	6.14	25.09	31.23	3.68	43.38	47.06	8.50	30.40	38.90
15.15748	3.69	36.01	39.70	7.21	51.90	59.10	5.31	48.59	53.90	14.96	18.33	33.30	10.54	35.38	45.92	6.22	25.18	31.40	3.73	43.49	47.22	8.57	30.54	39.11

Fig. 4.3 Example of numeric output from CPT capacity prediction

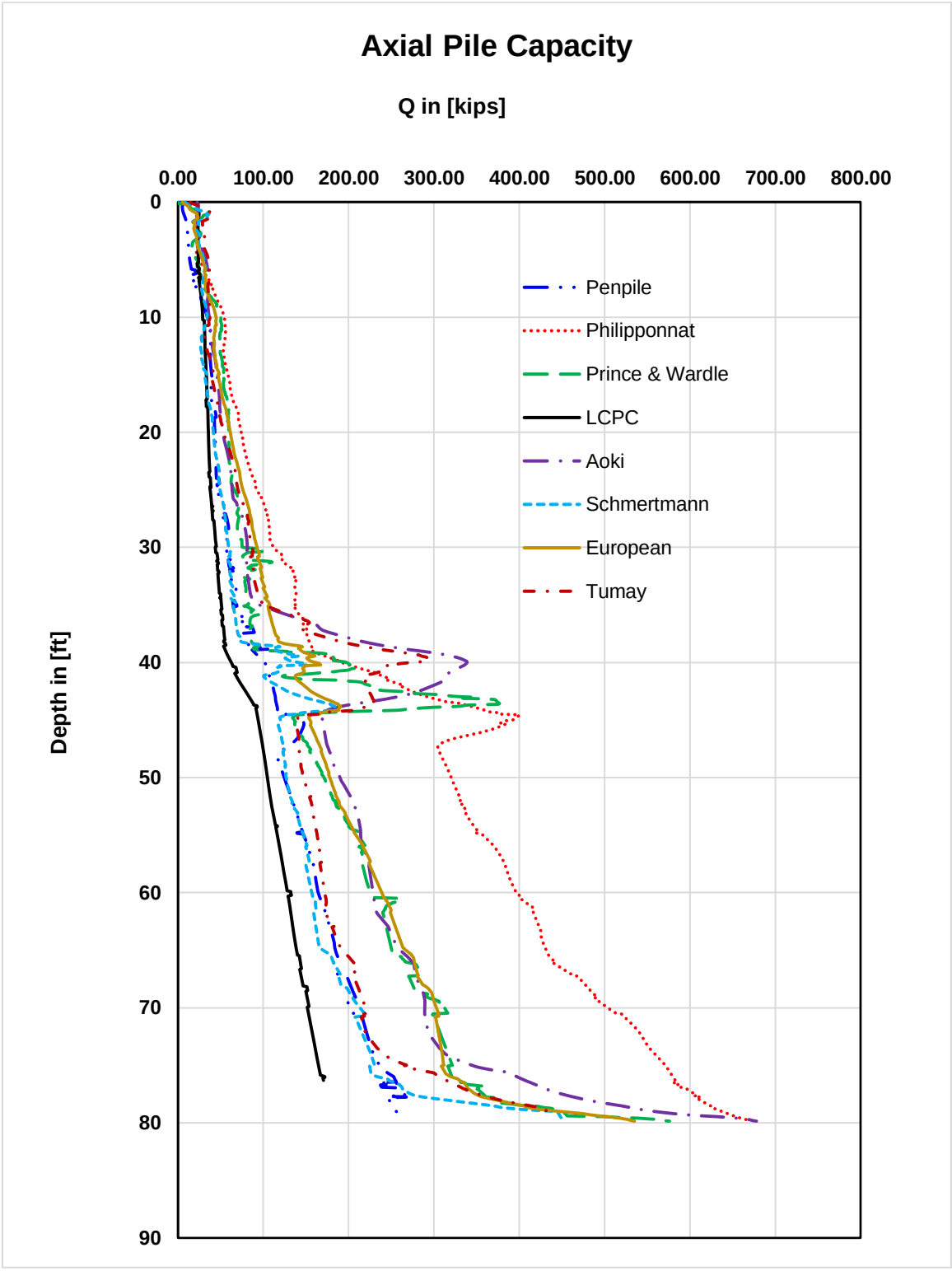

Fig. 4.4 Example of total axial capacity plot generated from CPT prediction

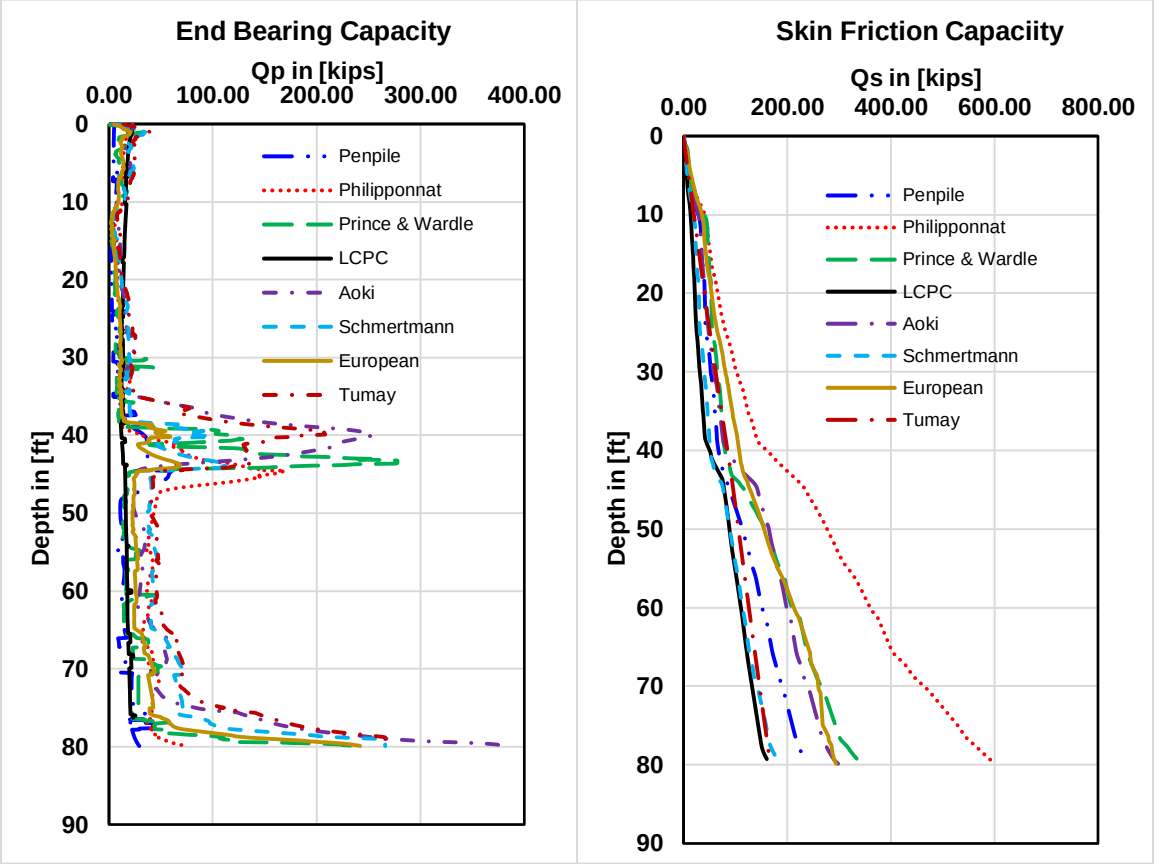

Fig. 4.5 Example of end bearing & skin friction CPT capacity plots

4.3 Dynamic Load Test Analysis

Pile load test data collected from NDOR on bridge construction projects was used for comparison and calibration of CPT prediction methods. Driving records from the PDA were selected per the procedure outlined in the methodology section 3.6. Multiple strike analysis was performed on studied pile where possible. PDA data was further analyzed by CAPWAP software for accurate ultimate load capacity determination. In addition to ultimate pile capacity, end bearing and skin friction proportions are available output. These capacities were recorded in a spreadsheet for further comparison.

4.5 Data Analysis

The following data tables contain a summary regarding the analyzed piles and CPT capacity predictions. 78 comparisons were made for initial study discussed here in after. For complete information regarding project information, driving details, and CPT end/skin capacities, refer to Appendices A&B.

Table 3.2 Pile and dynamic load test data summary.

Log ID	SN	Subst	Pile Type	Length in Place [ft]	Driving Eqn Ultimate [kips]	CW-total [kips]	CW-skin [kips]	CW-end [kips]
1	C05501305P	A1	HP12x53	45	124	163	151	12
2	S034 31644	A1	HP12x53	55	154	160	132	28
3	S034 31644	A1	HP12x53	57	176	171	147	24
4	S034 31644	A1	HP12x53	60	196	184	129	55
5	S034 31644	A2	HP12x53	45	64	75	9	66
6	S034 31644	A2	HP12x53	50	81	99	35	64
7	S034 31644	A2	HP12x53	55	131	152	132	20
8	S034 31644	A2	HP12x53	58	130	149	122	27
9	S034 31752	A1	HP12x53	34	223	251	101	150
10	S034 31752	A2	HP12x53	35	109	113	97	16
11	S034 31752	B1	HP12x53	40	259	313	3	311
12	S034 31752	B2	HP12x53	35	172	233	104	129
13	S077 09368	A1	pipe	80	393	448	273	175
14	S077 09368	A2	pipe	90	344	429	372	57
15	S077 09368	A2	pipe	92	397	450	96	354
16	S077 09368	B1	pipe	87	394	450	326	124
17	S077 09368	B2	pipe	87	382	430	269	161
18	S080 08295L	A1	pipe	32	298	452	429	23
19	S080 40436	P1	Type I	34	143	166	30	136
20	S081 08578	A1	pipe	74	173	163	134	29
21	S081 08578	A1	pipe	65	145	85	61	24
22	S081 08578	A1	pipe	70	163	98	76	22
23	S081 08578	A1	pipe	75	185	170	40	130
24	S081 08578	B2	pipe	75	91	137	89	48
25	S081 08578	B2	pipe	68	88	141	61	80
26	S081 08578	B2	pipe	72	99	116	37	79
27	S081 08578	B2	pipe	75	100	120	61	59

28	S080 40436	A1	pipe	55	125	192	141	51
29	S080 40436	A1	pipe	65	136	164	59	105
30	S080 40436	A1	pipe	75	144	133	47	86
31	S080 41341	A1	HP12x53	36	296	385	156	229
32	S080 41341	A1	HP12x53	40	402	401	118	283
33	S080 41341	A2	HP12x53	35	225	178	140	38
34	S159 01373	N3 (P3)	HP14x89	85	397	360	155	205
35	S159 01373	N2 (P2)	HP14x89	74	526	600	145	455
36	S085 0042	P1	pipe	37	71	56	13	43
37	S085 0042	P1	pipe	40	93	62	12	50
38	S085 0042	P1	pipe	42	104	71	21	50
39	S085 0042	P2	pipe	43	166	136	81	55
40	S085 0042	P2	pipe	46.5	147	138	70	68
41	S085 0042	P3	pipe	39	94	69	51	18
42	C006602905	A2	HP10x42	44.5	86	105	30	75
43	C006602905	A2	HP10x42	44	75	115	35	80
44	C006602905	A2	HP10x42	47	91	133	112	21
45	S080 43555	A1	HP12x53	45	89	153	107	46
46	S080 43555	A1	HP12x53	48	126	178	133	45
47	S080 43555	A1	HP12x53	52	145	206	130	76
48	S080 43555	A1	HP12x53	55	161	223	177	46
49	S080 43555	A2	HP12x53	40	172	186	133	53
50	S080 43555	A2	HP12x53	45	195	205	150	55
51	S080 43555	A2	HP12x53	50	214	276	227	49
52	S080 43555	A2	HP12x53	55	228	310	270	40
53	S080 43555	A2	HP12x53	60	280	388	305	83
54	S080 43555	P1	HP12x53	50	276	321	282	39
55	S080 43555	P1	HP12x53	53	327	391	317	74
56	S080 42094	A1	Pipe	42	184	180	145	35
57	S080 42094	A1	Pipe	45	174	165	99	66
58	S080 42094	A1	Pipe	50	148	152	70	82
59	S080 42094	A1	Pipe	55	205	221	109	112
60	S080 42094	A1	Pipe	60	192	199	125	74
61	S080 42094	A2	Pipe	47	230	252	136	116
62	S080 42094	A2	Pipe	50	220	255	140	115
63	S080 42094	A2	Pipe	55	238	270	188	82
64	S080 42094	A2	Pipe	60	256	282	124	158
65	S080 42094	P1	Type I	40	172	175	43	132
66	S080 42094	P1	Type I	45	206	188	71	117
67	S080 42094	P1	Type I	50	248	194	81	113
68	S080 42094	P1	Type I	55	191	159	93	66

69	S080 42094	P1	Type I	60	242	200	107	93
70	S080 44207	P4	HP12x53	55	176	170	138	32
71	S080 44207	P4	HP12x53	60	218	206	160	46
72	S080 44207	P4	HP12x53	65	238	236	149	87
73	S080 44207	P4	HP12x53	70	256	275	206	69
74	S080 44207	P4	HP12x53	73	240	314	241	73
75	S080 44207	P4	HP12x53	52	163	169	94	75
76	S080 44207	P4	HP12x53	57	162	170	147	23
77	S080 44207	P4	HP12x53	63	204	215	175	40
78	S080 44207	P4	HP12x53	69	263	332	237	95

Table 3.3 CPT prediction for total capacity.

CPT Methods Key 1) Penpile 2) Philipponnat 3) Prince & Wardle 4) LCPC 5) Aoki & De Alencar 6) Schmertmann 7) European 8) Tumay & Fakhroo

Log ID	CPT Depth [ft]	CW-total [kips]	CPT Method -Total Capacity [kips]							
			1	2	3	4	5	6	7	8
1	29.9	**163**	129.3	302.8	279.5	176.7	366.5	374.2	247.0	288.3
2	46.1	**160**	106.7	377.1	175.2	120.1	223.0	173.9	193.3	229.1
3	47.8	**171**	130.1	414.8	197.2	140.9	232.9	188.1	201.2	232.9
4	50.3	**184**	149.1	462.9	227.7	143.0	245.0	206.0	214.4	241.9
5	40.1	**75**	133.6	365.5	238.6	147.8	258.1	206.8	200.5	210.3
6	44.6	**99**	166.1	452.2	291.8	161.8	296.0	241.9	239.2	226.1
7	49.1	**152**	181.3	515.4	343.3	145.8	317.6	267.9	270.9	235.2
8	51.7	**149**	210.7	567.9	368.0	149.5	344.7	279.8	292.0	251.4
9	29.2	**251**	130.3	380.4	292.4	231.0	408.7	457.2	272.2	320.1
10	34.0	**113**	219.2	523.4	412.5	298.6	493.2	590.2	344.8	430.6
11	31.0	**264**	96.4	260.3	215.5	148.0	388.5	352.1	356.4	237.0
12	33.8	**264**	128.3	361.6	288.3	189.7	456.4	403.6	497.1	290.6
13	78.5	**448**	251.4	674.4	402.8	281.5	522.0	430.3	216.5	409.6
14	84.0	**429**	328.5	884.3	684.5	443.4	708.7	466.8	520.0	451.1
15	86.0	**450**	348.9	927.3	662.2	455.3	736.5	494.3	535.6	456.2
16	81.7	**450**	265.0	740.6	576.6	306.7	690.5	515.2	273.9	433.5
17	82.0	**430**	300.1	801.1	575.6	386.4	674.1	446.8	505.4	446.3
18	18.0	**345**	189.8	547.5	446.3	452.5	694.8	440.4	259.7	318.4
19	66.3	**166**	194.6	424.8	391.7	254.8	305.1	268.2	212.3	302.8
20	69.8	**85**	117.7	323.2	145.1	90.2	165.0	110.5	217.1	179.5
21	65.8	**98**	139.4	357.8	177.4	100.1	202.5	119.0	238.0	196.9

22	69.5	**163**	152.2	404.7	245.9	109.3	223.6	139.5	266.4	218.0
23	70.8	**170**	170.1	423.8	227.9	115.8	244.1	146.8	272.2	229.1
24	81.0	**141**	348.5	617.6	532.0	192.7	521.3	313.5	368.8	330.7
25	85.0	**116**	384.7	757.6	616.5	225.3	468.9	379.7	405.3	318.0
26	86.0	**137**	387.1	754.6	661.1	233.1	503.8	422.0	442.2	343.8
27	86.5	**120**	390.2	772.1	677.6	235.6	515.3	433.0	453.0	352.4
28	63.3	**192**	228.0	586.1	352.0	192.5	341.5	217.8	230.4	227.1
29	73.3	**164**	268.7	677.2	399.9	214.0	385.9	254.8	280.9	267.6
30	83.3	**133**	312.2	769.0	464.9	238.2	449.7	310.1	345.5	325.0
31	36.0	**385**	186.9	288.4	459.2	72.2	513.6	366.8	281.5	417.7
32	40.0	**401**	245.9	457.3	433.0	131.1	458.4	501.1	376.6	429.8
33	34.0	**178**	134.1	278.2	339.7	78.5	452.1	402.1	318.4	423.8
34	83.0	**360**	216.9	687.6	345.8	177.9	521.0	419.0	392.5	559.1
35	74.0	**600**	172.1	530.0	420.2	120.6	552.5	487.5	384.3	610.0
36	46.1	**56**	109.8	167.1	125.4	63.2	101.3	106.0	122.6	127.1
37	49.1	**62**	120.7	186.2	138.1	68.3	118.1	112.9	135.0	140.9
38	51.1	**71**	128.0	196.9	143.3	71.8	127.7	124.1	146.9	147.7
39	52.5	**136**	127.9	209.3	182.8	75.3	135.7	130.2	156.5	156.0
40	56.0	**138**	153.3	247.0	184.6	88.2	174.3	176.0	198.5	191.7
41	55.0	**69**	115.2	193.8	132.1	77.3	121.0	123.1	149.5	156.2
42	45.0	**105**	73.3	192.0	171.1	65.7	340.4	240.7	227.2	251.9
43	45.5	**115**	76.7	206.3	178.7	70.4	354.7	244.1	250.2	253.5
44	47.5	**133**	93.3	276.4	209.4	85.1	400.5	254.4	310.9	259.4
45	56.7	**153**	216.0	436.1	323.4	106.2	244.5	232.1	317.7	200.0
46	59.7	**178**	237.8	487.7	358.0	109.5	272.9	251.8	348.4	214.6
47	62.7	**206**	261.2	539.8	408.5	122.0	313.5	293.1	392.3	243.6
48	65.7	**223**	288.4	612.0	478.0	130.2	343.5	329.5	428.3	266.1
49	51.0	**186**	200.0	389.4	305.1	98.8	221.1	219.4	281.4	207.4
50	56.0	**205**	249.6	485.0	382.7	112.0	316.0	260.0	337.1	261.3
51	61.0	**276**	294.6	614.6	467.2	128.9	340.4	329.1	387.1	276.4
52	66.0	**310**	324.3	691.1	558.7	143.4	387.6	385.7	441.5	312.1
53	71.0	**388**	364.2	795.0	652.0	157.3	447.9	432.3	495.2	357.2
54	69.1	**321**	317.7	705.6	575.1	140.1	392.8	393.6	436.5	310.3
55	72.1	**391**	343.9	767.0	629.3	148.6	440.4	418.0	467.5	345.4
56	46.0	**180**	184.0	460.0	297.5	153.0	357.8	193.9	181.8	284.0
57	49.0	**165**	192.3	499.7	349.7	162.3	341.6	190.8	183.3	232.7
58	54.0	**152**	232.1	530.8	291.9	176.9	436.5	242.4	229.1	297.9
59	59.0	**221**	291.6	672.1	366.5	202.9	506.0	280.2	241.0	328.9
60	64.0	**199**	284.7	759.3	494.3	243.8	532.6	400.2	313.7	363.5
61	50.4	**252**	242.3	598.6	432.0	178.5	497.1	410.7	373.1	443.0
62	53.4	**255**	253.0	663.6	461.3	201.5	491.3	344.9	339.8	427.4
63	58.4	**270**	249.3	711.5	410.4	236.0	407.4	231.7	278.3	270.7

64	63.4	**282**	267.9	732.3	409.4	248.4	466.0	236.4	293.5	287.9
65	48.5	**175**	216.7	588.1	397.9	218.6	473.0	409.0	331.8	421.9
66	52.5	**188**	231.5	597.5	252.1	254.8	410.2	212.2	181.6	265.4
67	57.5	**194**	245.0	710.8	406.2	285.6	480.8	328.0	240.6	312.1
68	62.5	**159**	287.0	793.4	568.7	326.0	595.5	459.8	314.5	387.4
69	68.5	**200**	315.7	914.9	430.3	367.5	583.1	338.5	320.5	350.9
70	62.5	**170**	286.4	753.0	543.4	206.3	497.7	425.9	297.6	306.2
71	67.5	**206**	327.3	842.7	552.1	208.3	512.7	416.1	285.8	289.8
72	72.5	**236**	339.4	931.2	615.1	225.7	556.6	489.5	320.5	335.3
73	77.5	**275**	365.3	1028.4	649.0	238.0	602.2	533.1	339.8	377.3
74	80.5	**314**	383.1	1089.1	683.2	246.4	632.6	548.6	343.4	392.4
75	59.5	**169**	287.3	703.0	472.6	195.3	478.8	408.7	282.8	310.4
76	64.5	**170**	299.8	797.4	558.3	211.9	489.1	431.5	297.9	295.2
77	70.5	**215**	325.9	883.8	595.4	220.4	542.8	466.2	311.3	317.3
78	76.5	**332**	359.8	1008.5	644.8	235.5	592.1	526.7	337.5	371.0

CHAPTER 5 DATA EVALUATION

5.1 Introduction

Evaluation of the data was conducted primarily to determined which of the CPT prediction methods most accurately determines axial capacity compared to dynamic load test data. Evaluation was conducted for total capacity, end bearing, and skin friction resistances.

The first method for comparison was calculating a direct ratio of CPT predicted capacity to PDA measured capacity. Plots of measured (PDA) and predicted (CPT) pile capacities were prepared to assess the relative accuracy of each CPT based methods. Figure 5.1 presents this data for total capacity, end bearing, and skin friction. The 45-degree linear line passing diagonally through the data points shows ideal prediction where PDA result is equal to CPT result. The dashed lines are a linear regression fit of the data points to give a better indication of relative performance.

Second, a statistical comparison was made to further understand the accuracy of each prediction method. The paired t-test was chosen for this study. The test determines the significance of the difference between the predicted (CPT) and measured (PDA) capacities. A brief background on the paired t-test is discussed in the following section.

5.2 Paired T-test

The paired t-test evaluates the difference between two dependent measurements. The paired t-test indicates measurements are taken twice on same subject (Heumann et al. 2016). The soil condition, the pile type, diameter, and depth are equivalent for any given pairs of pile capacities. Thus, the only difference is the method of analysis, specifically

PDA vs CPT measured capacity. Let $D = X - Y$ denote the difference between variable X and Y. In this case, variable X and Y represent pile capacity from a PDA and a CPT based method respectively. With this test, we will evaluate if $\mu_D = 0$, where μ_D is the mean of the difference D. The t-statistics $T(D)$ on the difference D is given by:

$$T(X,Y) = T(D) = \frac{\overline{D}}{S_D}\sqrt{n} \tag{26}$$

If the t-statistics value is closer to zero, it means the difference between the variable X and Y is small or in other words the error is small. Conversely, if the difference between datasets is large, then the variables being compared are significantly different. The p-value is commonly used to conduct a hypothesis test on the compared values. The null hypothesis is that there is no significant difference between PDA & CPT data pairs. When the p-value is less than .05 (using 95% confidence), the alternative hypothesis is accepted, meaning there is significant difference between the load test and predicted measurements. In practical terms, a p-value of .80 represents an 80% probability that the error between the two quantities is zero. Based on this concept, bar graphs were compiled to compare p-values of the eight capacity prediction methods.

5.3 Complete Dataset Analysis

Initially, the entire dataset was evaluated for the three bearing measurements discussed above. The following figures in this section present evaluation information outlined above. The CPT/PDA ratio figures offer prediction trend and relative accuracy indication. Individual data plots for each of the eight methods are shown.

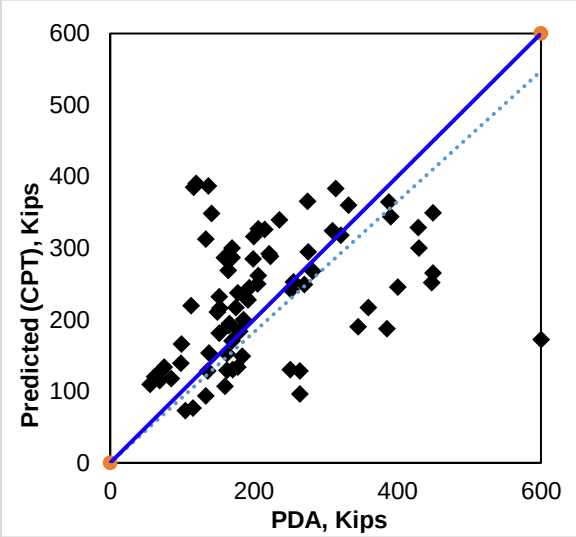

(a) Penpile

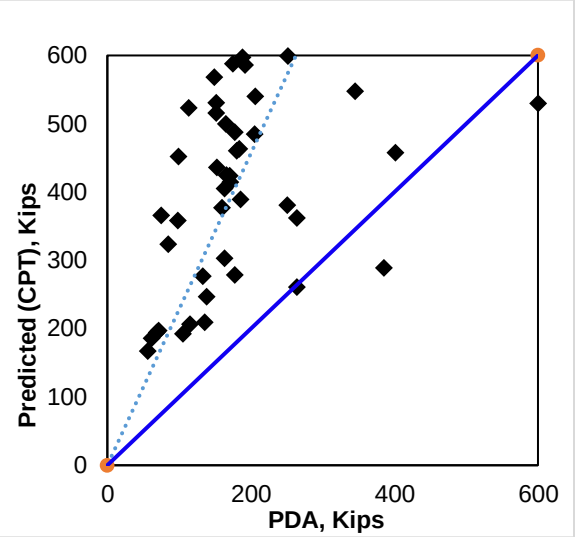

(b) Philipponnat

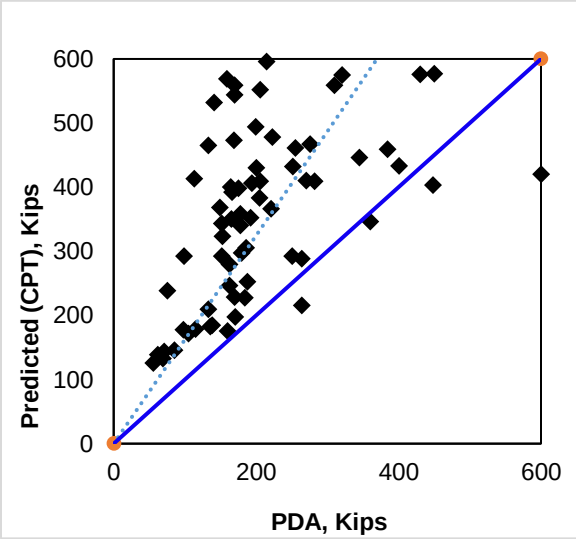

(c) Prince & Wardle

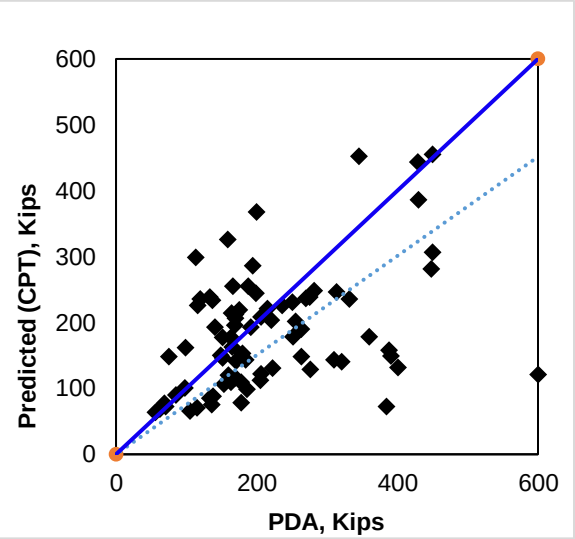

(d) LCPC

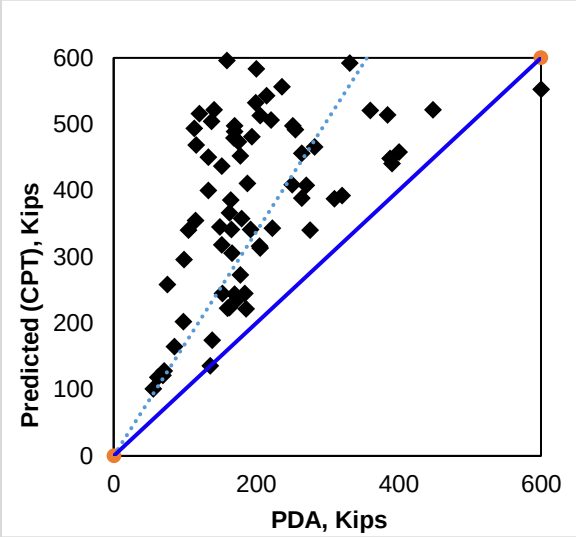

(e) Aoki

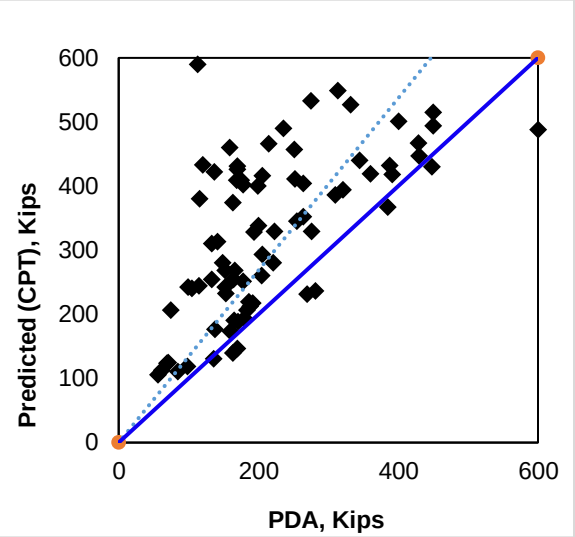

(f) Schmertmann

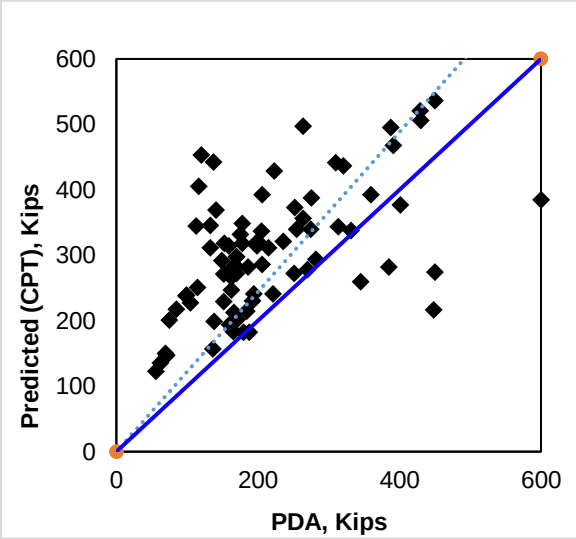

(g) European

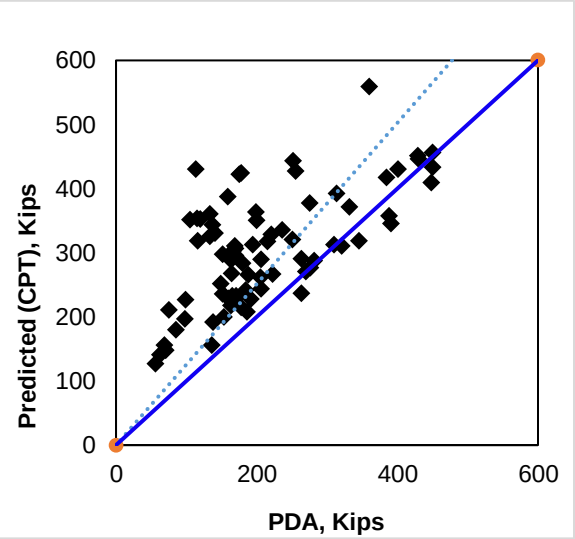

(h) Tumay & Fakhroo

Fig. 5.1 Total Capacity - PDA vs CPT methods

Total bearing capacity analysis results suggest that Penpile and LCPC methods are the most accurate CPT prediction methods. The Penpile method has an average prediction ratio of (CPT/PDA) of 1.24 while LCPC was the only method to under predict total

capacity with an average ratio of 0.97. These two methods also had the smallest standard deviation among the eight methods. Penpile gave a linear fit with the slope closest to one. In general, all of the methods appear to noticeably overestimate total capacity, evidenced by the majority of data points and dashed linear fit line falling above the 1:1 line.

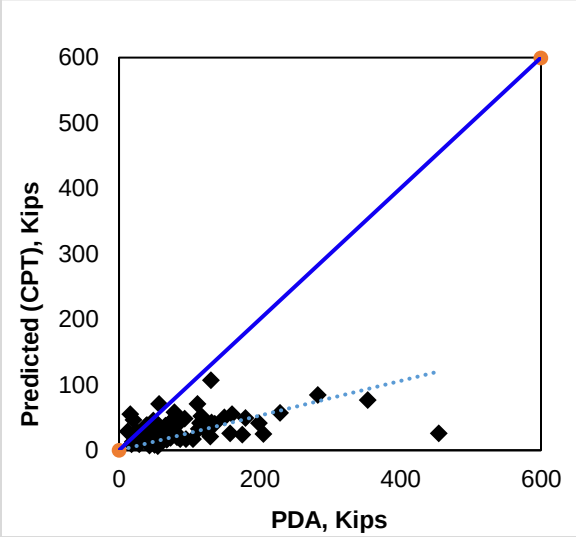

(a) Penpile

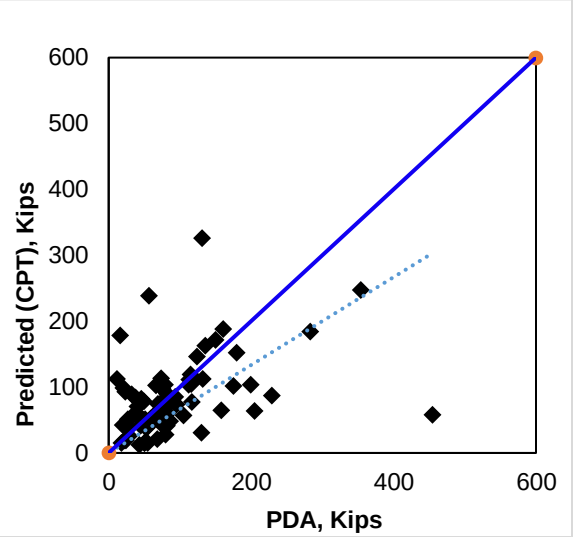

(b) Philipponnat

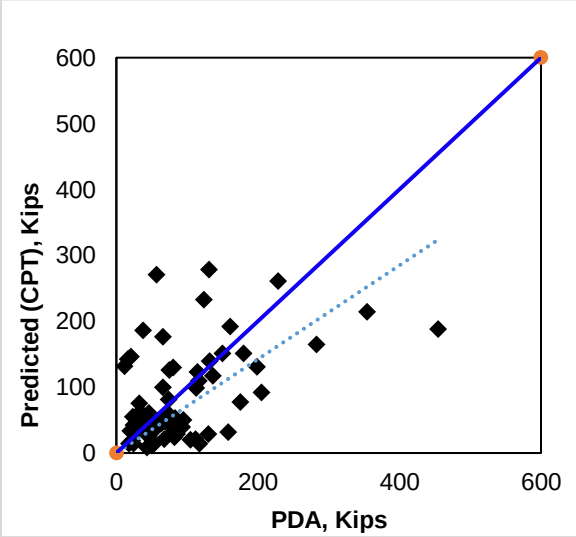

(c) Prince & Wardle

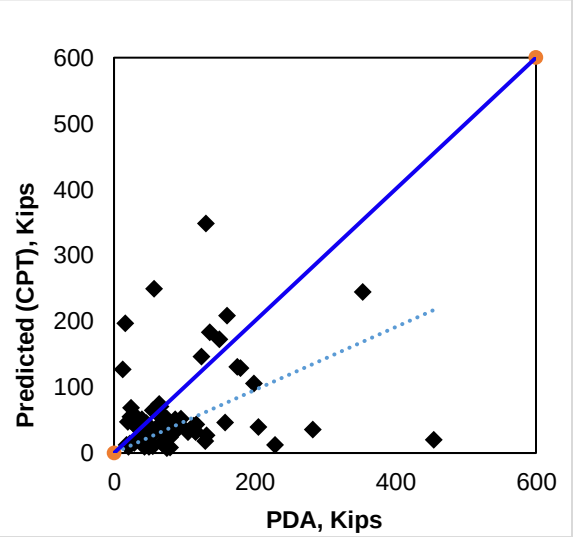

(d) LCPC

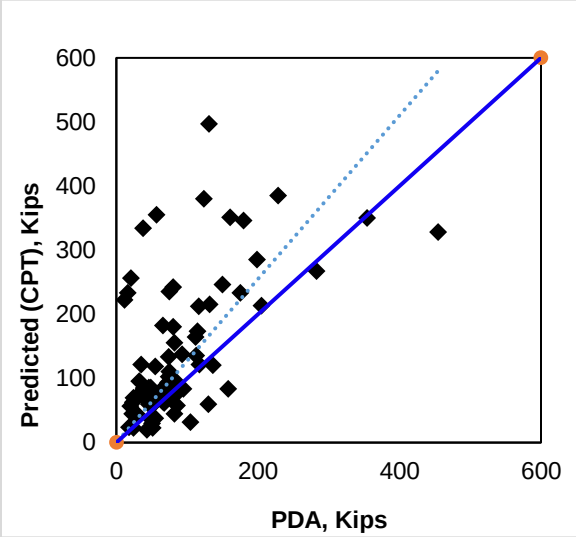

(e) Aoki

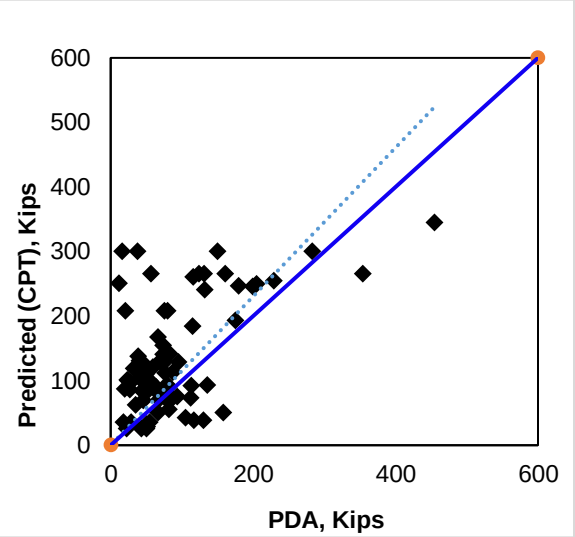

(f) Schmertmann

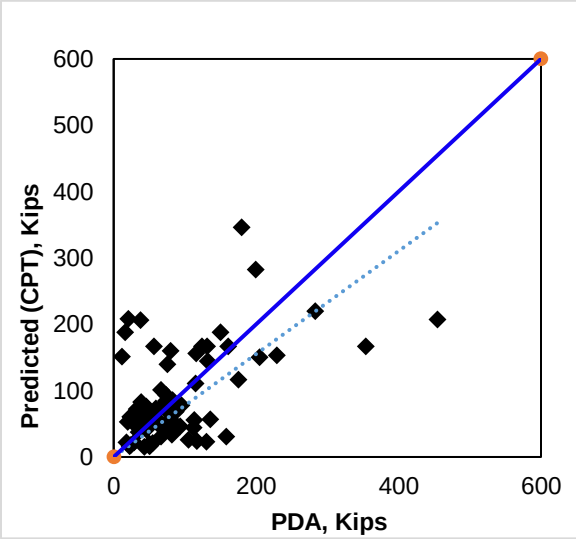

(g) European

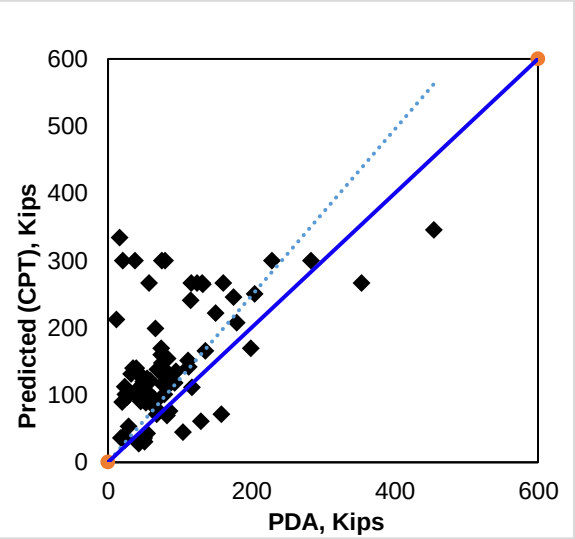

(h) Tumay & Fakhroo

Fig. 5.2 End Bearing Capacity - PDA vs CPT methods

Evaluation of end bearing capacity did not yield well defined results compared to total capacity. Based on the average prediction ratio, LCPC is the clear top performer with a 1.03 ratio. However, looking at Figure 5.2 (d), the data points do not appear to agree with this near perfect prediction. The majority of points are well below the 45° line less a few large over predictions, which is supported by LCPC having a higher standard deviation than four other methods. Additionally, the linear trendline has a slope much lower than one. Other potential quality performing methods for end bearing prediction include Philipponnat, Prince & Wardle, and European. These methods had prediction ratios of 1.35, 1.31, and 1.52 respectively. While these methods overpredict capacity more so than LCPC, standard deviation is lower, and graphical trends suggest potentially better prediction quality. Only Penpile underpredicted end bearing, with the other seven methods over predicting capacity by a factor up to about 2.5 times the PDA value.

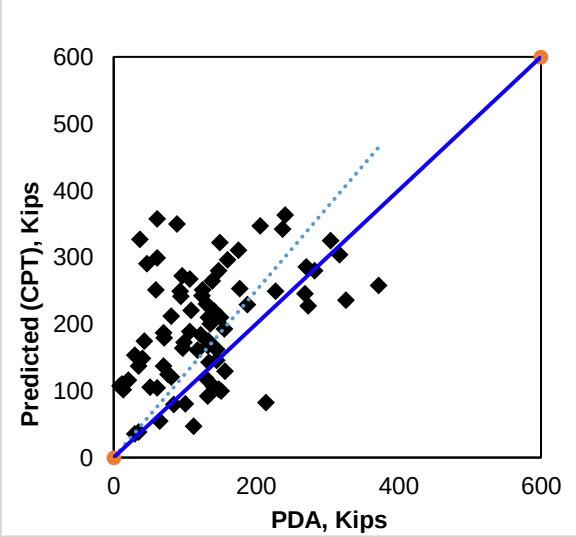

(a) Penpile

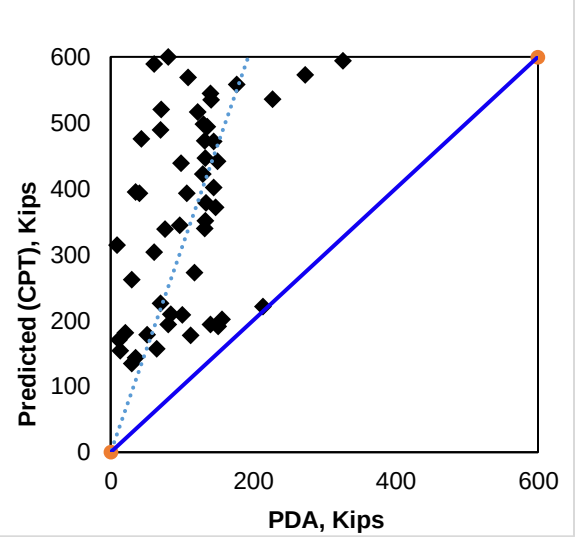

(b) Philipponnat

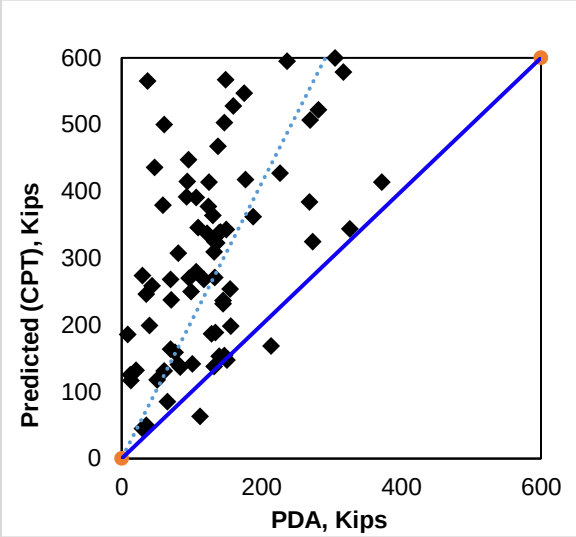

(c) Prince & Wardle

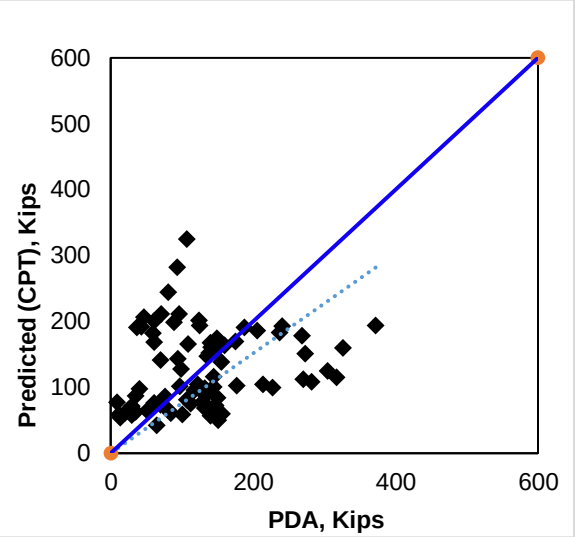

(d) LCPC

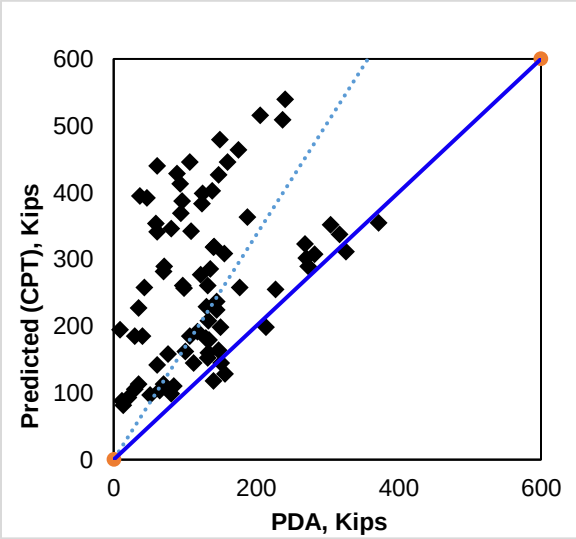

(e) Aoki

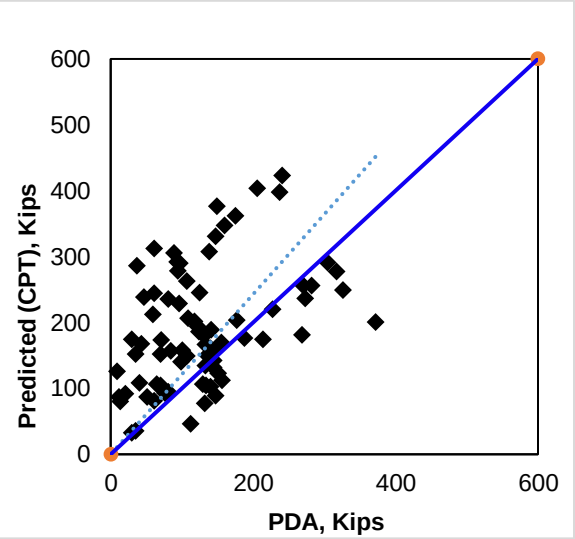

(f) Schmertmann

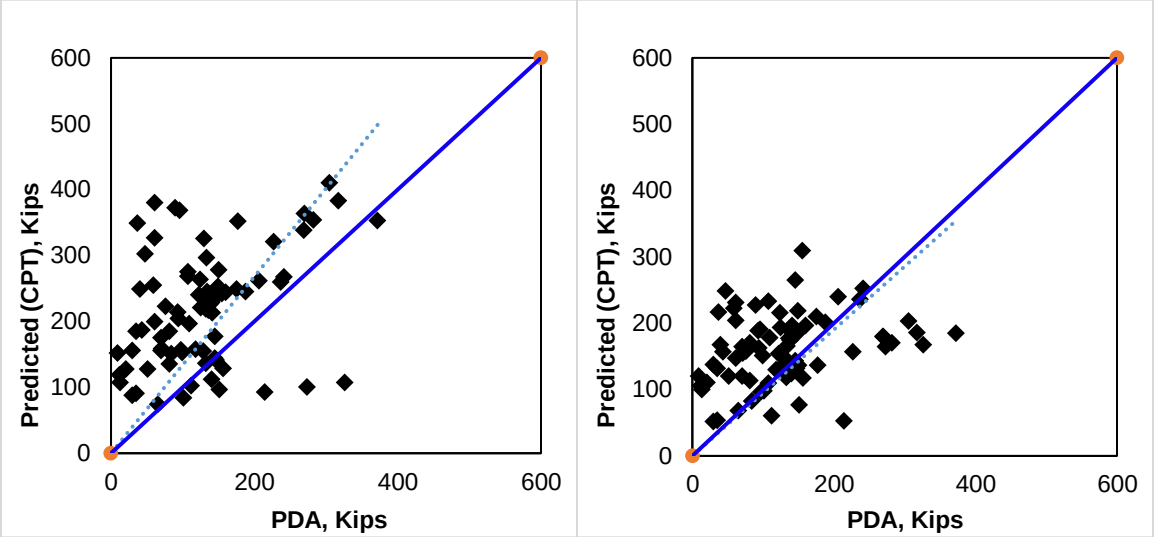

(g) European (h) Tumay & Fakhroo

Fig. 5.3 Skin Friction Capacity - PDA vs CPT methods

Every CPT method overpredicted skin friction capacity, with half in excess of 2.5 times the dynamic load test capacity. LCPC had the lowest average prediction ratio of 1.52, followed by Tumay & Fakhroo overpredicting frictional resistance by an average factor of 1.99. Standard deviation for skin friction was generally higher than deviation values for end bearing and total capacity, suggesting less accurate prediction. Again, LCPC capacity shown in Figure 5.3 (d) has a linear fit slope further from one compared to plots (h) & (f). LCPC appears to over predict at lower PDA skin friction capacities and under predict at resistance values greater than approximately 200 kips. This does not necessarily discredit LCPC prediction but the behavior should be considered.

5.4 Initial Statistical Analysis

Paired t-tests were performed on the entire set of comparisons. The goal of this statistical evaluation was to conduct hypothesis testing of PDA vs CPT axial capacity and identify statistically significant correlation. Secondly, by plotting bar charts, a relative

comparison of performance between the eight CPT capacity methods is apparent. While the null hypothesis may be rejected, some methods may still show potential for accurate capacity prediction. The higher the p- value, the higher probability that the CPT method's capacity will match the dynamic load test value. Charts for total capacity, end bearing, and skin friction were formulated once again, these are presented below.

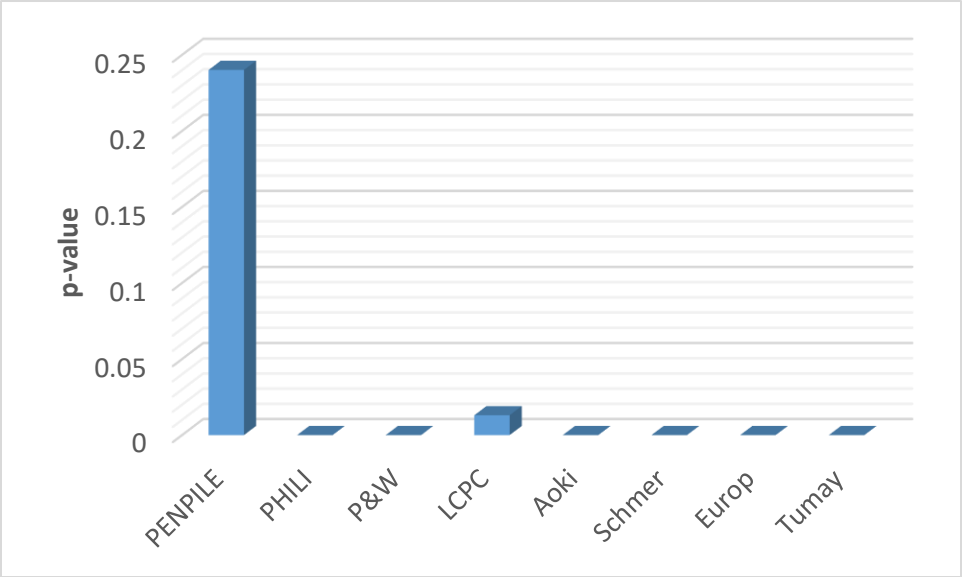

Fig. 5.4 CPT Accuracy Level – Total Capacity

Results of the t-test for total pile capacity, reported in Figure 5.4, showed that Penpile method was the best CPT based method by a large margin. The Penpile method had a p-value of 0.24 or 24%. The second most accurate method for total capacity was the LCPC method with a p-value of 0.013. This value however is below p-critical value of 0.05 for hypothesis testing. These two methods were rated the highest by the simple prediction ratio comparison, however the in reverse order. The large difference in p-values, with the LCPC value too low to reject the null hypothesis, suggests that the Penpile method more accurately predicts total pile compacity versus LCPC despite LCPC

having a CPT/PDA ratio closer to one. The other six methods did not reject the null hypothesis. Lower statistical performance by a large margin is observed, indicating poor prediction accuracy.

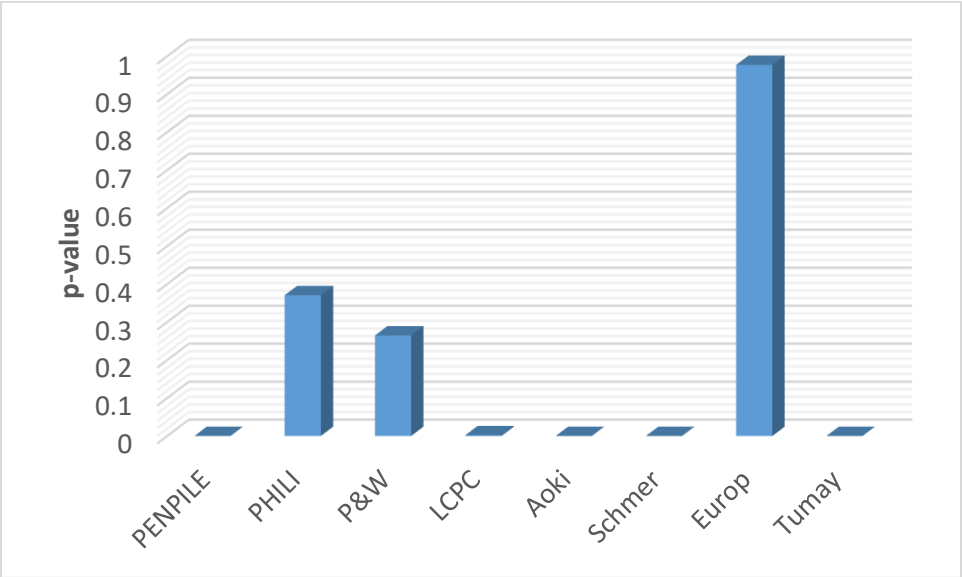

Fig. 5.5 CPT Accuracy Level – End Bearing

Statistical evaluation of end bearing prediction indicated three CPT methods rejected the null hypothesis of the t-test. European, Philipponnat, and Prince & Wardle were the top three methods, while the remaining five methods had p-values lower than p-critical. Figure 5.5 clearly shows the European method is the most accurate method (p-value 97%), followed by Philipponnat and Prince & Wardle having similar accuracy with p-values 0.37 and 0.26 respectively. The European method had the 5th ranked prediction ratio and standard deviation for end bearing capacity. Philipponnat and Prince & Wardle methods were similarly the 2nd and 3rd ranked CPT methods based on the evaluation in section 5.3. All three of these methods showed higher prediction accuracy values for end

bearing compared to the top methods for total capacity prediction, especially the European method.

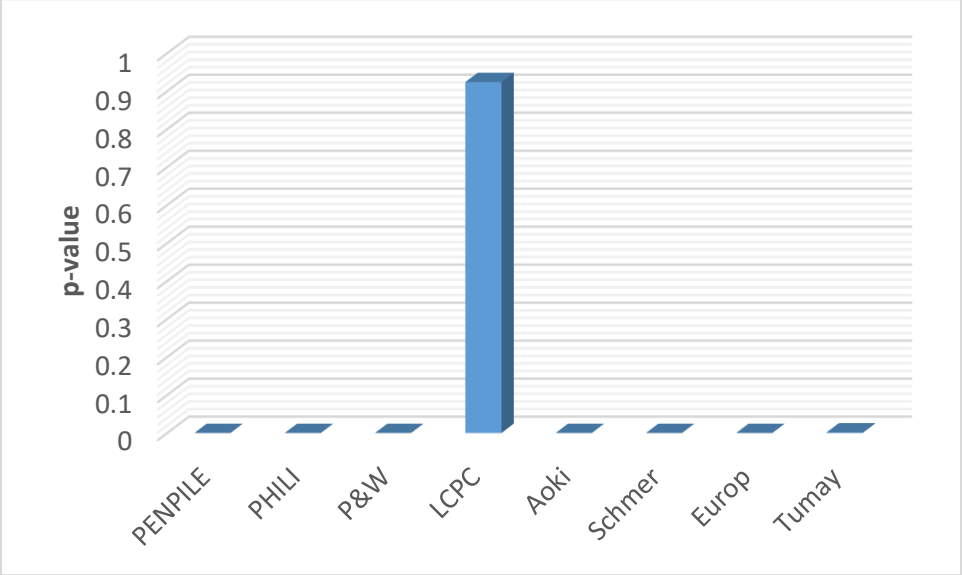

Fig. 5.6 CPT Accuracy Level – Skin Friction

The paired t-test of skin friction capacity gave results in agreement with the ratio analysis conducted in section 5.3. LCPC was the only CPT method with a p-value (0.92) greater than p-critical, indicating good accuracy. Tumay & Fakhroo which ranked 2nd by the previous evaluation, also finished 2nd by the statistical test, however the p-value was only 0.001, well below 0.05, meaning poor accuracy. While the rest of the CPT methods strongly overpredict the skin friction resistance, visual inspection of Figure 5.3 suggests that there may be some other methods showing some potential for quality prediction based on close grouping. Further investigation into the skin friction will be discussed later in the paper in an effort to identify other viable CPT methods.

5.5 Discussion of Initial Evaluation

Sections 5.3 and 5.4 evaluated the quality of CPT based capacity prediction for 78 comparison of dynamic load test data and CPT data. Total capacity, end bearing resistance, and skin (side) friction resistance was evaluated for each comparison. The relative under prediction or over prediction of eight CPT methods was determined by calculating a CPT/PDA capacity ratio for each dataset. Most methods appeared to overpredict all three measured capacities, with skin friction being the most significant over prediction on average. Second, performance was measured on a statistical basis using the paired t-test. The p-value gave indication of the probability that the predicted CPT pile capacity would match load test information (higher p-value being more accurate). Statistical tests indicated that end bearing prediction by the CPT methods was the most accurate of the three measured quantities, with skin friction only being predicted with some accuracy by the LCPC method. Table 5.1 below summarizes the performance of the eight methods with comparison to ranking found in a similar study conducted by Abu-Farsakh and Titi (2004) for Louisiana DOT. The ranking of methods for this study shown here is based on the statistical testing only, while the Abu-Farsakh & Titi ranking is an aggregated score for total capacity only.

Table 5.1 Summary of ranking CPT methods from initial statistical evaluation

CPT method	Total Capacity	End-Bearing	Skin Friction	Abu-Farsakh & Titi (2004)
Penpile	1st	-	-	9th
Philipponnat	-	2nd	-	4th
Prince & Wardle	-	3rd	-	7th
LCPC	2nd	-	1st	1st
Aoki & de Alencar	-	-	-	5th
Schmertmann	-	-	-	5th
European	-	1st	-	1st
Tumay & Fakhroo	-	-	2nd	8th

The table above indicates agreement with previous study that LCPC should be a quality prediction method, which was found to be the case for total capacity and skin friction. Additionally, the European CPT method was the top performer for end bearing prediction, again in accordance with LTRC's study. Conversely, Penpile, Philipponnat, and Prince & Wardle methods demonstrated accurate prediction in some instances despite lesser ranking found by LTRC.

The lack of a clearly most accurate CPT methods and discrepancy between this study and previous work by LRTC motivated further investigation into performance assessment. Different methods showing categorically varying accuracy also suggests that perhaps a hybrid CPT prediction method may be a viable approach to increase prediction quality for Nebraska pile and soil conditions. Possible causes for the discrepancies in results are likely found in differences in regional soils and pile types investigated.

5.6 Criterion Based Evaluation

After initial evaluation of the eight CPT methods discussed in section 5.3 and 5.4, the results indicated that the prediction methods demonstrated accuracy for some comparisons, but not on a consistent basis. Thus, bearing resistance mechanism was taken into further consideration. Comparisons were separated by dominant bearing type, specifically, end bearing or skin friction resistance controlled pile. While all pile in the real world experience a combination of resistance, an effort was made to practically separate based on pile type. Of course, soil bearing strata is also an important consideration. Determining end bearing in firm IGM or rock formations is fairly straight forward. Conversely, determining unit skin friction along the pile shaft and identifying the most prominent contributing layers is difficult and often varies even within a single substructure's pile group. A simplified approach was the first step to identify bearing type. In conjunction with NDOR classification, all HP piles were considered end bearing controlled pile. Steel pipe and prestressed concrete pile were considered to obtain the majority of their capacity from skin friction.

Once again CPT/PDA prediction ratio, standard deviation, and t-test statistical analysis was performed on the entire 78 comparison pairs. Analysis was initially sorted by individual pile type. However due to sample size and comparable findings discussed here in after, piles were categorized into simply end bearing or skin friction piles. The distribution of sampled projects resulted in a sample population of 40 end bearing pile and 38 skin friction pile comparisons. Once again total capacity, end bearing capacity, and skin friction capacity were evaluated. This sorting led to 6 categories for CPT prediction accuracy evaluation.

5.7 Sorted Ratio Analysis

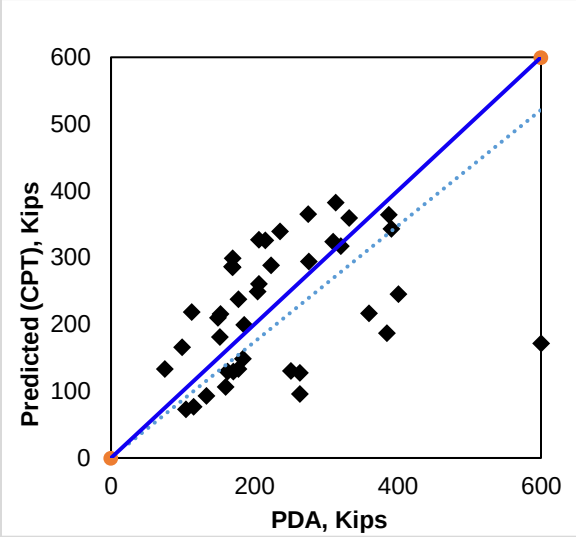

(a) Penpile

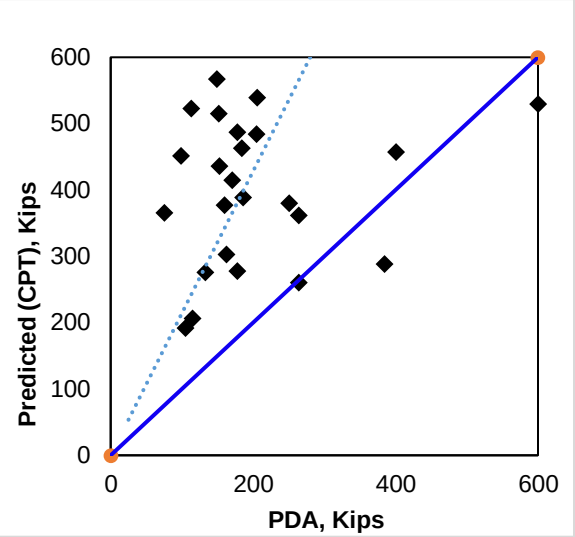

(b) Philipponnat

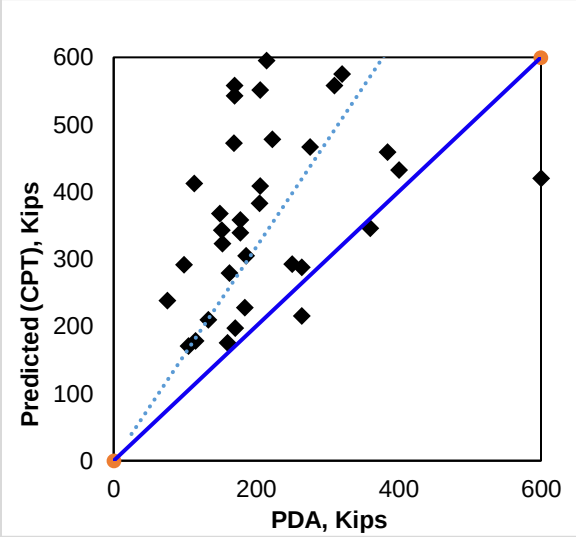

(c) Prince & Wardle

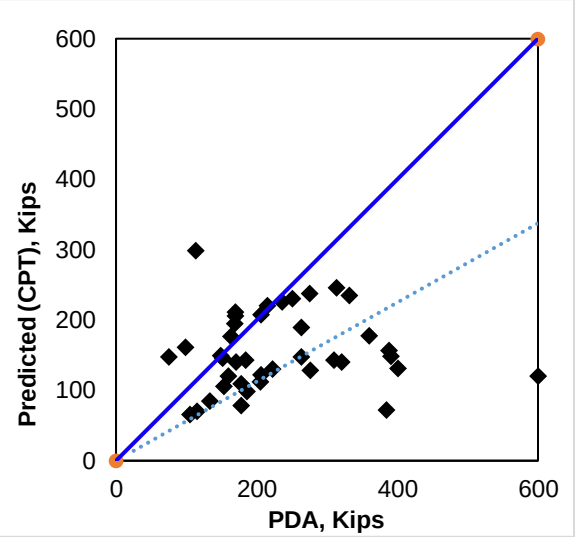

(d) LCPC

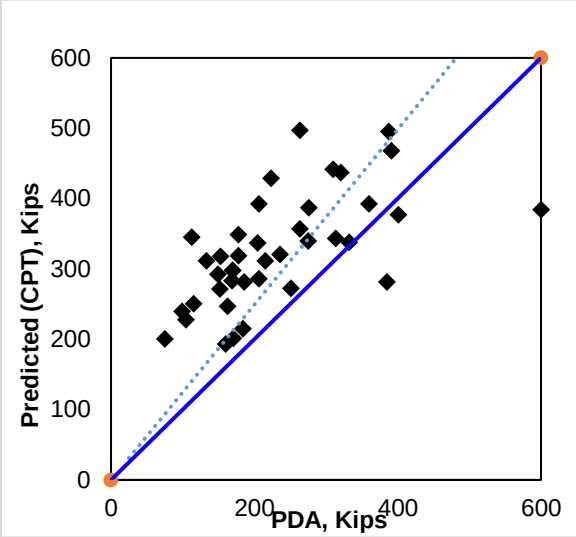

(e) Aoki

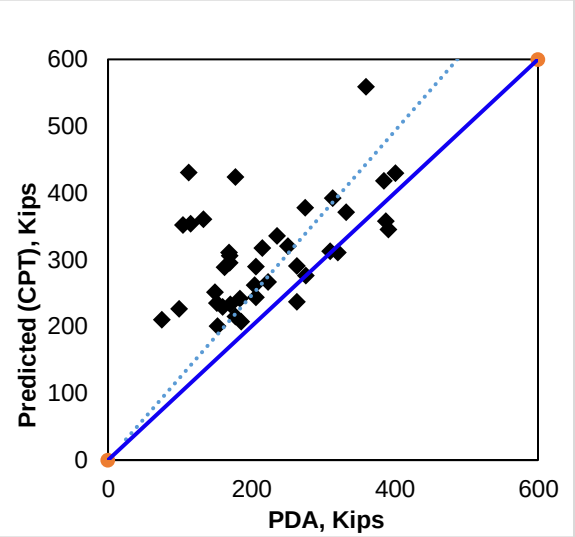

(f) Schmertmann

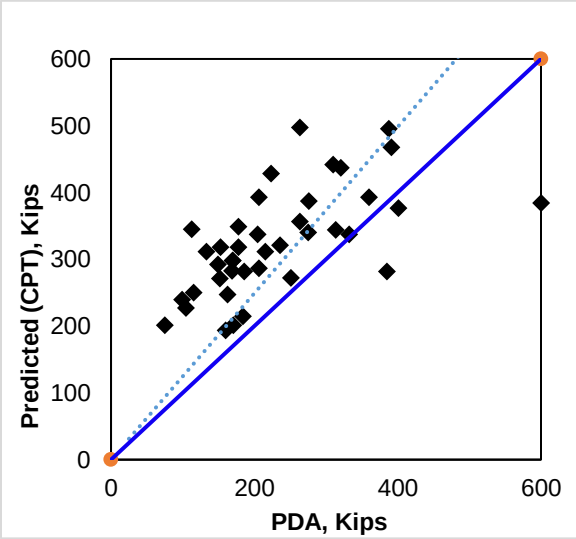

(g) European

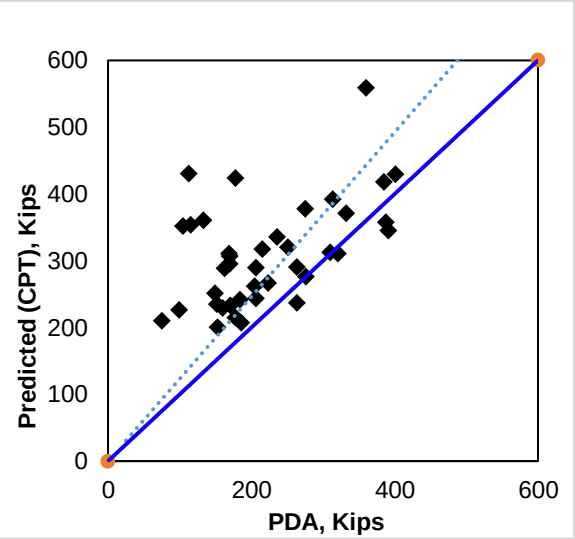

(h) Tumay & Fakhroo

Fig. 5.7 End Bearing Pile - Total Capacity - PDA vs CPT methods

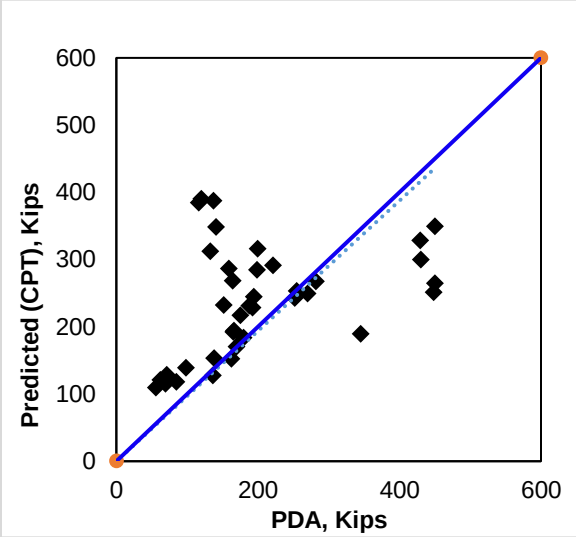

(a) Penpile

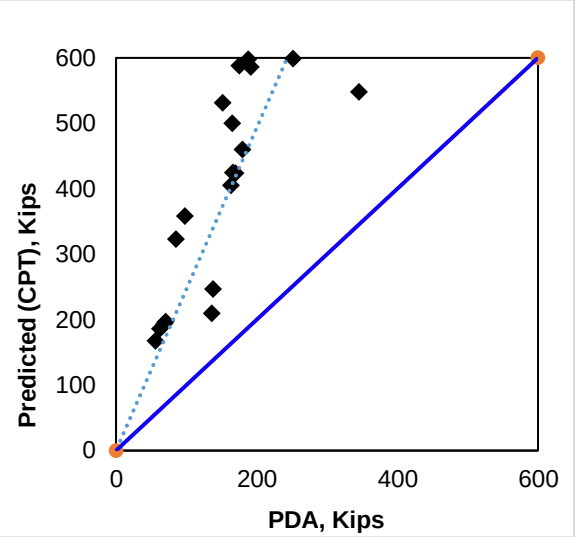

(b) Philipponnat

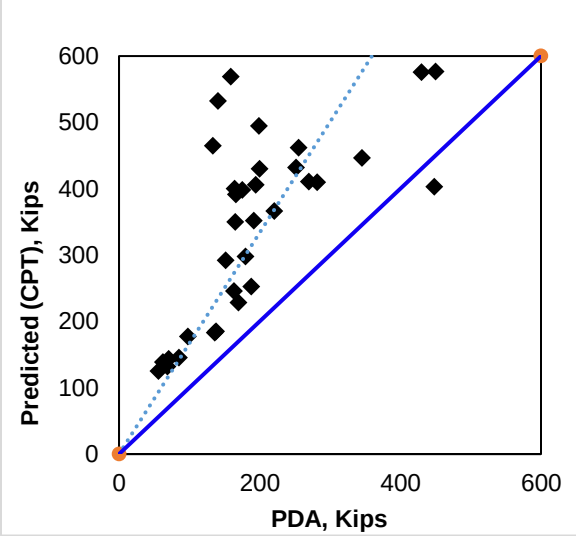

(c) Prince & Wardle

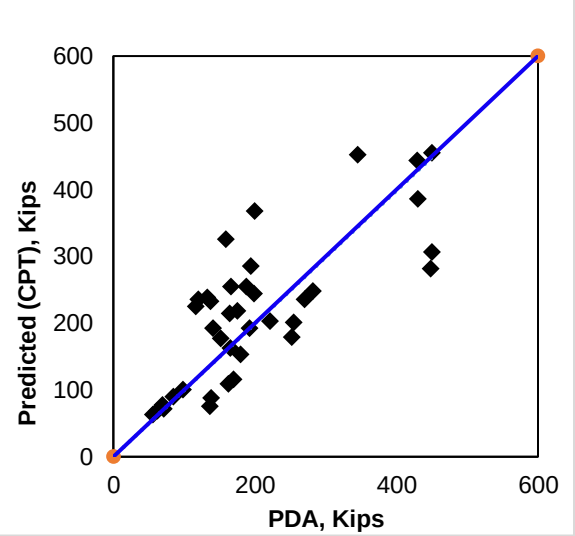

(d) LCPC

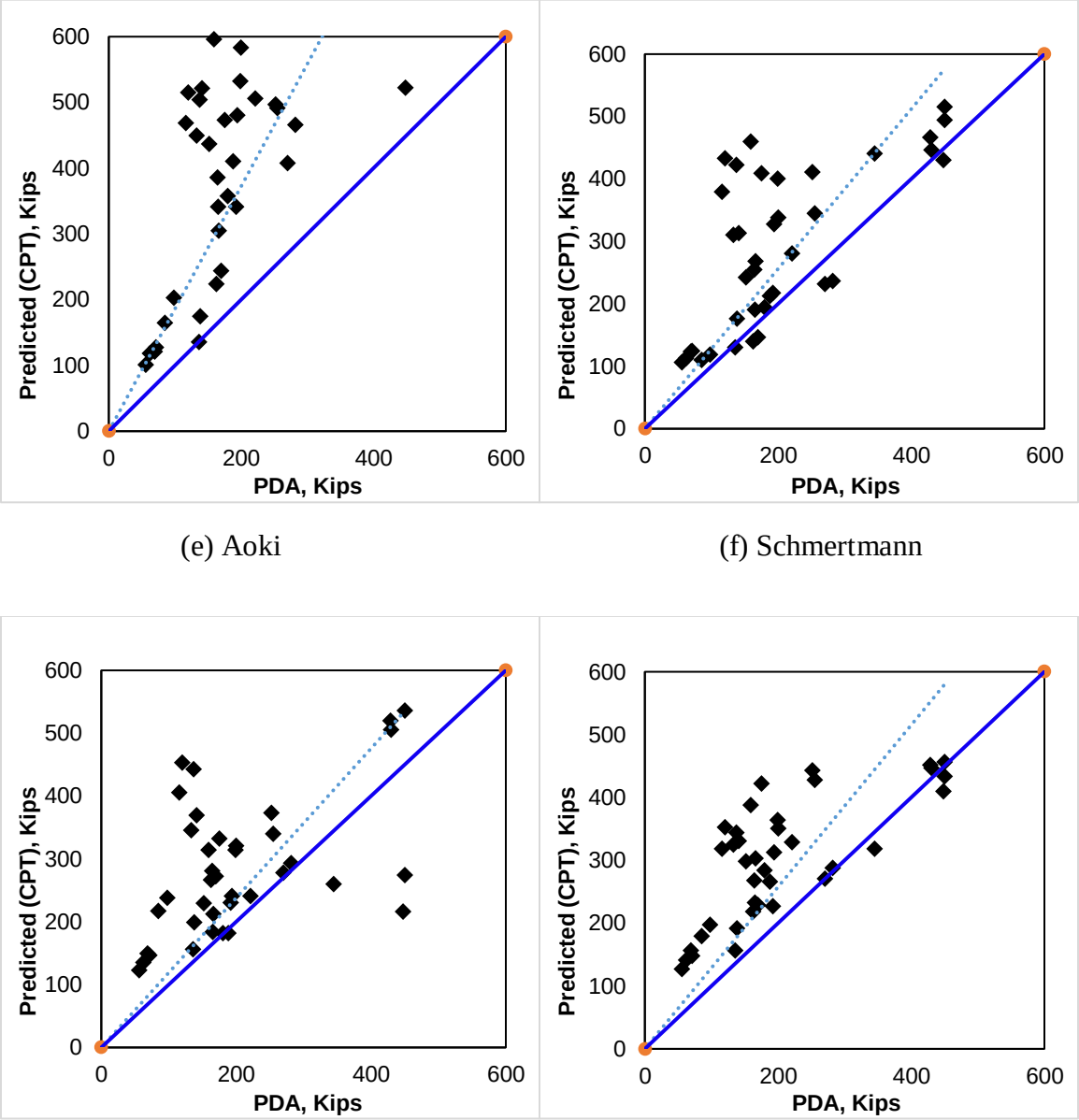

(e) Aoki (f) Schmertmann

(g) European (h) Tumay & Fakhroo

Fig. 5.8 Skin Friction Pile - Total Capacity - PDA vs CPT methods

Total bearing capacity analysis yielded similar results to the unsorted evaluation. In general methods showed overprediction for total capacity except for LCPC method. There was a noticeable shift in prediction ratio between end bearing versus friction piles. End bearing CPT/PDA ratios decreased for all eight methods, while skin friction pile

prediction ratios generally increased. This evidence points to more significant over prediction of skin friction piles, and possibly the unit skin friction in general. For the case of end bearing piles, the top two methods were once again Penpile and LCPC methods, with ratios of 1.08 and 0.80 respectively. Friction pile results showed the same two methods with the best accuracy, however in this instance LCPC had a 1.15 ratio while Penpile was second with 1.41. Standard deviation decreased by at least 20% for both Penpile and LCPC methods for end bearing pile but increased about 10% for skin friction pile. Such behavior indicates the methods predicted total capacity more reliably for HP pile compared to either pipe or concrete pile. Tumay & Fakhroo, and European methods showed reasonable ratios consistently around 1.60 for all total capacity predictions. Standard deviations improved significantly for European in end bearing pile while Tumay & Fakhroo showed deviation improvement only for friction piles.

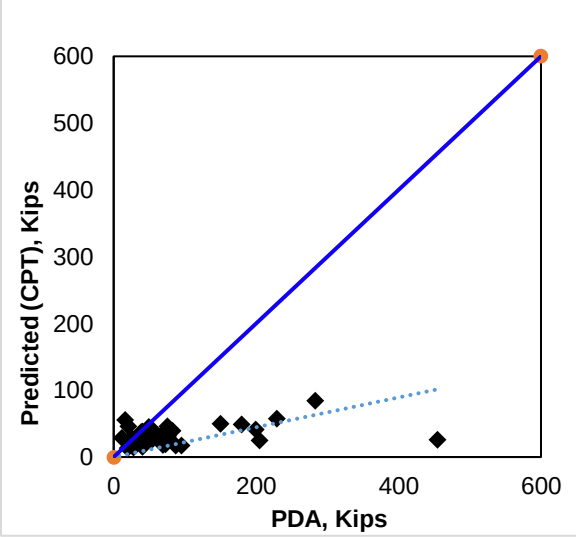

(a) Penpile

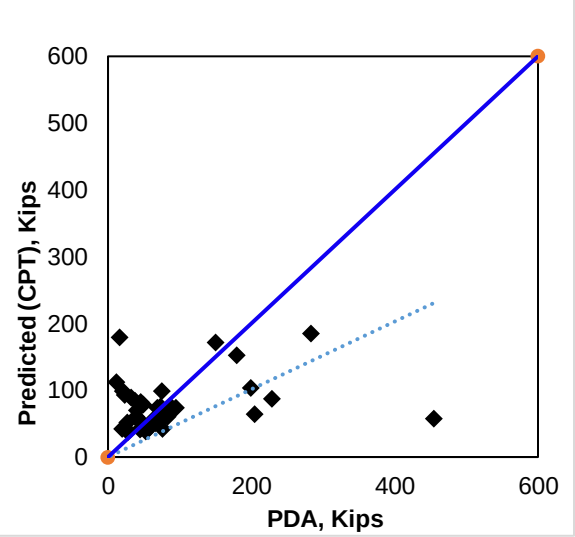

(b) Philipponnat

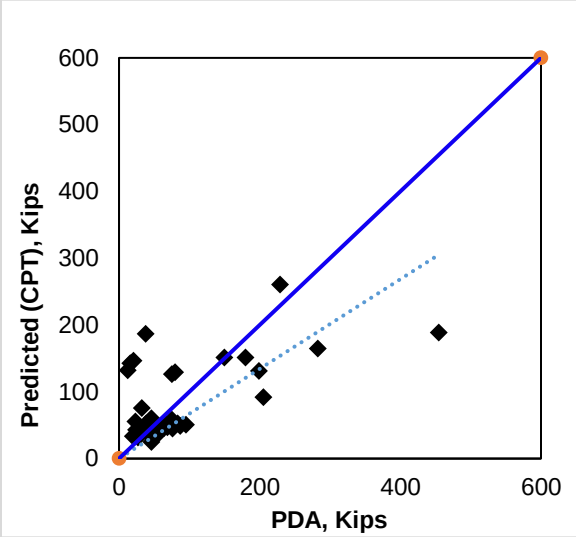

(c) Prince & Wardle

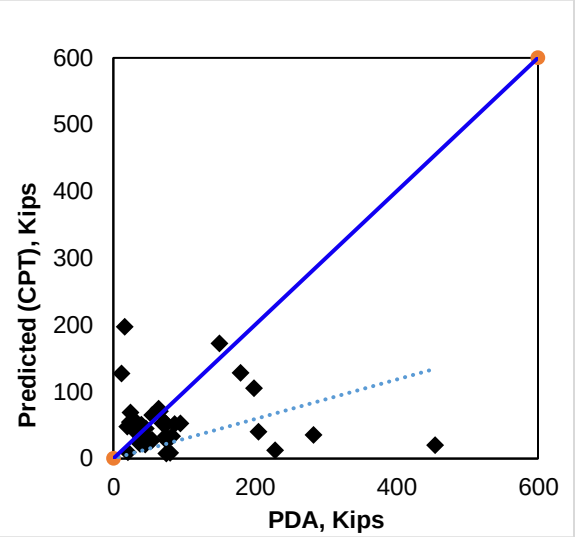

(d) LCPC

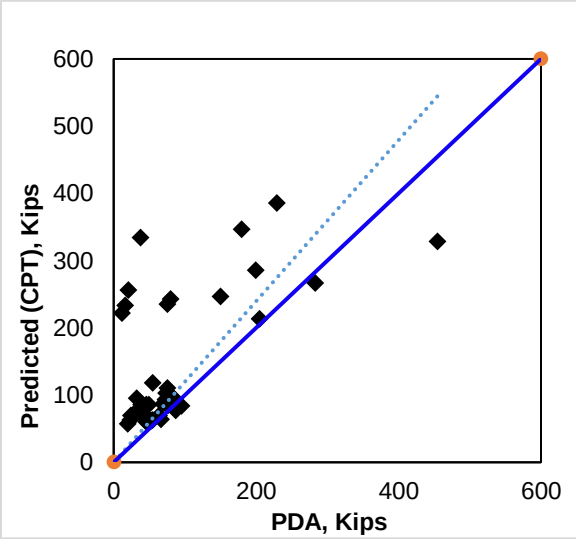

(e) Aoki

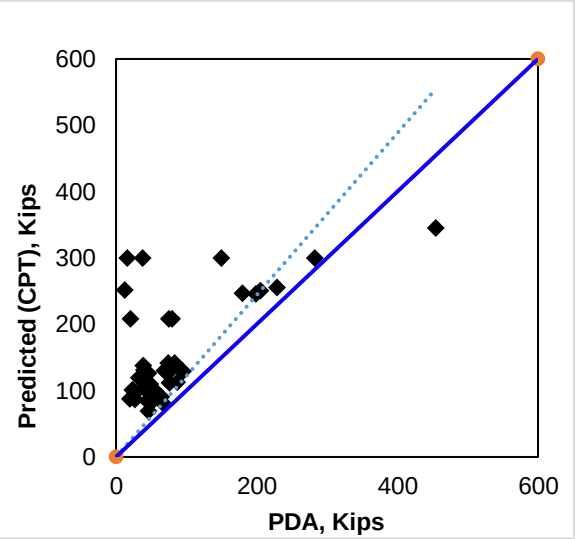

(f) Schmertmann

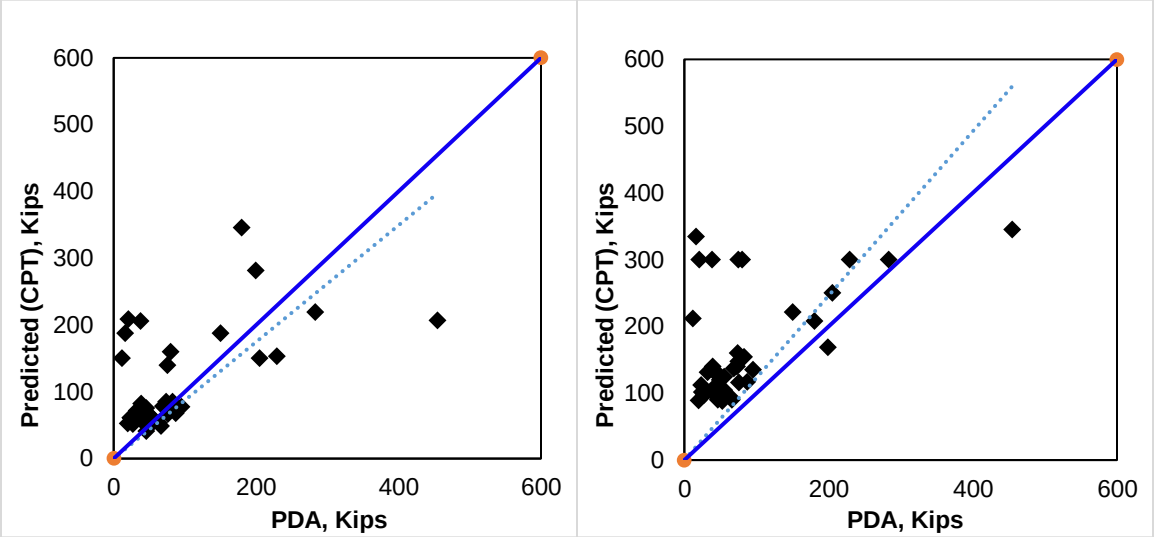

(g) European (h) Tumay & Fakhroo

Fig. 5.8 End Bearing Pile – End Bearing Capacity - PDA vs CPT methods

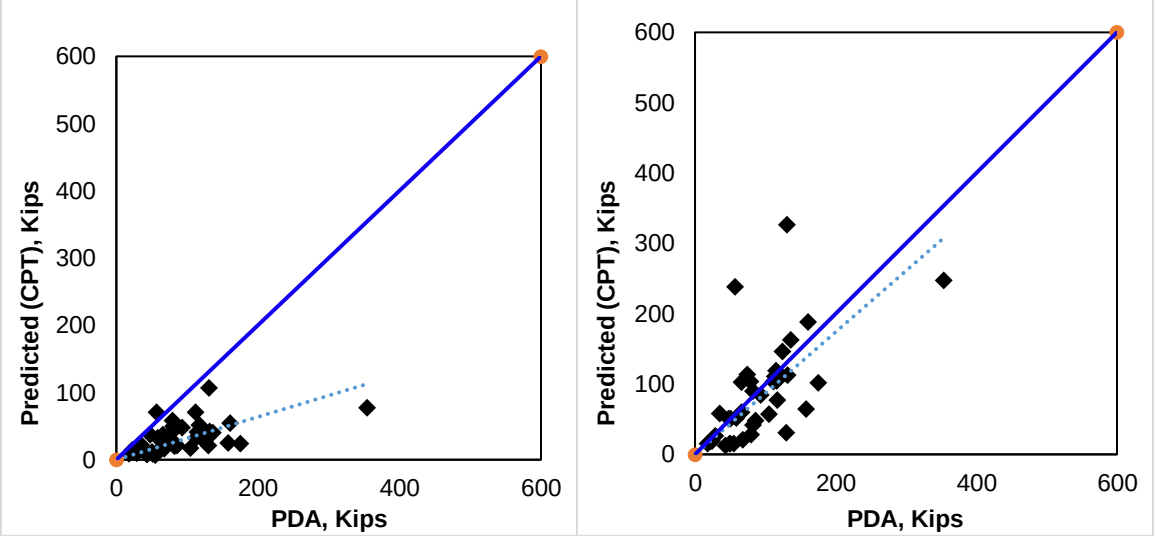

(a) Penpile (b) Philipponnat

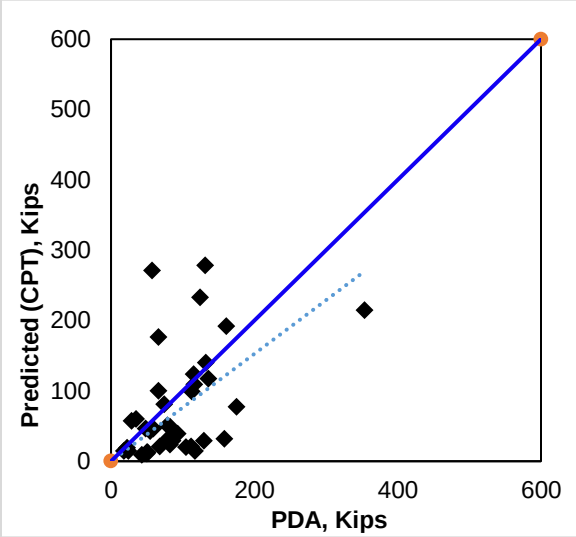

(c) Prince & Wardle

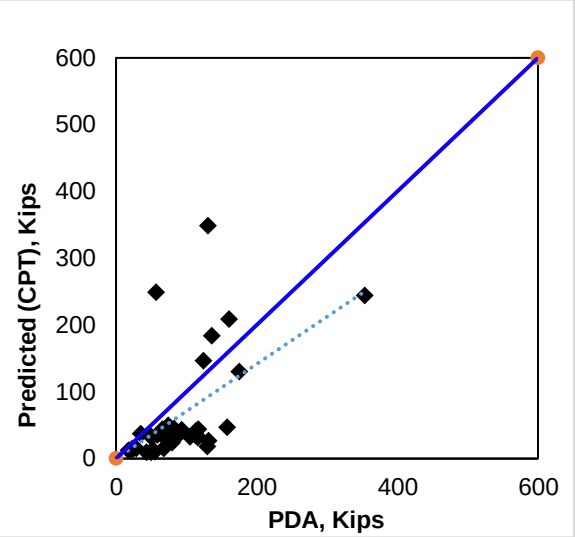

(d) LCPC

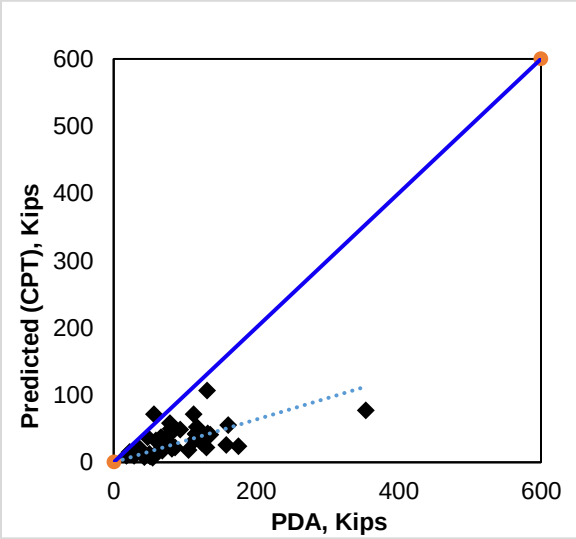

(e) Aoki

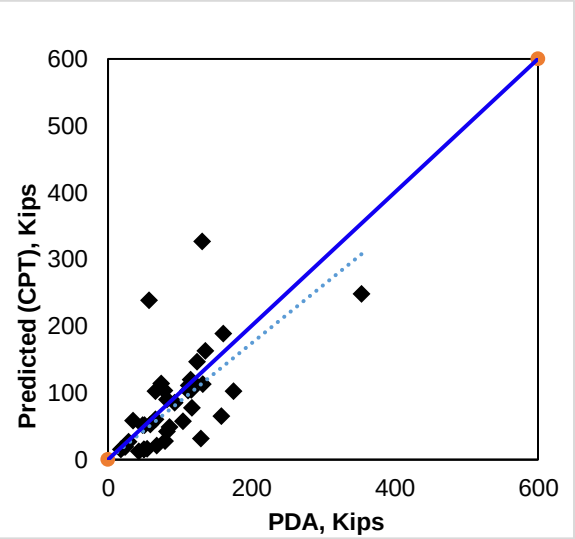

(f) Schmertmann

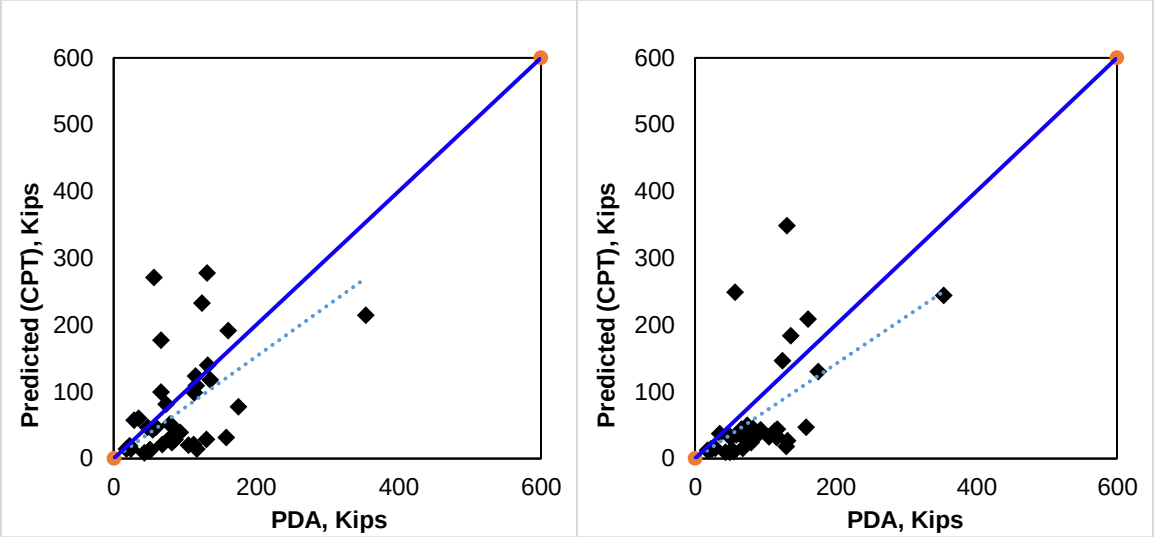

(g) European (h) Tumay & Fakhroo

Fig. 5.9 Skin Friction Pile – End Bearing Capacity - PDA vs CPT methods

Baseline evaluation of end bearing showed some of the most accurate CPT/PDA ratios among all three capacity types. Once sorted, there was apparent movement in both directions from the ideal 1:1 line. For the case of end bearing pile, prediction ratios increased for all eight methods, with over prediction shown for all methods other than Penpile. LCPC and Penpile had ratios of 1.37 and .69 respectively, while Philipponnat and Prince & Wardle were almost identical at 1.70 for 3rd best prediction. Standard deviation increased for all eight methods for end bearing pile by approximately 30%.

Evaluating the friction piles for end bearing capacity showed a decrease in the prediction ratio for most methods. Five of the eight methods now showed ratios less than one, or under predicted end bearing compared to the load test data. Philipponnat and Prince & Wardle had ratios closest to one with 0.96 and 0.91 respectively. Schmertmann and European methods also had ratios of 1.27 and .77 respectively, suggesting fairly

close prediction. The most significant result of pile type classification in for end bearing capacity was evident in the standard deviation for pipe and concrete piles. All eight methods showed at least 50% reduction in the deviation value, with three methods yielding over 70% reduction. Comparing this behavior with the end bearing piles makes a clear case that the CPT methods were struggling predicting end bearing capacity for end bearing pile compared to the end bearing for pipe or concrete piles. Overall, as was the case with the initial unsorted analysis, end bearing prediction seemed to show more accuracy over multiple methods compared to the total capacity prediction. Figures 5.8 & 5.9 present the CPT/PDA ratios of end bearing capacity for each pile classification.

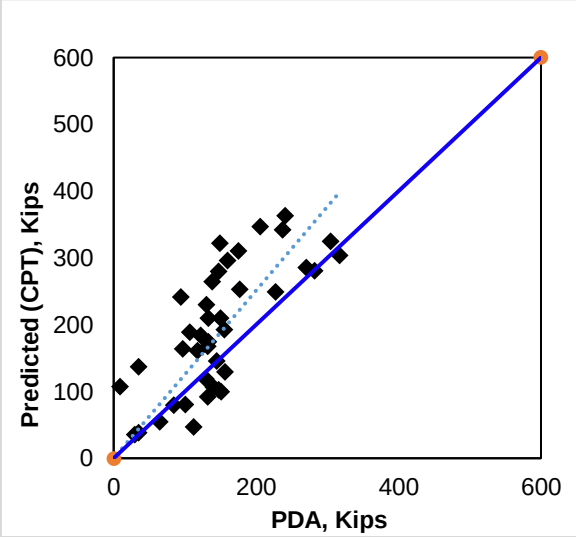

(a) Penpile

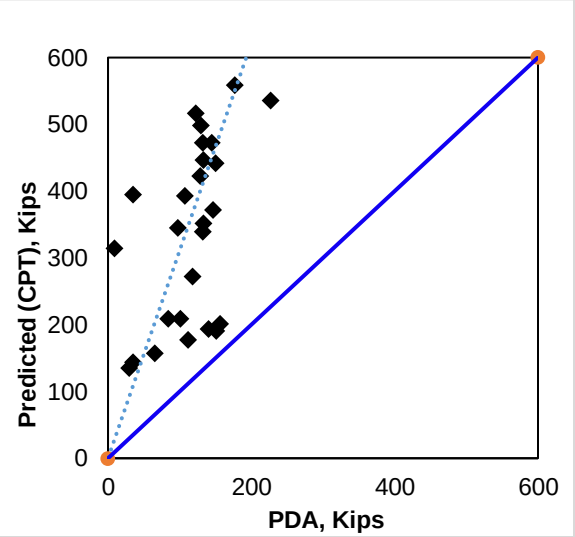

(b) Philipponnat

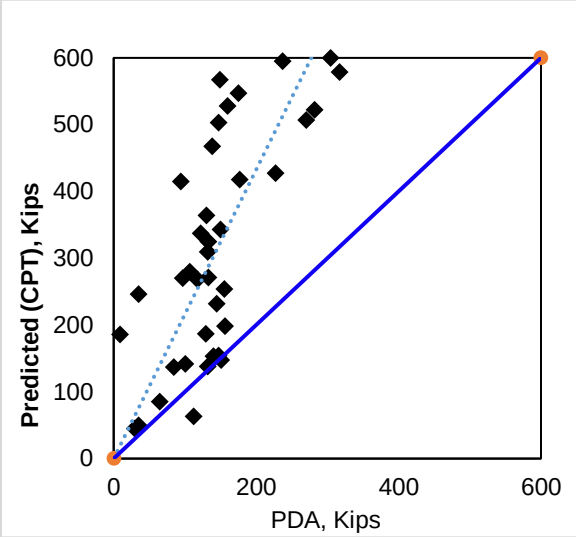

(c) Prince & Wardle

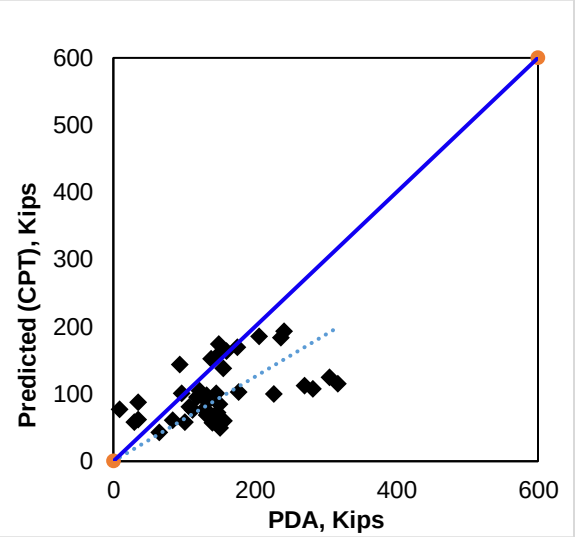

(d) LCPC

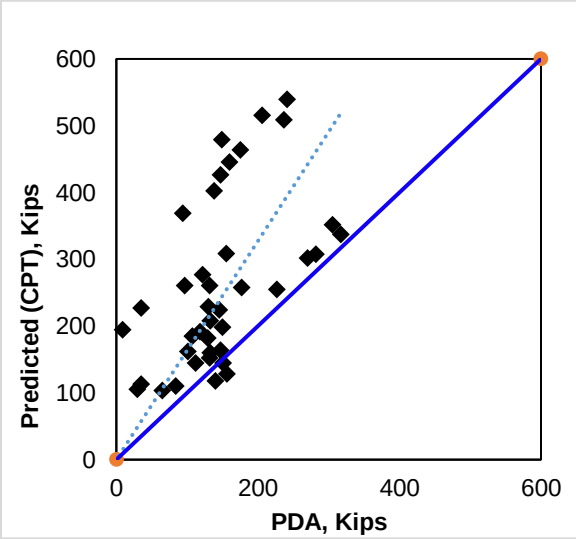

(e) Aoki

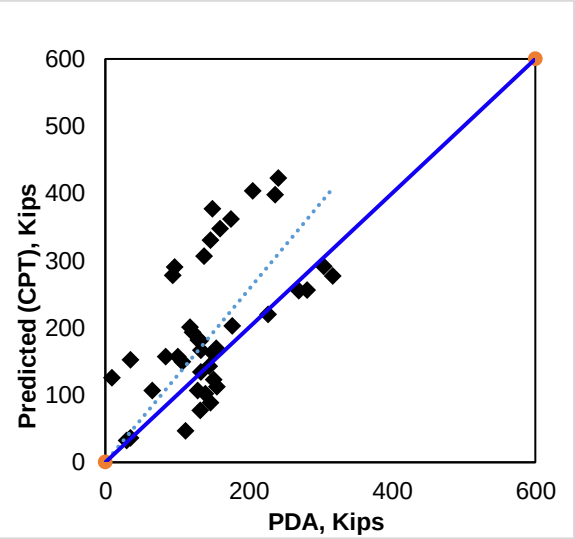

(f) Schmertmann

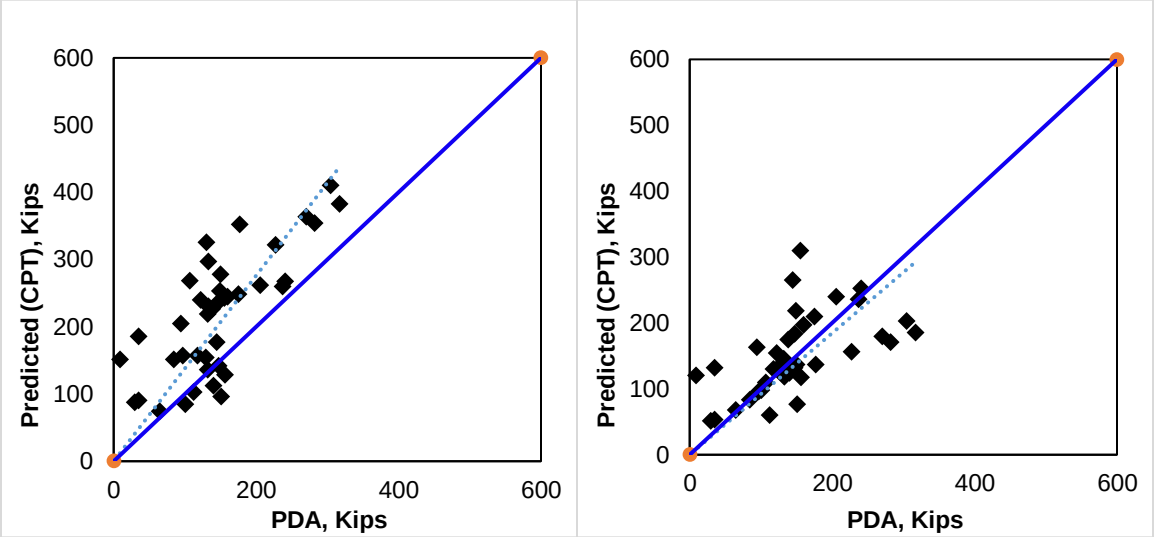

(g) European (h) Tumay & Fakhroo

Fig. 5.10 End Bearing Pile – Skin Friction Capacity - PDA vs CPT methods

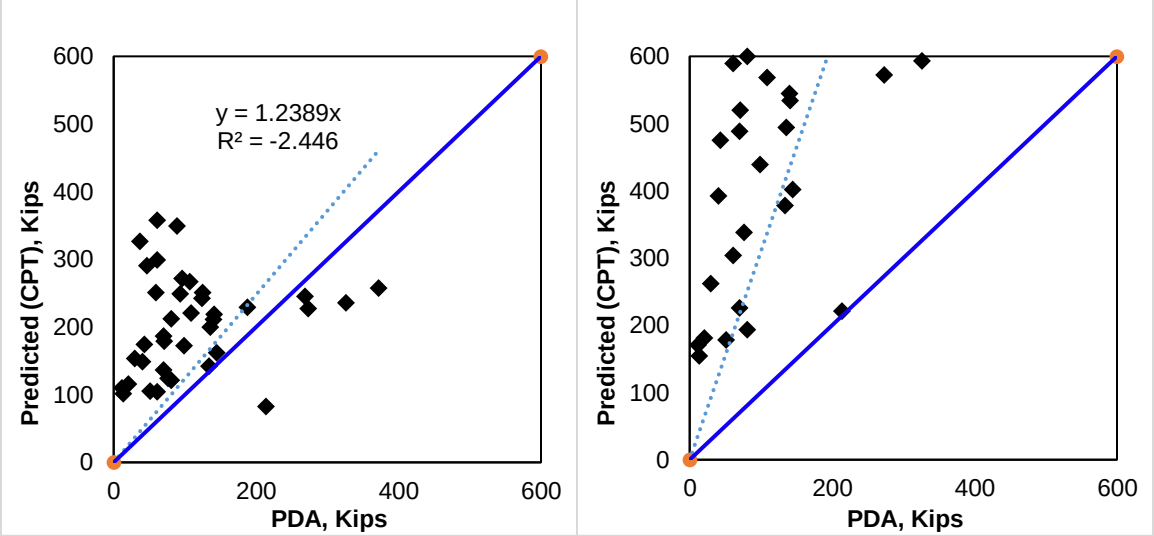

(a) Penpile (b) Philipponnat

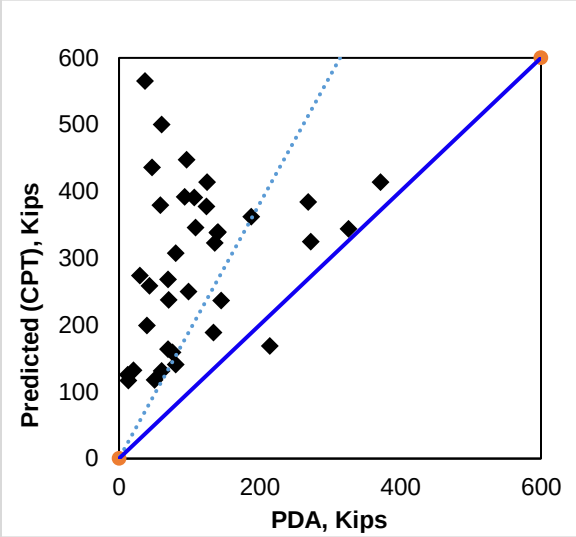

(c) Prince & Wardle

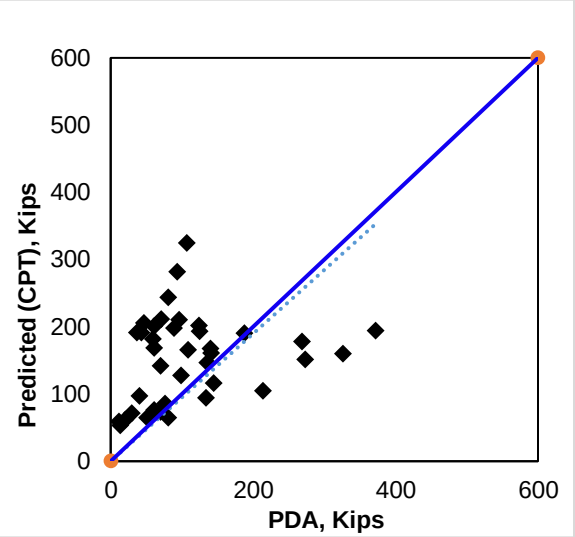

(d) LCPC

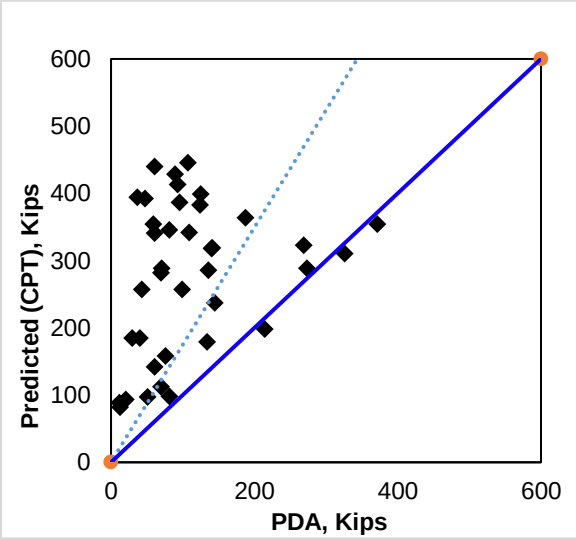

(e) Aoki

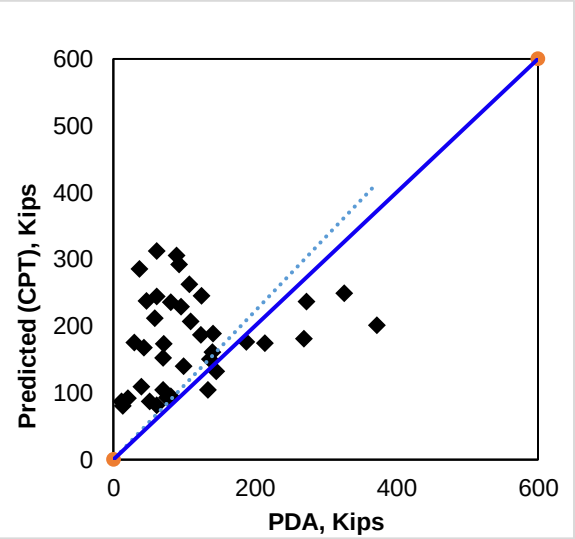

(f) Schmertmann

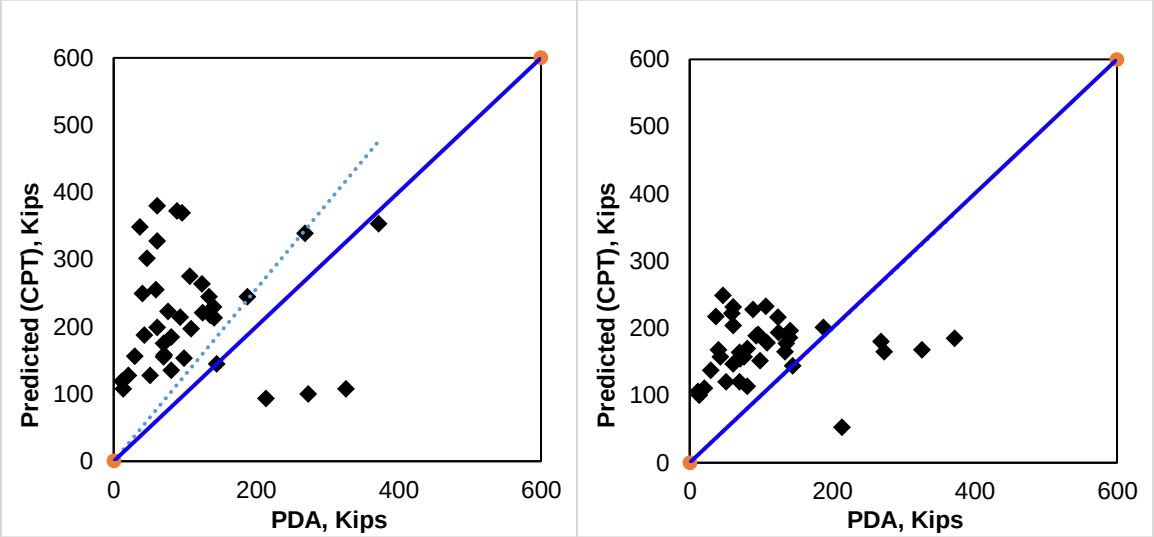

(g) European (h) Tumay & Fakhroo

Fig. 5.11 Skin Friction Pile – Skin Friction Capacity - PDA vs CPT methods

Skin friction capacity was found to be strongly overpredicted by all eight CPT bearing capacity methods upon analysis of the entire dataset. Once sorted, HP piles once again showed this over estimation, however with the exception of the Schmertmann method, there was a decrease in the CPT/PDA ratio relative to the baseline data. Top three performers for end bearing pile prediction all lowered ratios below 2.0. Most accurate was LCPC with a ratio of 1.01, followed by Tumay & Fakhroo and Penpile showing 1.43 and 1.63 respectively. These three methods also shared the lowest standard deviations, with LCPC having the lowest among the top three. Standard deviation decreased by about 20% for the sorted end bearing pile compared to the deviation calculated for the entire set of comparisons. Tumay & Fakhroo and Penpile gave the largest decrease in deviation for HP pile's skin friction capacity.

Separate evaluation of side friction piles resulted in all eight predictive methods increasing the ratio, with some of the largest over estimates of pile capacity versus the dynamic load test data. Five of the eight CPT methods had ratios greater than 3.0. Visual inspection of Figure 5.11 above confirms this, and also indicates that over prediction is most significant at lower skin friction (PDA) values, becoming slightly more accurate at higher load test points. The lowest ratios for friction piles in this assessment belonged to LCPC, followed by a tie for second between Schmertmann and Tumay & Fakhroo. Consistent with lower prediction ratios, these three methods also had the lowest standard deviation values. The deviation values were almost identical to those found by the same methods for end bearing pile prediction of skin capacity. Conversely to end bearing pile, there was a significant increase in standard deviation for the sorted friction pile group's friction capacity compared to baseline numbers found previously. Once again, the behavior in the filtered evaluation is useful to see because it was not apparent in the initial numbers. With this new information, skin fiction prediction seems to be more accurate for end bearing piles compared to friction piles based on the prediction ratio.

5.8 Sorted Statistical Analysis

Similar to the procedure outlined in the previous section, the data set was sorted by pile type for further statistical evaluation. The same six categories for the two pile classifications and three bearing quantities were followed. The paired t-test was performed again, allowing for direct comparison to baseline information found in the initial statistical assessment.

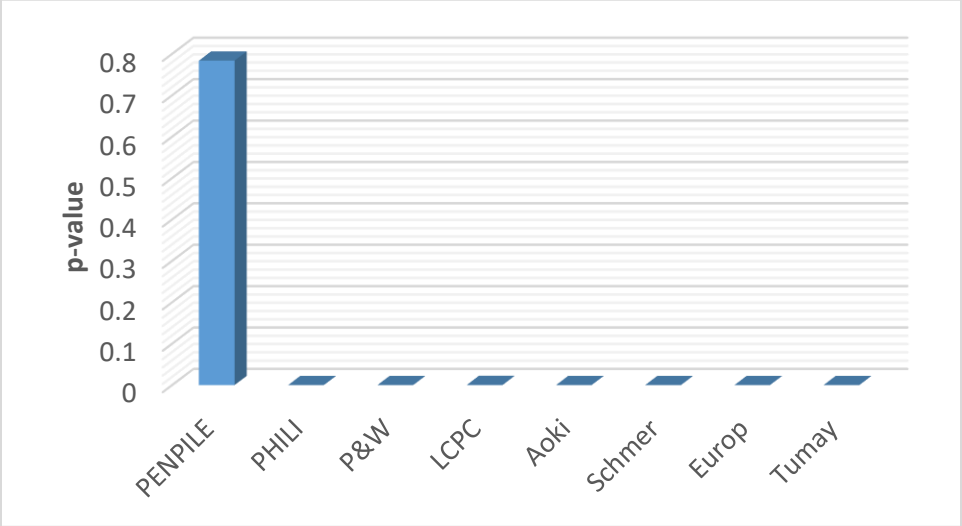

Fig. 5.12 CPT Accuracy Level – Total Capacity-End Bearing Pile

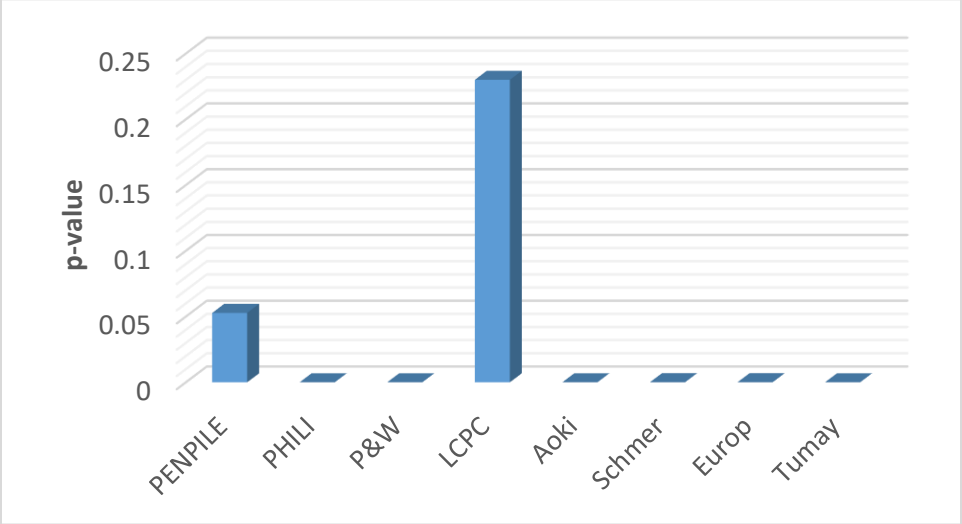

Fig. 5.13 CPT Accuracy Level – Total Capacity-Skin Friction Pile

Evaluation of the entire data set by the statistical paired t-test indicated that Penpile and LCPC methods were the most accurate CPT based capacity predictions. Once comparisons were sorted by pile bearing mechanism, the t-test was used again on the two populations. End bearing or HP pile analysis indicated that the Penpile method was by far the most accurate with a p-value of 0.78. Second ranked was again LCPC,

however the p-value (2.5e-4) did not exceed p-critical = 0.05. For reference, unsorted analysis gave p-values of 0.24 and 0.01 for the two respective methods. Next, steel pipe and prestressed concrete piles, considered friction piles, were evaluated with the paired t-test. LCPC ranked first with a p-value of 0.23, while Penpile was next best with p-value = 0.052, slightly greater than p-critical. Considering both categories and the baseline t-test results, it is apparent that the methods moved in opposite directions for the different bearing behavior classification. End bearing piles were better predicted by Penpile method, yielding accuracy increase of 54% compared to the original p-value. Similarly, LCPC method appeared to predict the total capacity of friction pile more accurately. An improvement of 22% from the first analysis in this category was realized. Conversely, LCPC's p-value decreased below p-critical for end bearing pile, while Penpile's accuracy decreased 19% for skin friction pile. Figure 5.13 indicates the negligible accuracy of the other methods not discussed in detail in this section.

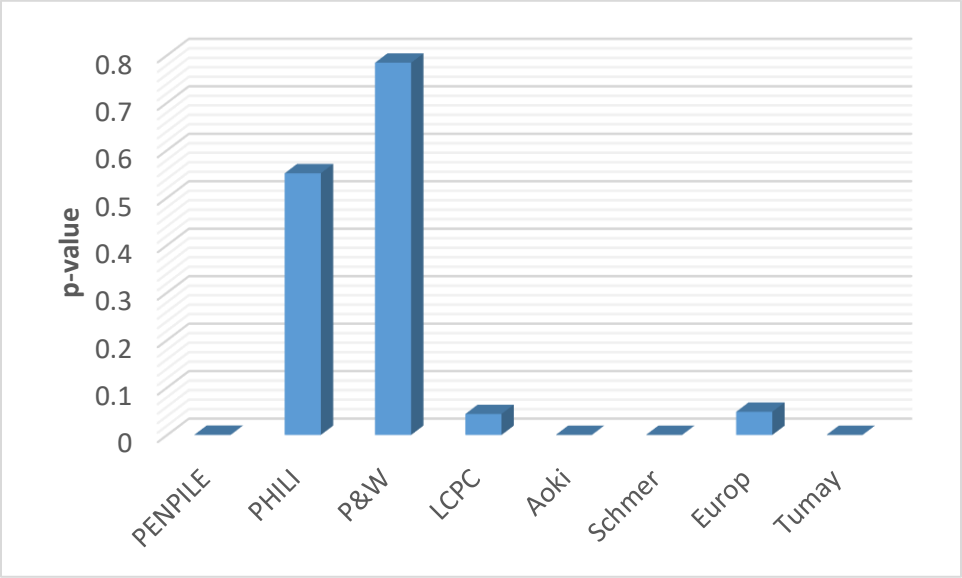

Fig. 5.14 CPT Accuracy Level – End Bearing Capacity-End Bearing Pile

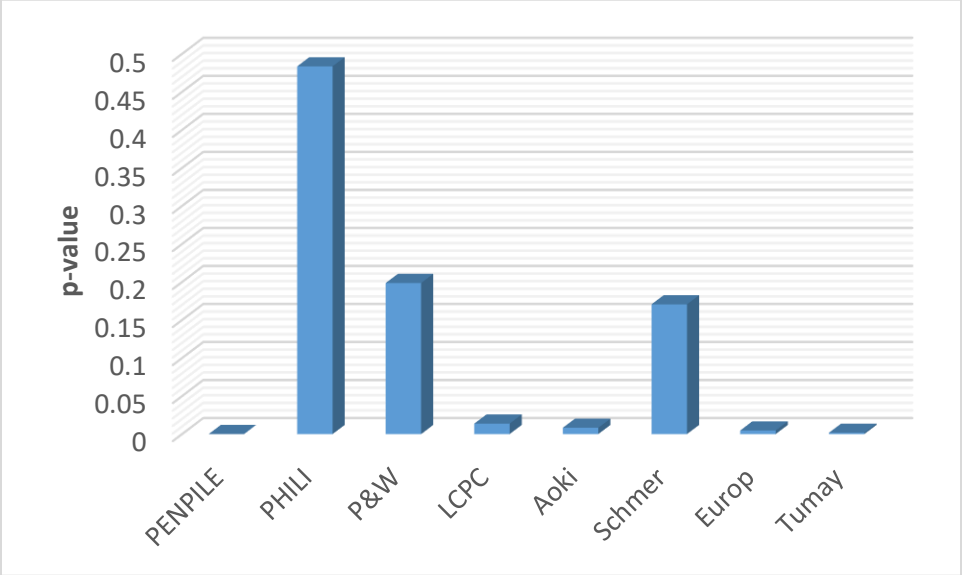

Fig. 5.15 CPT Accuracy Level – End Bearing Capacity-Skin Friction Pile

Next, end bearing capacity was further evaluated using the pile bearing type classification procedure. For HP piles, Prince & Wardle was the most accurate method with a p-value of 0.78. Philipponnat method followed with an accuracy of 55%. LCPC and European methods were the only other methods of mention, however p-values for both were just below p-critical. This relative performance is plotted in Figure 5.14 above. Baseline values from the entire data population indicated that both methods were among the best performers. Prince & Wardle had p-value 0.26 while Philipponnat's p-value was 0.37. A 52% and 18% respective increase in prediction accuracy realized for the CPT methods in end bearing pile.

Friction pile gave similar results to the end bearing pile, however for this case the Philipponnat method was the most accurate method while Prince & Wardle was second. These methods had p-values 0.48 and 0.19 respectively for end bearing capacity of friction piles. Additionally, the Schmertmann method indicated reasonable accuracy with

a p-value of 0.17. By evaluating the skin friction classified piles independently, Philipponnat indicated an increase of 11% while Prince & Wardle did have a slight decrease in accuracy with the p-value decreasing about 7%.

Overall, end bearing capacity evaluation upon the sorted pile types showed improvement in accuracy measures. Both Prince & Wardle and Philipponnat methods were indicated to be fairly accurate methods by the initial analysis, and this was reinforced by the sorted data. Accuracy numbers generally increased for both pile types with each method distinguishing itself for end and friction piles respectively. Interestingly, the European method had extremely high accuracy when the entire comparison population was evaluated but was not a top measuring method in either of the sorted analysis This may suggest some form of averaging or extremes mitigation in the larger dataset leading to a reduction of total error. Conversely, Schmertmann had very poor accuracy initially, but was a very close third rank for pipe and concrete pile end bearing prediction. This is confirmed by the decrease in standard deviation and lowering of the prediction ratio for these pile (accompanied increase for HP pile). Observation of Figure 5.15's plot of relative performance, argues this method may be worthy of further consideration in this category. In summary, the bearing mechanism acting on the different pile studied appears to play a role in measured capacity compared to the empirical CPT methods. The CPT prediction's over or under estimations of end capacity was clarified by studying pile types separately.

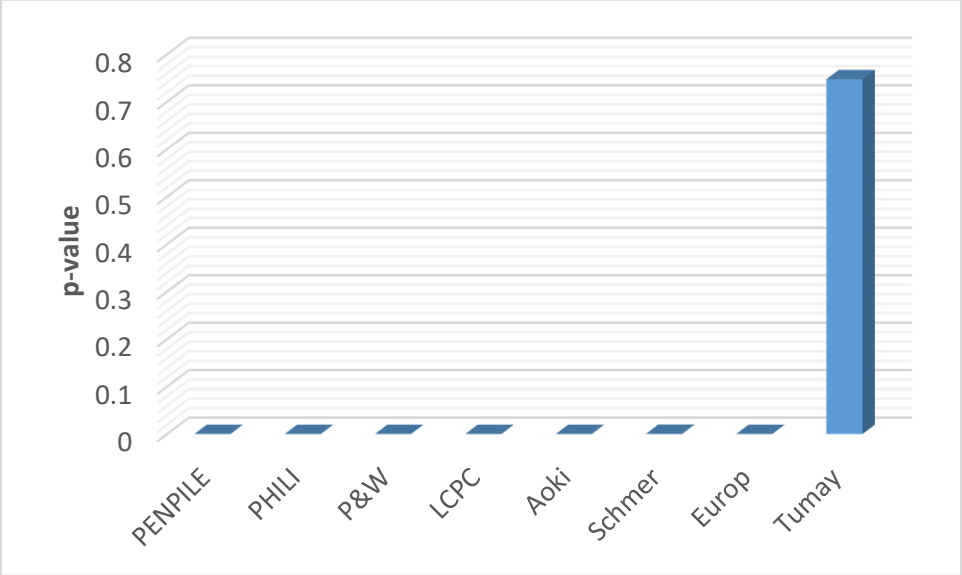

Fig. 5.16 CPT Accuracy Level – Skin Friction Capacity-End Bearing Pile

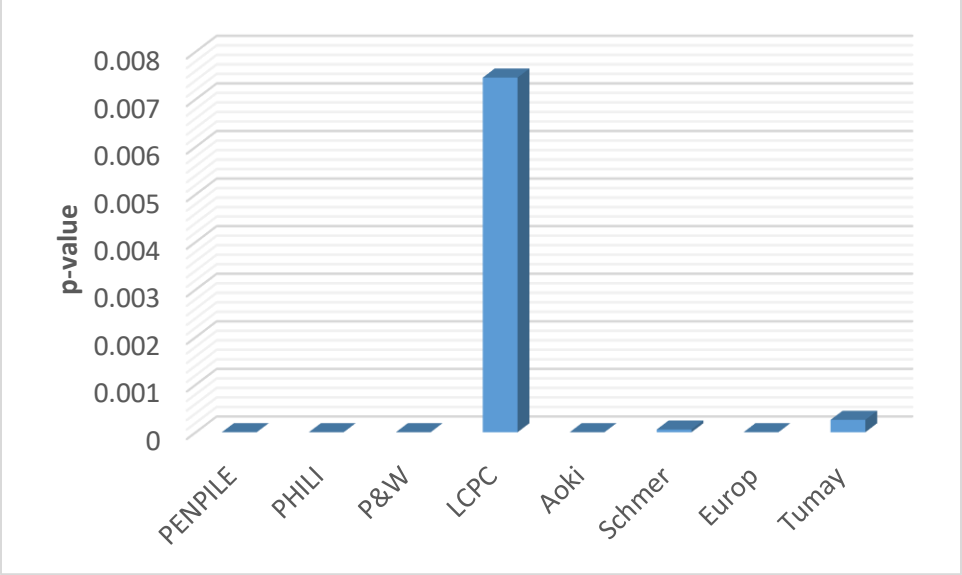

Fig. 5.17 CPT Accuracy Level – Skin Friction Capacity-Skin Friction Pile

Skin friction capacity was the final criterion for sorted evaluation of statistical performance of the eight CPT predictive methods. Results from the full dataset indicated that LCPC was the lone accurate method for skin friction capacity with a p-value around 90%. Tumay & Fakhroo ranked second but had an accuracy less than p-critical. First, HP piles were evaluated. The paired t-tests seen in Figure 5.16 show that Tumay & Fakhroo had very good accuracy with p-value = 0.75. Schmertmann's method was ranked second but showed very low accuracy. Prediction for side friction classified piles showed very limited accuracy in this set of comparisons. LCPC was ranked highest by the t-test followed by Tumay & Fakhroo. However, the y-axis of Figure 5.17 clearly indicates that the accuracy of these two methods for skin friction prediction is significantly lower relative to accuracy various methods measured in the other five categories in this section. P-values for both methods were well below p-critical on the order of 0.1%.

The most significant change observed in the skin friction capacity sorted analysis was the new performance measures of LCPC. Similar to the phenomenon discussed above for the European method's accuracy in end bearing prediction, a muted response is perhaps being measured in the initial evaluation. The scatter plots of the LCPC methods skin friction (Figures 5.10 & 5.11) suggest that the method was under predicting for HP piles and over predicting for the majority of side friction pile comparisons. Despite this, linear fit and deviation values improved, so this method still offers prediction potential later in the study.

5.9 Summary of Performance Evaluation

Upon completion of initial evaluation of the entire dataset, subsequent tests were performed on sorted subsets. Classification was based primarily on the concept of pile type and dominant resistance behavior for the different piles. This logic established six categories constructed from the three bearing capacity measures (total, end, skin) and the two pile types, end bearing pile and skin friction pile. The results of this new assessment clarified that data, and established situations where individual methods excelled or performed poorly. In addition, there was skepticism of confidence in some accuracy numbers found from the first analysis. By sorting the data and evaluating more refined datasets, it became apparent that in some situations "averaging" effects were perhaps taking place. This means that a method may have been over predicting x group of piling, and under predicting y group of piling. The net result was an apparent accuracy, but rather a net effect rather than a highly accurate (individual basis) method. Additionally, total capacity may have indicated quality prediction, but component proportions were inaccurate. Similar to section 5.5, summary tables with performance ranking are presented below. These tables are based only on t-test results and are not an entirely comprehensive view. Differing from the previous summary tables, below performance is presented separately for end bearing and friction piles. Again, the final column from Abu-Farsakh & Titi (2004) is the comprehensive rank found by that particular study for total capacity and are shown for consideration purposes rather than direct comparison based on identical sorting or ranking criteria.

Table 5.2 Summary of ranking CPT based methods for end bearing piles

CPT method	Total Capacity	End-Bearing	Skin Friction	Abu-Farsakh & Titi (2004)
Penpile	1st	-	-	9th
Philipponnat	-	2nd	-	4th
Prince & Wardle	-	1st	-	7th
LCPC	2nd	-	-	1st
Aoki & de Alencar	-	-	-	5th
Schmertmann	-	-	2nd	5th
European	-	3rd	-	1st
Tumay & Fakhroo	-	-	1st	8th

Table 5.3 Summary of ranking CPT based methods for skin friction piles

CPT method	Total Capacity	End-Bearing	Skin Friction	Abu-Farsakh & Titi (2004)
Penpile	2nd	-	-	9th
Philipponnat	-	2nd	-	4th
Prince & Wardle	-	3rd	-	7th
LCPC	1st	-	1st	1st
Aoki & de Alencar	-	-	-	5th
Schmertmann	-	3rd	-	5th
European	-	-	-	1st
Tumay & Fakhroo	-	-	2nd	8th

CHAPTER 6 COMPTUTATIONAL MODELING

6.1 Introduction

A numeric modeling study was conducted to better understand the mechanisms relating the CPT device and driven pile. Two main objectives for the study were defined. First, determine influence depths above and below the pile tip, then compare to those suggested by the eight CPT capacity prediction methods. Second, obtain q_b/q_c ratios, and compare to the empirical method's recommendations for cohesive and granular material. These measures further investigate the empirical processes studied in the project to validate more than capacity accuracy, but rather aid to determine if the mechanics are reasonable. FLAC 2D *v8* finite difference software was used to build models replicating CPT penetrometer, pile, and soil strata conditions.

An attempt was made to replicate actual CPT profiles from the project, which could then be further studied with cone and pile penetration. The two selected projects were 77-2(1025) (Wahoo Bypass) and 80-9(811) (I-80 & Capehart Rd). The projects were select because two different pile types were represented, as well as primary bearing strata consisting of dense sand and glacial till respectively. Modeling of the soil layers, and subsequent penetration behavior of CPT/pile proved to be substantially more complex than expected. Though the process of the computational modeling shifted, Figure 6.1 confirms agreement between horizontal and vertical stresses, and subsequent q_c values of the actual CPT profiles can be obtained. Proceeding forward, six simplified models were studied for resultant behavior. The models consisted of combinations of soft/stiff cohesive material and loose/dense granular material. While exact confirmation

of measured CPT to empirical predictions were not obtained, understanding of behavior in stratified conditions was thoroughly investigated.

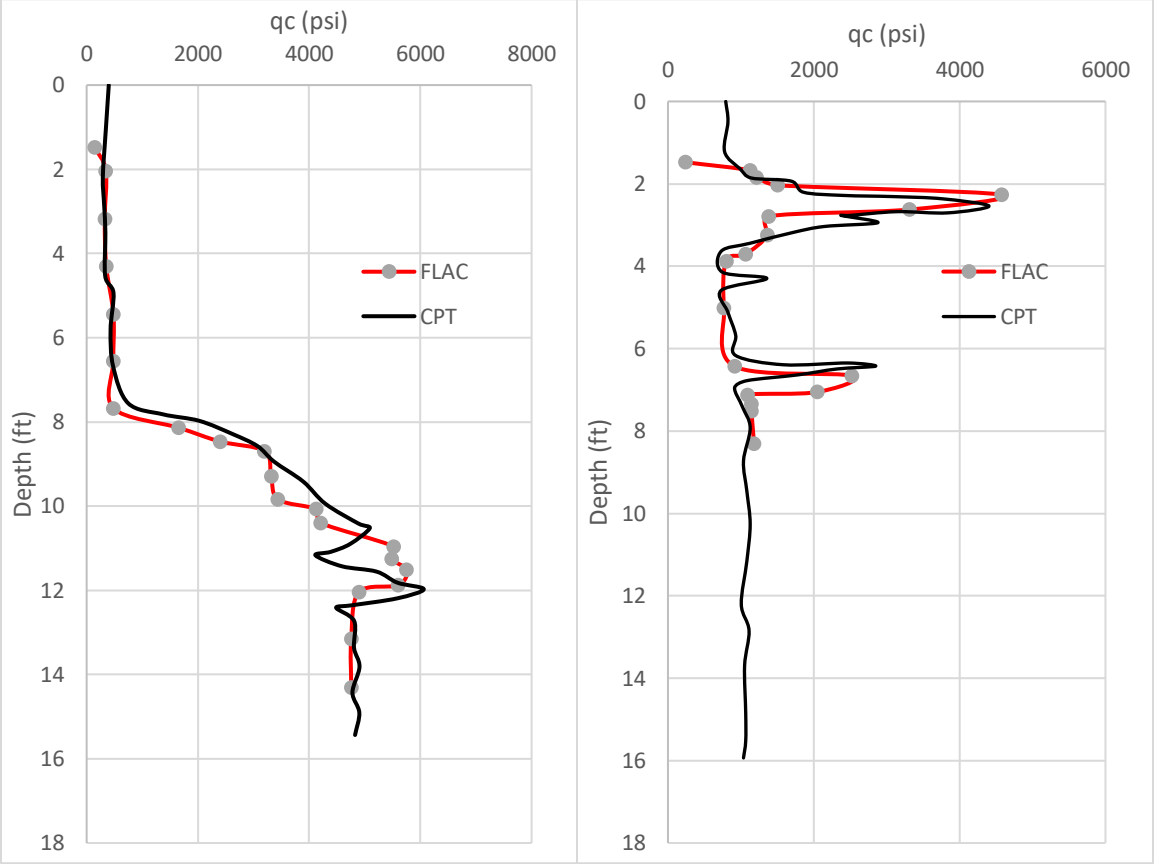

a) S077 09368 b) S080 43555

Fig. 6.1 Calibrated FLAC CPT profiles

6.2 Modeling Parameters

Equilibrium equations and strain compatibility were used for the study. The soil constitutive model assumed for all scenarios was the Mohr-Coulomb criterion, considering elastic-perfectly plastic failure. Pore pressure effects were not included into the study. Linear strain terms and explicit time step evaluation were applied in the FLAC models. Boundary conditions for the modeling consisted of an axis symmetric model,

with displacement partially restrained on the y-axis and full restrained at the x-axis. See details below in Figure 6.2 for complete boundary condition details. Initial conditions applied to the models included gravity loading for overburden stresses throughout the model. Coefficient of lateral earth pressure was determined by the relationship in equation 27, with poisson's ratio varying by material. Unit weight of soil considered was 18kN/m^3 for all soils.

$$K_0 = \frac{\nu}{1-\nu} \tag{27}$$

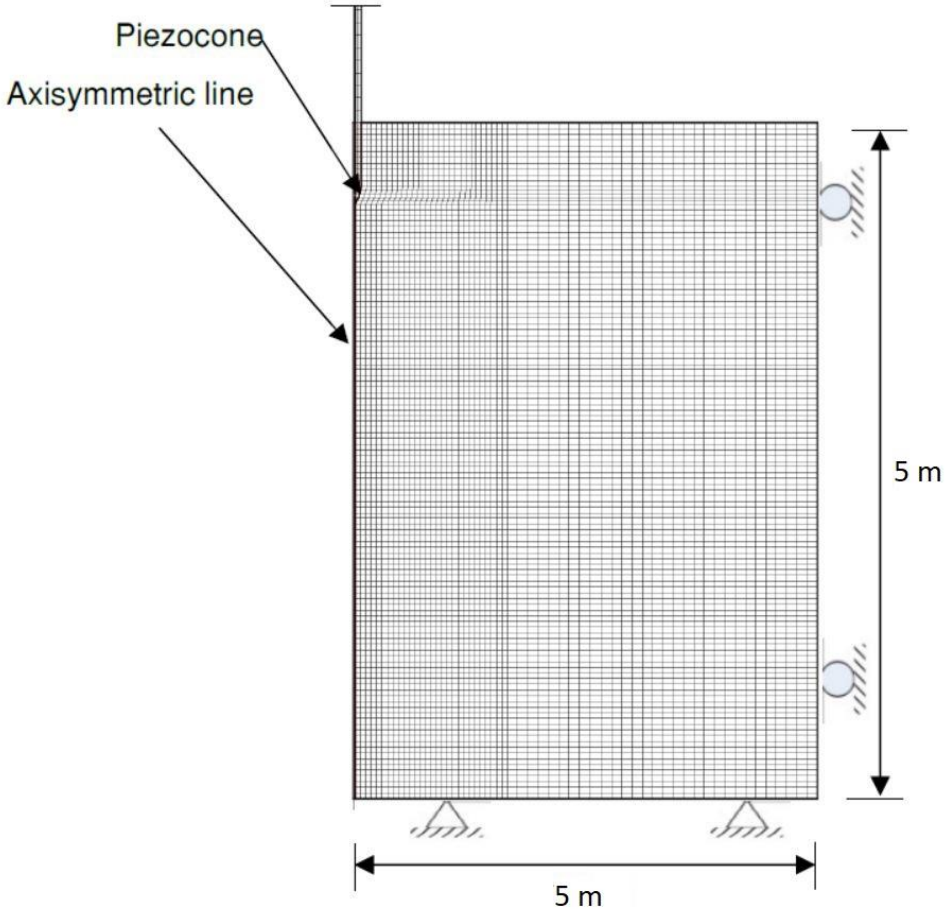

Fig. 6.2 Model setup and boundary conditions

Models were constructed for 5m x 5m blocks, with strata changes implemented at 2.5m. Cohesive materials were assumed to have φ = 0, and c = 100kpa for soft and 200kpa for stiff material. Granular materials were defined with c = 0, and φ = 30° or φ = 40° for loose and dense material respectively. Interface values were 2/3 of internal friction angle and 60% of cohesion compared to bulk material properties. Pile shape was modeled as circular, with D = 0.3m, similar to the typical 12.75" NDOR pipe pile. Due to numerical instabilities, the end section was modified from a flat steel plate to a conical point. According to Randolph (1994), driven circular pile a rigid cone of soil can be assumed beneath the pile tip in sandy soils. The assumption was transferred to cohesive conditions for this study, however actual penetration behavior may vary with a flat bottom. All models were run with CPT penetration and pile penetration for comparison.

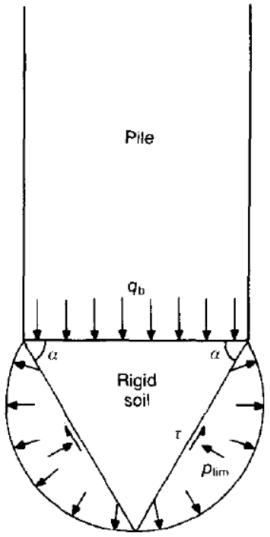

Fig. 6.3 Rigid soil mas below pile tip (Randolph, 1994)

6.3 Model 1 – Cohesive soft overlying stiff

Model 1 consisted of entirely cohesive material. Only cohesion values were modified to increase or decrease material strength and stiffness. The simulation represents common driving conditions in Nebraska where overlying soft materials such as alluvium or loess are encountered, prior to the pile being driven into stiffer bearing layers. Figure 6.4 depicts the model construction with pile penetration. At the surface, slight heaving can be observed due to the pile's displacement properties.

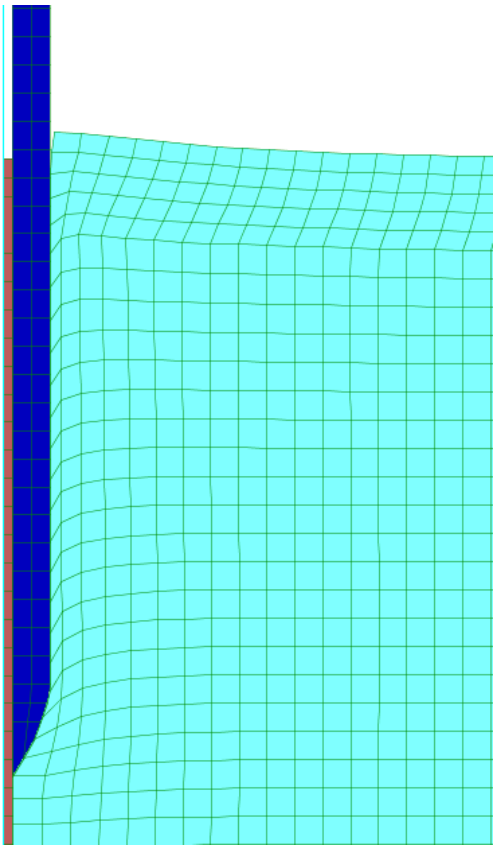

Fig. 6.4 Pile penetration and resulting surface heave

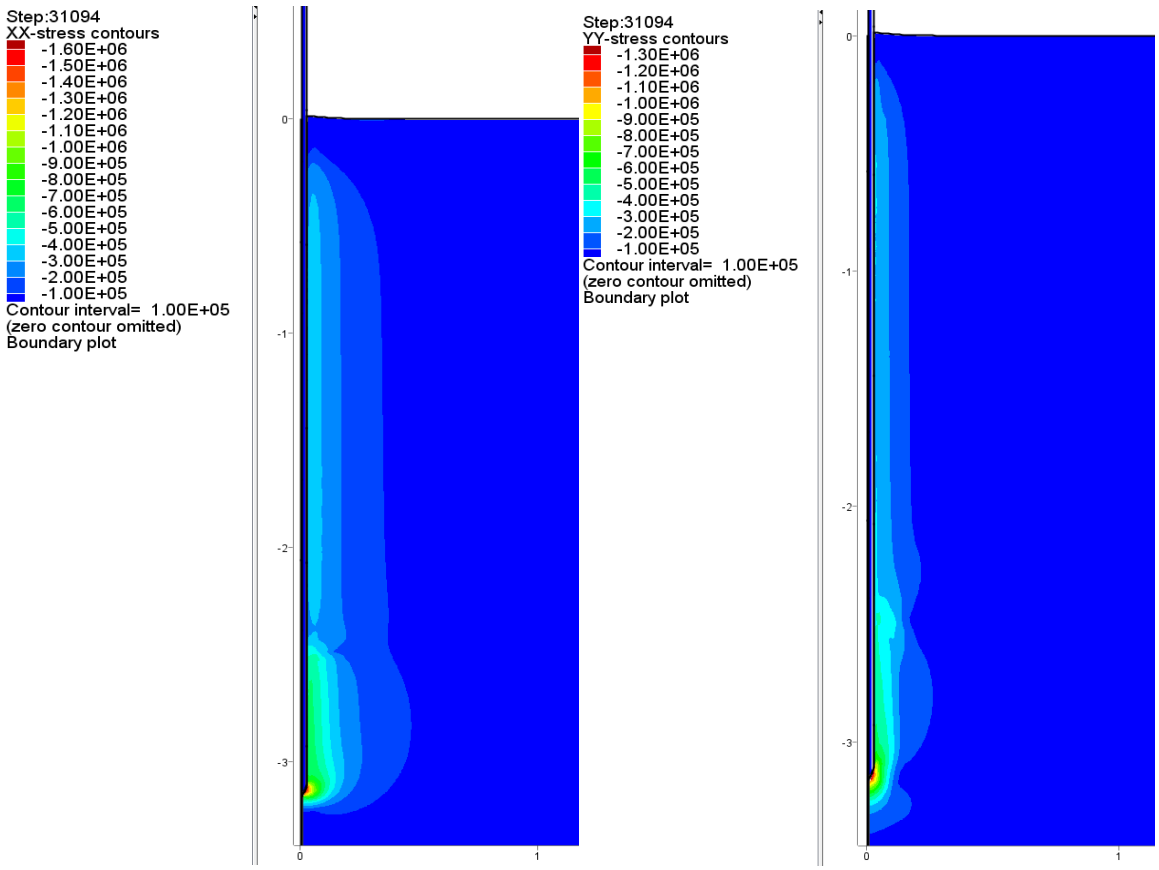

Fig. 6.5 CPT horizontal and vertical stresses at 3m (stiff)

Figure 6.5 shows the small zones of influence around the CPT cone, with both horizontal and vertical stresses clearly higher in the stiffer material below 2.5m. Vertical stress contours influence about .3m or 8D. Compare to the following figure of pile penetration stress distributions where horizontal and vertical stress contours are impacted at approximately 1m distances respectively.

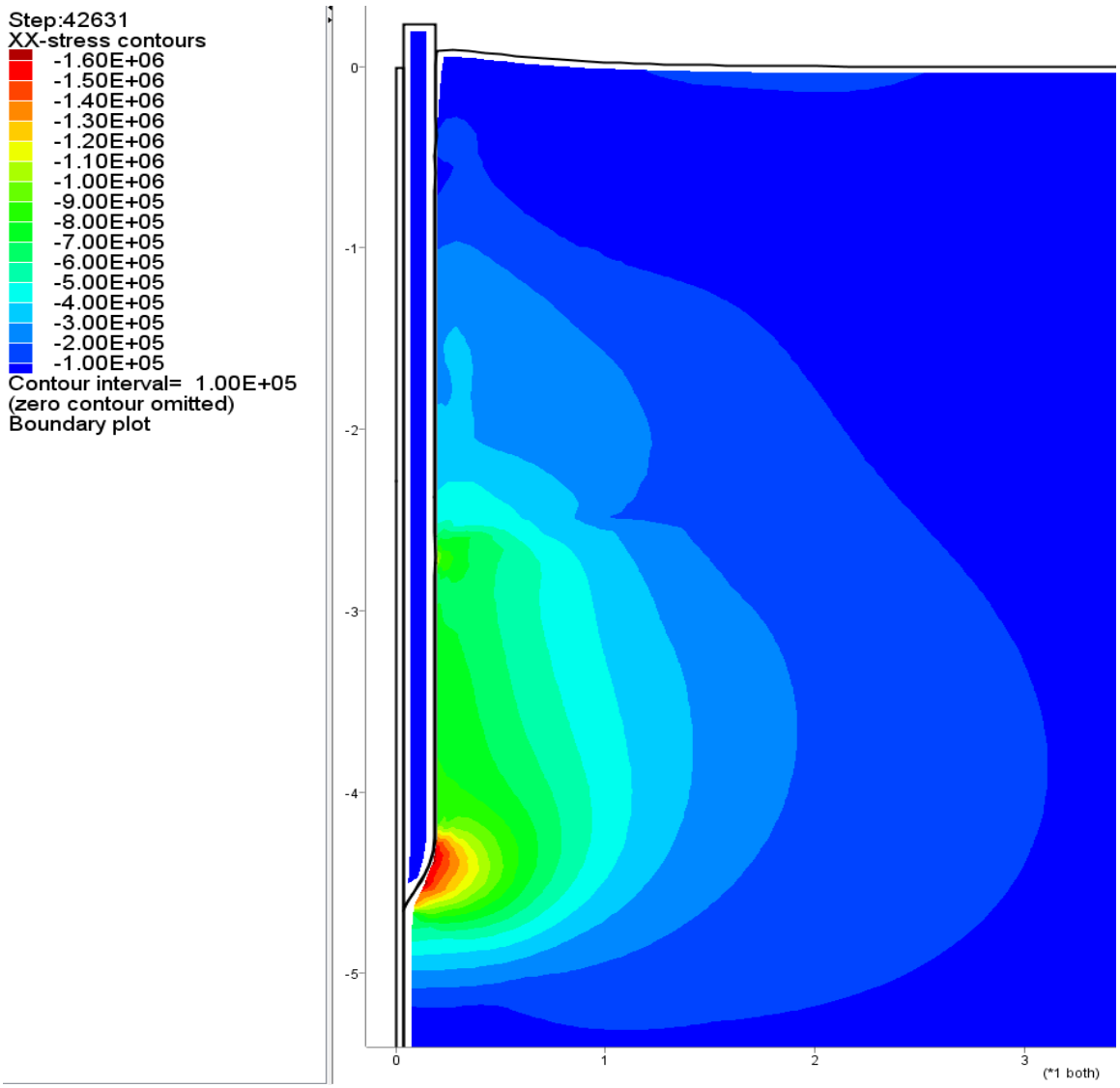

Fig. 6.6 Pile horizontal stress at 4.5m penetration (stiff)

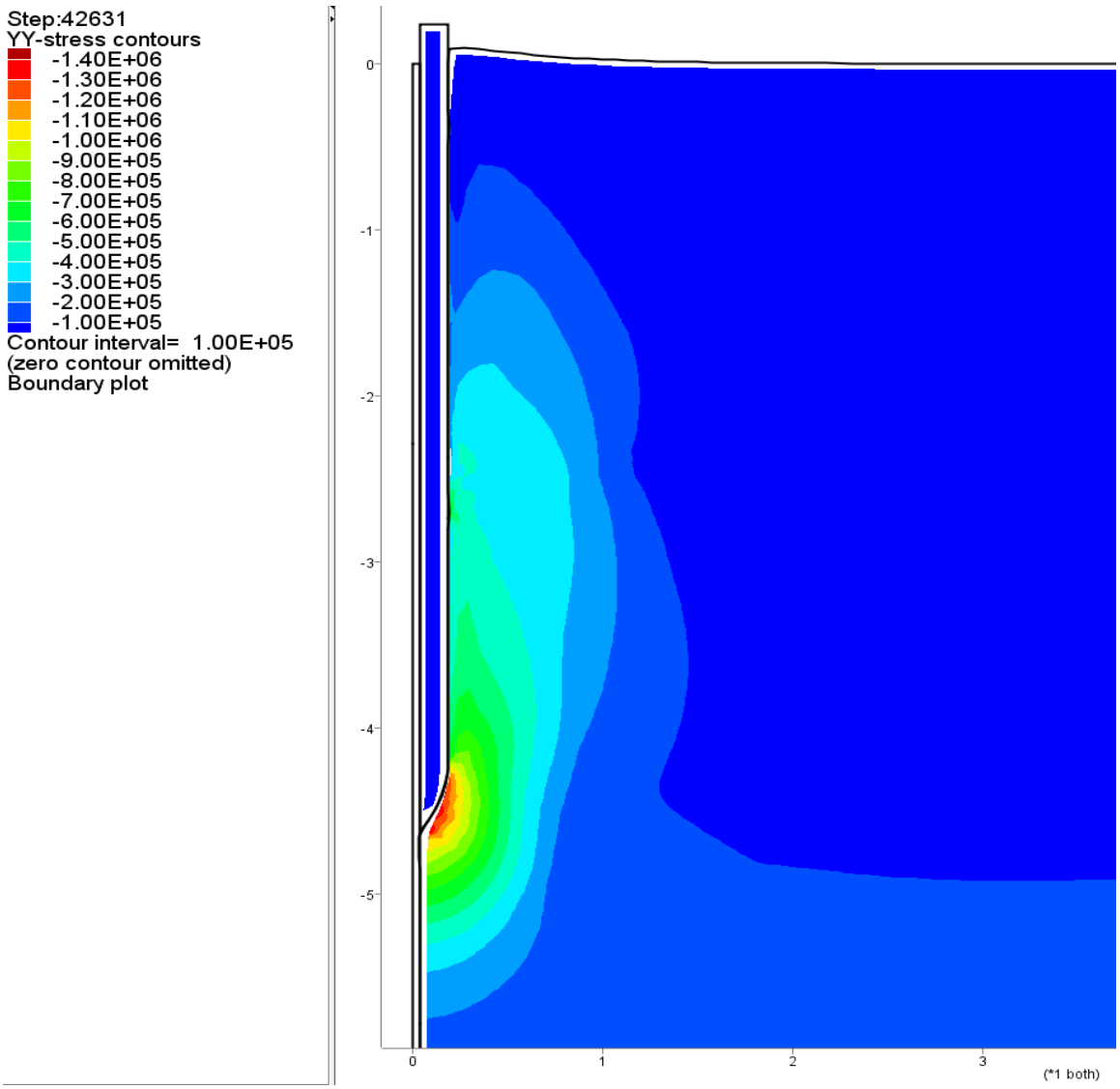

Fig. 6.7 Pile vertical stress at 4.5m penetration (stiff)

Finally, horizontal and vertical stress logs taken at history points along the cone/soil penetration interface were exported to calculate q_b and q_c values for comparison. A tip resistance plot was prepared with corresponding material changes reflected at 2.5m or 8ft depth. Influence depths above and below the pile tip are estimated on the plot. Additionally, q_b/q_c ratios were determined by comparing the pile resistance value to the CPT at the point where CPT resistance reached steady state conditions.

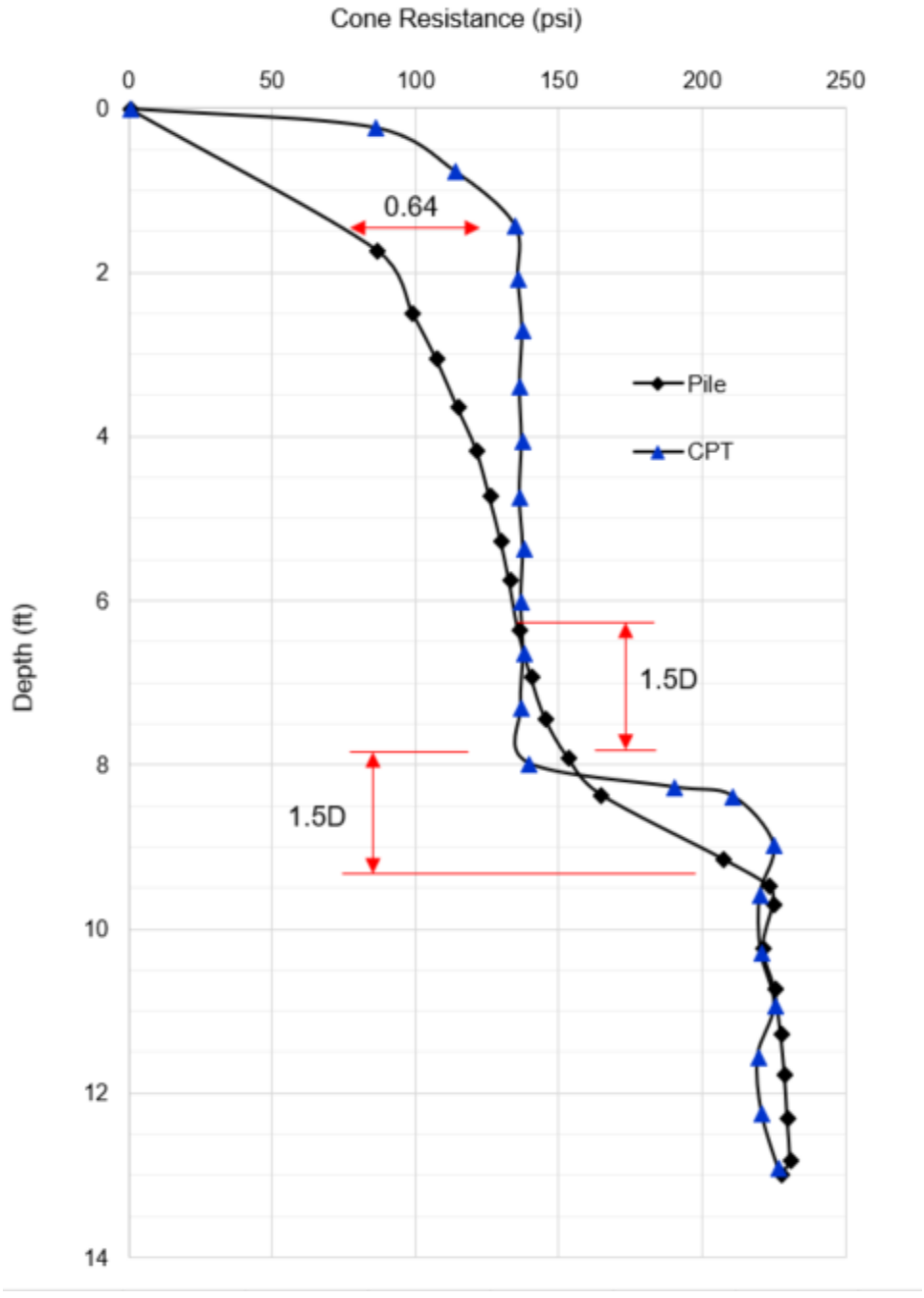

Fig. 6.8 CPT vs Pile tip resistance Model 1

CPT cone and pile responses indicate different response and strength mobilization times. Figure 6.8 shows the CPT tip resistance reaching a steady state near 135 psi within the first 1.5 ft of penetration. Conversely, the pile does not mobilize this resistance until a depth of 6.5 ft. Calculated q_b/q_c ratio in soft cohesive material (layer 1) is 0.64. Influence depths appear to be about 1.5D above and below the pile tip. It is evident that the pile begins to feel the underlying stiffer layer at 6.5ft, where the pile resistance exceeds the q_c value. The CPT records almost instantaneous resistance increase at the soft/stiff interface, reaching steady conditions within 0.25 ft. The final portion of the plot indicates good agreement between the pile and penetrometer.

6.4 Model 2 – Cohesive stiff overlying soft

Next, a completely cohesive soil model was maintained, but the order of layers was reversed. The situation is perhaps less likely than model 1 to be encountered, however it represents a study on the effect of loss of bearing capacity due to underlying weak materials. Cohesion values were not changed from model 1. Slightly larger differences in stiffness were investigated, however deformation discrepancies occurred. Figure 6.8 again shows the longer mobilization period for the pile compared to the CPT. The pile reached steady conditions (225 psi) between 5.0 and 5.5ft. This is slightly earlier compared to model 1 in the soft cohesive soil. Reduction in strength of the pile began at 7.0 ft (1.0D). Influence above the pile tip was calculated to be near 1.5D, similar to the previous conditions. This suggests that the pile feels weaker layer earlier than the CPT, which may lead to CPT over prediction if proper consideration is not given to underlying layers. The q_b/q_c ratio in the stiff cohesive layer was 0.70, slightly higher than the soft material, and in agreement with the shorter mobilization length.

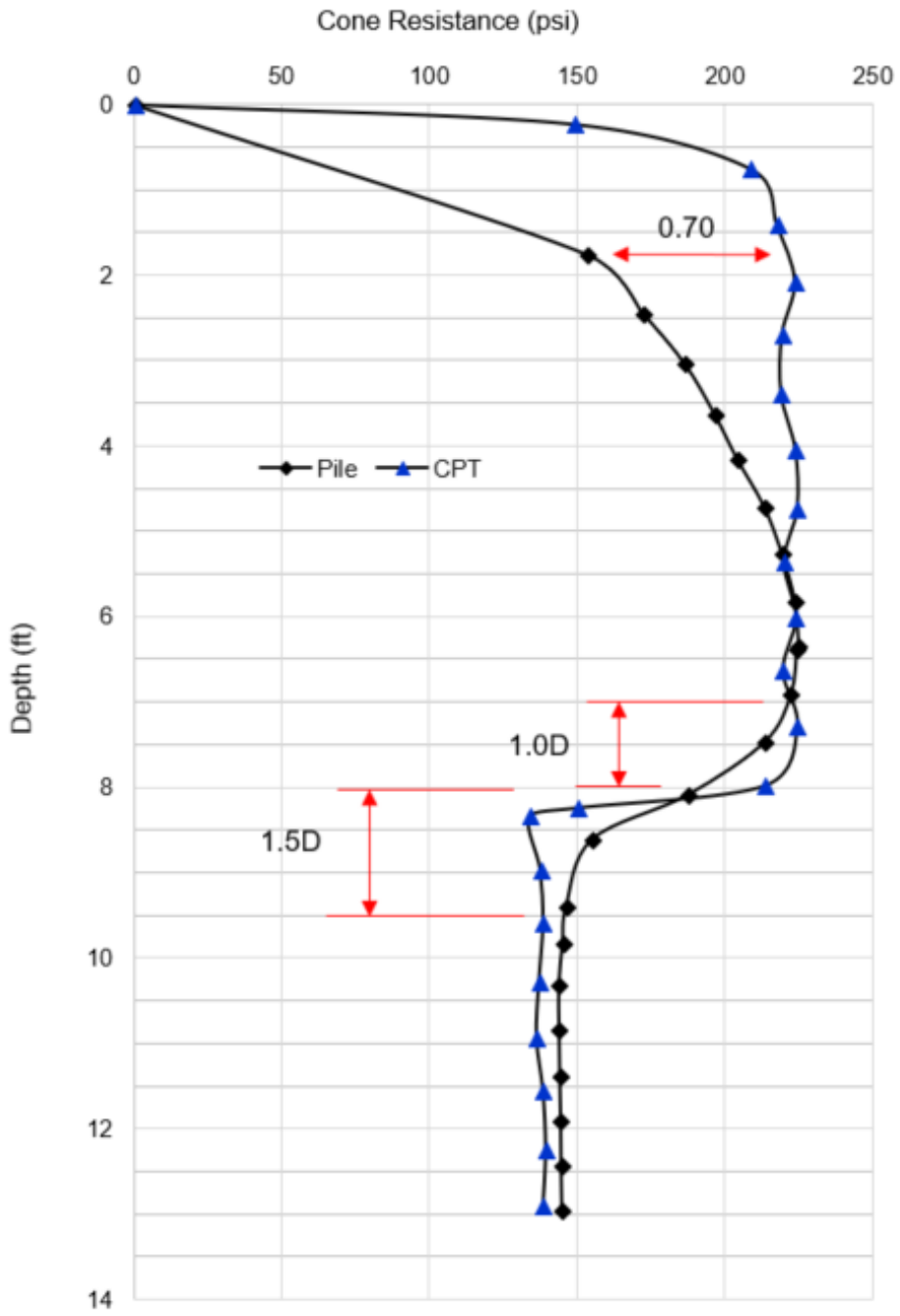

Fig. 6.9 CPT vs Pile tip resistance Model 2

6.5 Model 3 – Granular loose overlying dense

Model 3 consisted of granular material, assumed to have no cohesion. Internal friction angle was the only parameter changed between the two layers, with higher phi values assumed to correspond to denser sand/gravels. In granular materials the resistance is derived from frictional strength, which means the horizontal stress adds a large contribution to the resistance felt by the cone or pile. For the case of the conical tip, this is proportional to the 60 ° angle at the interface. Figure 6.10 demonstrates the relative deformation of the loose material interacting with the underlying dense sand.

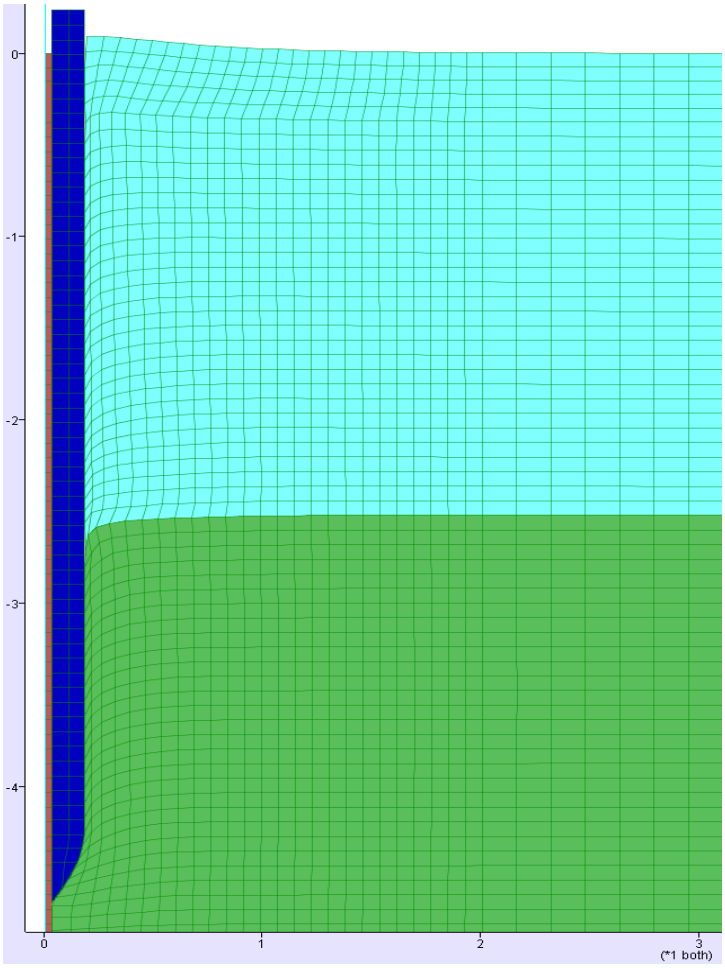

Fig. 6.10 Granular deformation Model 3

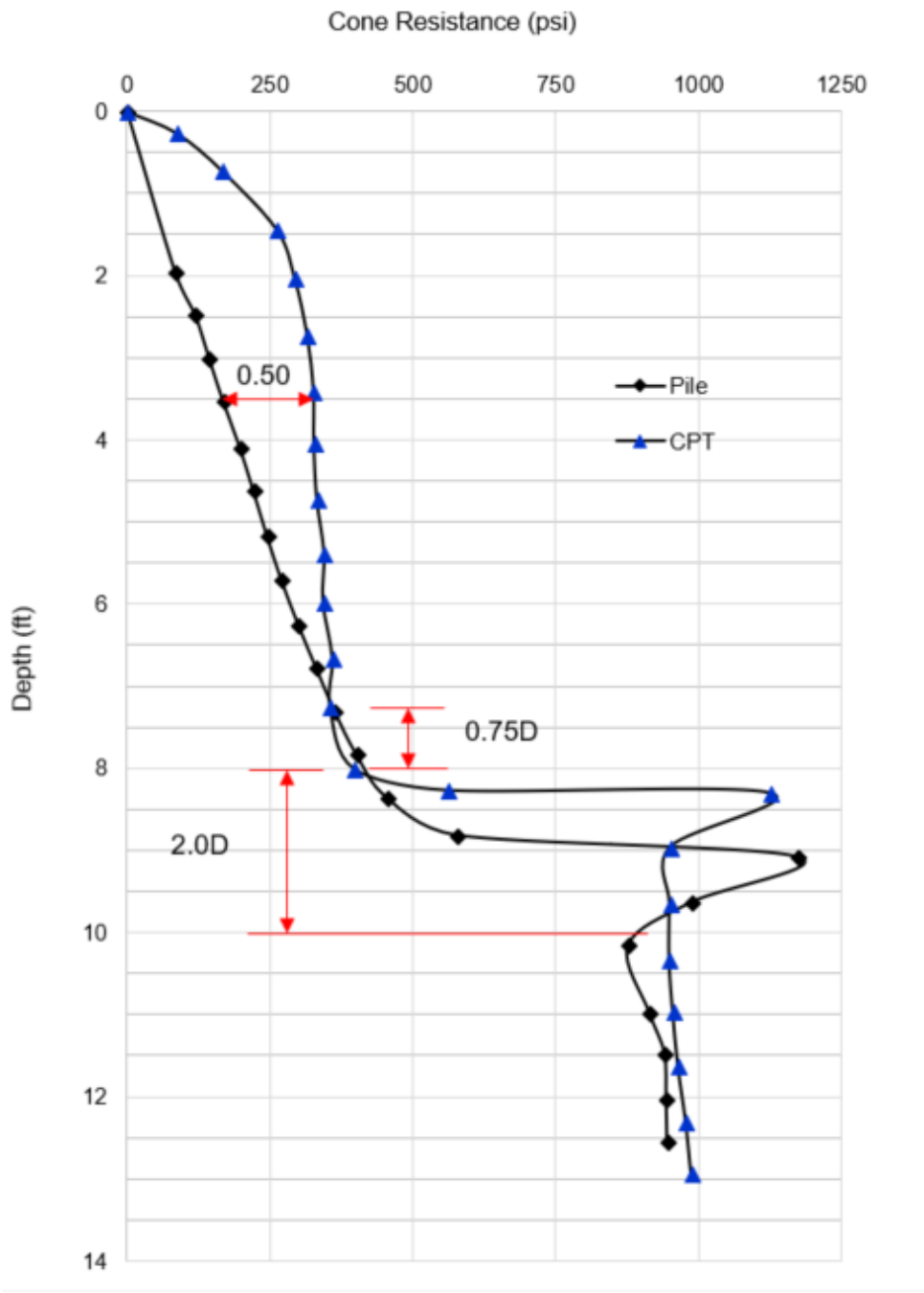

Fig. 6.11 CPT vs Pile tip resistance Model 3

Model 3 indicated the first time there was a measurable mobilization period for the CPT, where the steady state was not reached until 3.5 ft (325 psi). The model also verified a higher tip response in the loose sand compared to the soft cohesive material as expected. The pile penetrated with a linear resistance mobilization trend, requiring almost the entire depth of layer 1 to reach the q_c value. The q_b/q_c ratio determined for this analysis was 0.50. Influence depth below the pile tip was only, 0.75D suggesting minimal impact from dense sand until actual pile embedment has taken place. Conversely, influence above the tip was at least 2.0D in the loose sand. Similar to the cohesive material, the weaker strata show a more significant influence length. Once the CPT/pile reach the dense sand, resistance immediately increases to over 1000psi. Furthermore, a node to the right for both plots is evident in the dense sand. This response is similar to behavior observed in a direct shear test where dilation occurs, and the initial interlocking of highly angular particles must be overcome followed by a residual strength. A slight lag is observed in the pile response compared to the CPT which has a nearly horizontal resistance increase curve at the layer boundary. The tip resistance in the dense sand is over 4x the value observed in the strictly cohesive stiff soil.

6.6 Model 4 – Granular dense overlying loose

Dense material over loose material offered another chance to observe the effect of weaker strata not directly in contact with the pile, but potentially impacting the bearing capacity. The scenario is possible in many of Nebraska's alluvial environments where alternating layers of loose and dense poorly graded sands/gravels are present, which is certainly relevant to bridge foundations. Influence depths were calculated at 1.5D above and below the pile tip for this scenario. The CPT's mobilization period was shorter than

observed in the loose sand, however it is still longer than cohesive conditions. A similar linear pile resistance development period can be seen in Figure 6.12, with a brief steady state, before the loose underlying material begins to decrease the pile resistance. The CPT quickly indicates the drop in strength, while the pile maintains some resistance from the dense sand above. The q_b/q_c ratio in dense granular material proved to be the lowest among the models, corresponding to the slow mobilization of strength. The difference in pile resistance when encountering dense material between models 3 & 4 was an unexpected result. Possible explanation for such behavior could be due to short vs deeper pile embedment lengths suggests White & Bolton (2005). Another key outcome from this model was the discrepancy in steady state below 10ft, with q_c exceeding q_b. Further investigation into the volumetric strain gave insight into the behavior. Large strains observed in Figure 6.14 (pile) compared to Figure 6.13 (cone) for the case of a constant elastic modulus would increase the confining pressure. This points to the larger soil deformation of the pile inducing a densification effect on the loose material, that the smaller CPT cone simply cannot achieve. As a result, the pile experiences a slightly higher end resistance in the same material compared to the CPT profile.

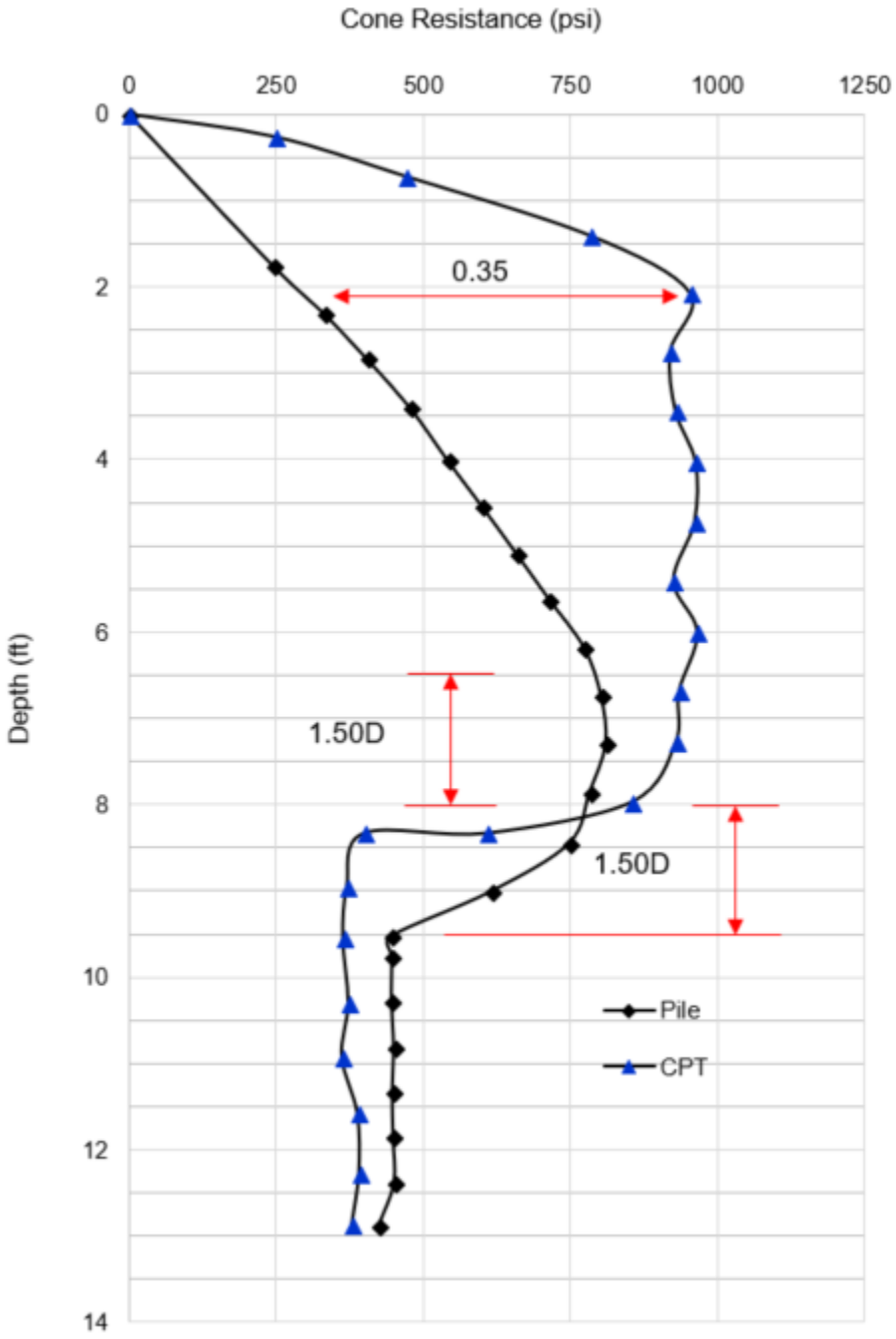

Fig. 6.12 CPT vs Pile tip resistance Model 4

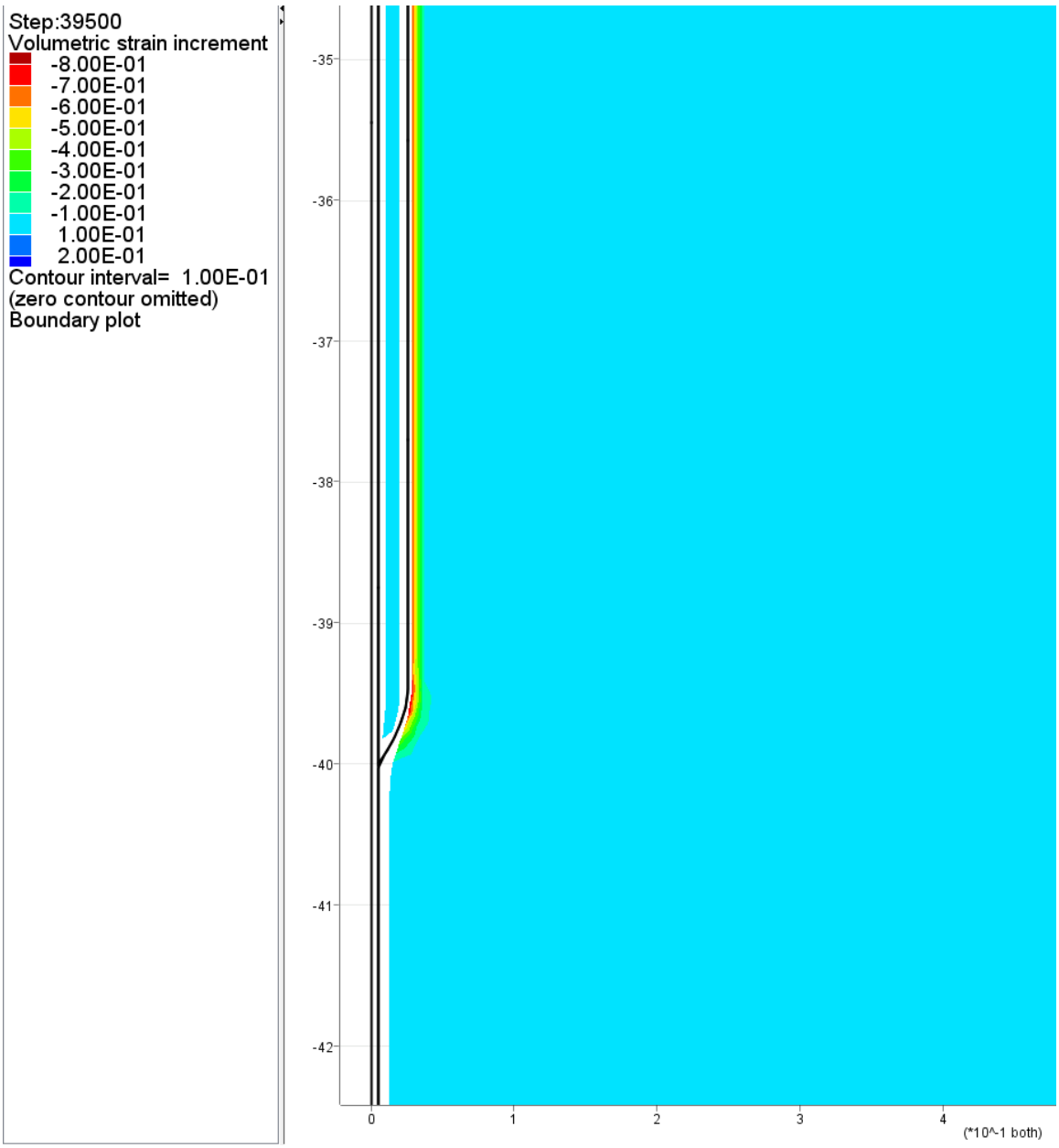

Fig. 6.13 CPT volumetric strain Model 4

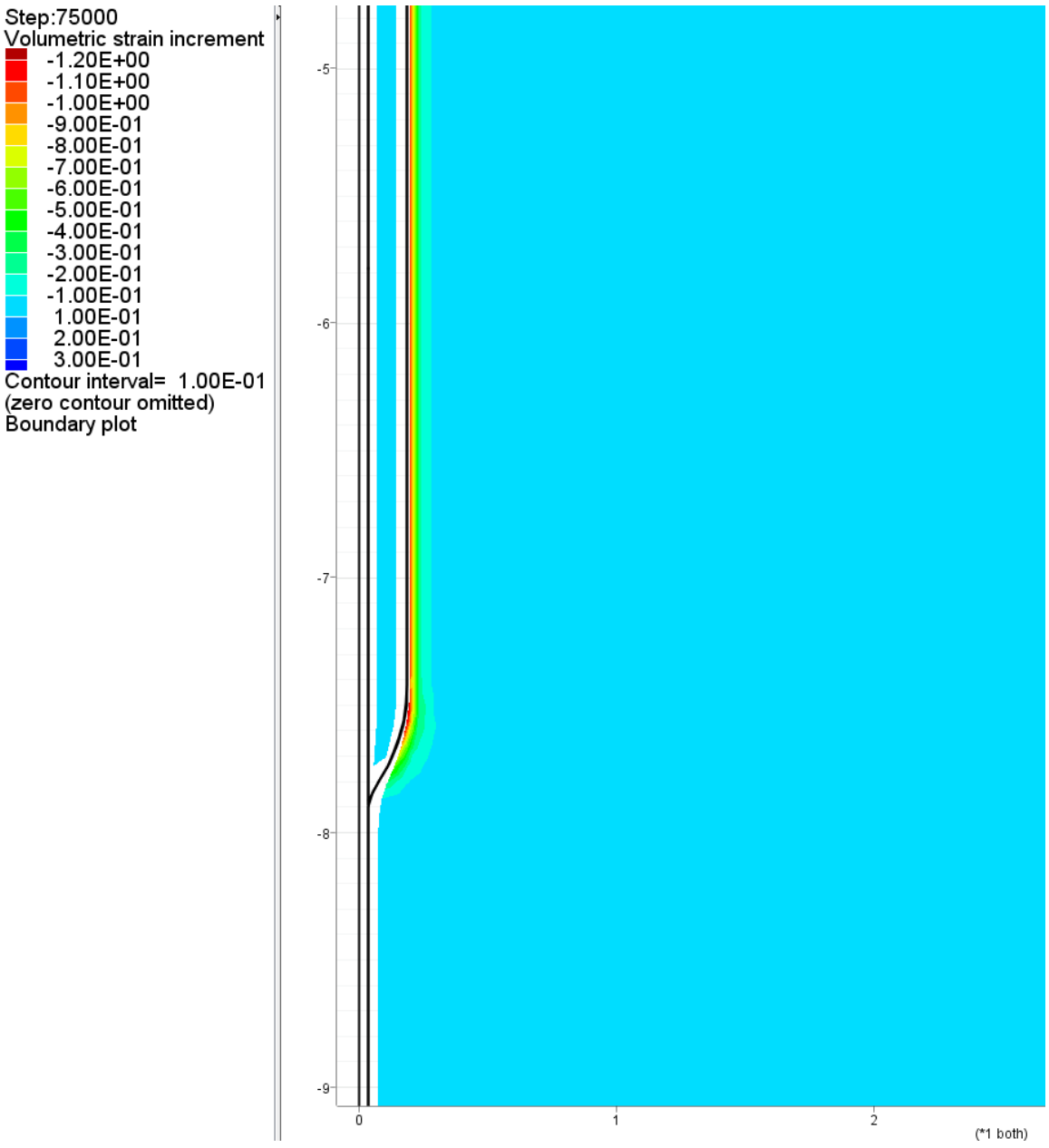

Fig. 6.14 Pile volumetric strain Model 4

6.7 Model 5 – Granular/Cohesive dense over soft

The final two models considered mixed soil conditions, combining granular and cohesive material. Model 5 evaluated an often-considered critical bearing state, that is dense sand underline by soft cohesive material. Pile designers typically avoid placing a pile toe in these scenarios due not only to capacity reduction, but also the potential for settlement. Similar behavior observed in model 4 held true in this model regarding CPT and pile behavior in the dense sand. An identical q_b/q_c ratio of 0.35 was observed. Pile resistance mobilization was again linear and slow, and in this case never reached steady state due to the influence of the soft lower layer. Influence depths of 1.5D above and below the pile tip were determined for the model. The CPT recorded a quick response to the reduction in tip resistance found in layer 2, while the pile showed a staged decrease. Prior to contact the pile slowly decreased end capacity, then quickly dropped to steady conditions by 10 ft. The lower portions of the plot indicate quality model performance at 145psi in the soft soil.

6.8 Model 6 – Cohesive/Granular soft overlying dense

Model 6 evaluated a very common bearing condition and was encountered at project 77-2(1025) discussed earlier in the chapter. Both the CPT and pile quickly mobilized the strength in the soft cohesive upper layer. Steady state was reached in the first 3.0 ft. A q_b/q_c ratio of 0.74 was found in this study, agreeing with the piles brief mobilization length. The pile corresponded to the CPT's rapid detection of the dense lower layer with only a 0.5 ft lag observed. A larger influence depth of 2.0 above the tip can be seen, which is consistent with previous findings for soft materials. Unexpectedly, there is no apparent influence below the pile tip gained from the dense sand layer. While

not initially intuitive, this could perhaps be explained the difference in cohesive and granular strengths. First, the horizontal stress dominates the dense sand condition, while it is minimal for layer 1. Large deformation takes place in the cohesive layer one. The cohesive material is essentially independent from horizontal stress and friction, while the sand layer is limited in vertical stress impact and cohesion. This leads to independent behavior at the layer interface and thus little influence obtained below the pile tip. Figure 6.16 shows the rapid pile response once in contact with the dense layer.

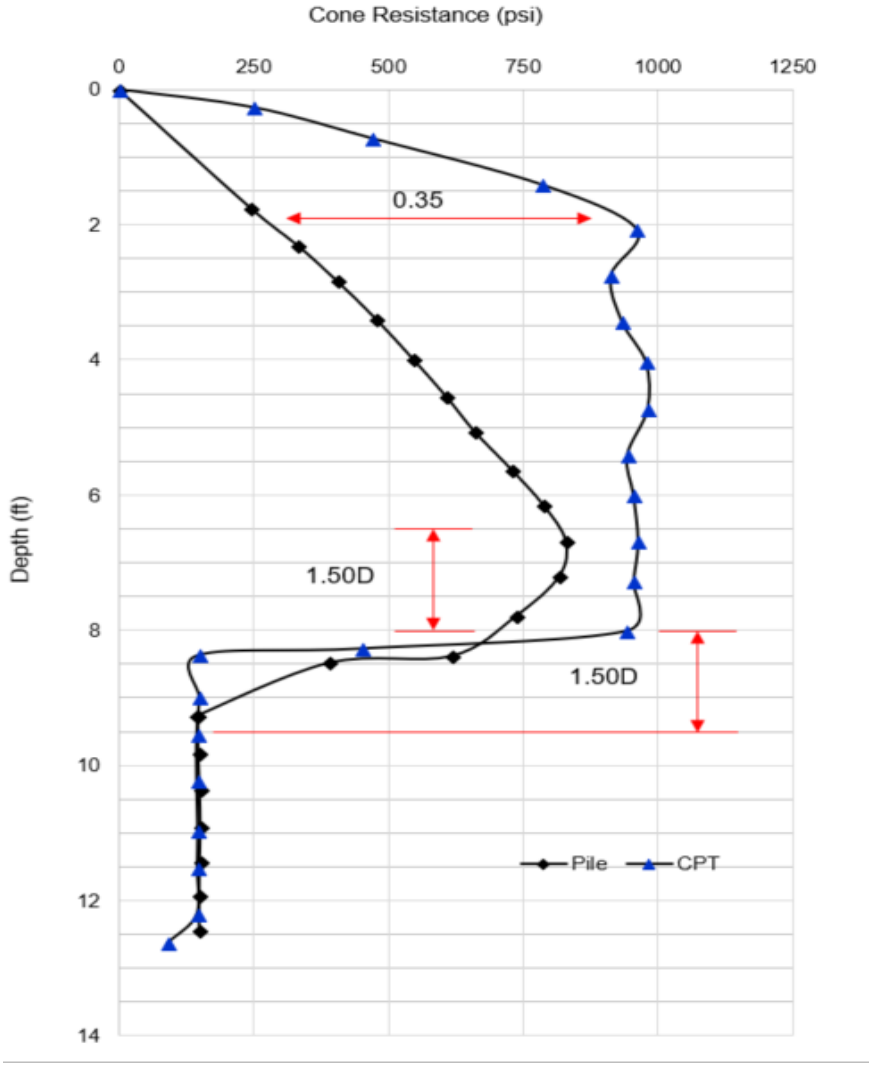

Fig. 6.15 CPT vs Pile tip resistance Model 5

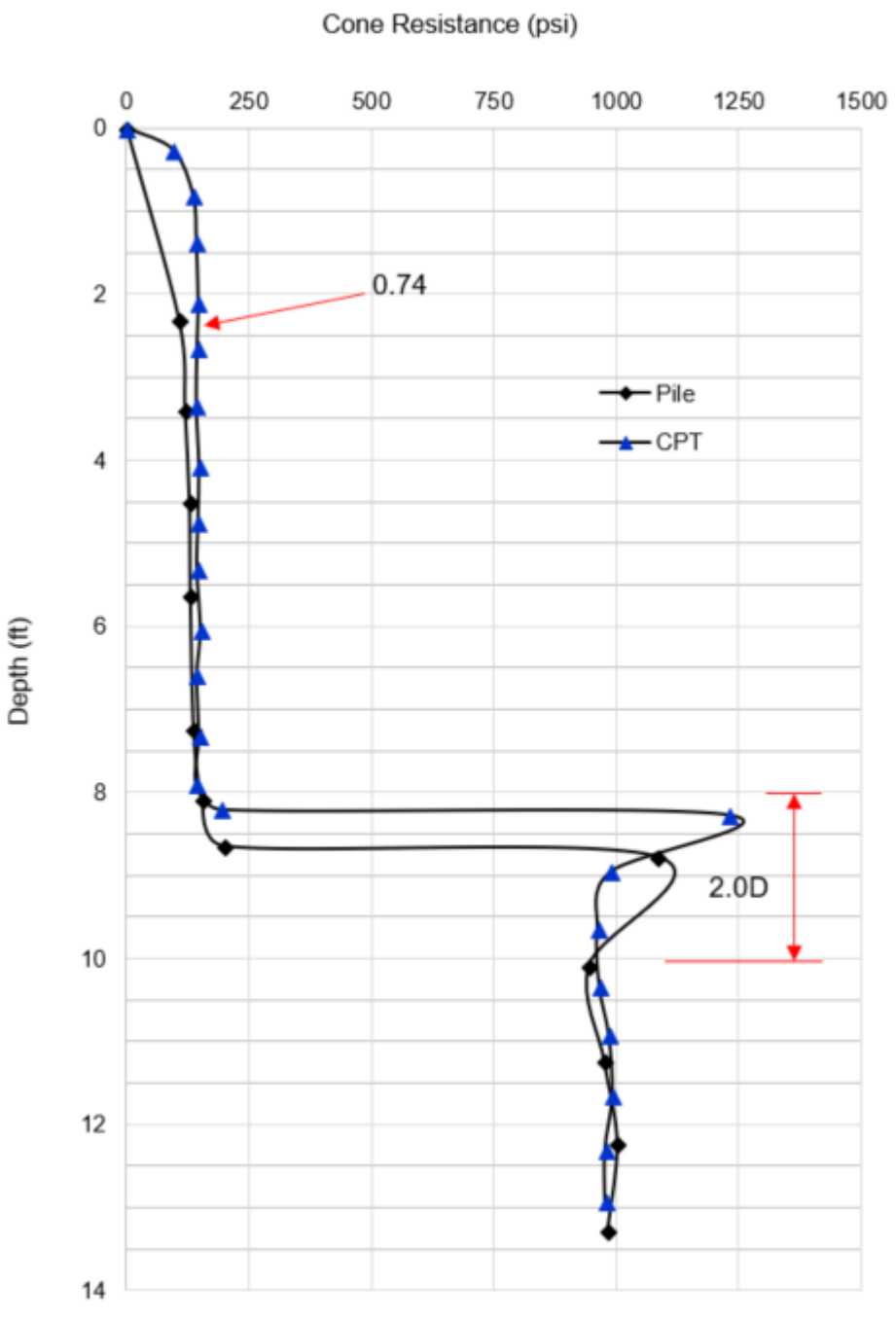

Fig. 6.16 CPT vs Pile tip resistance Model 6

6.9 Numerical Study Summary

The computational modeling offered further insight into the behavior of driven pile compared to the CPT. Numeric verification of measured CPT profiles was achieved for two projects. Various soil stratifications were studied to obtain q_b/q_c ratios and additionally influence depths for the pile case were derived. Pile to CPT end resistance factors were found to be 0.60 – 0.75 for cohesive materials. For granular materials, values were 0.35 for dense sand/gravel and 0.50 for loose material. These values correspond with reduction ratios suggested by empirical methods studied. Values found from the models were slightly higher than the empirical methods, with Prince & Wardle indicating 0.35 for all driven pile, and Philipponnat reporting 0.35-0.4 (sand/gravel) and 0.50 (clays). Influence depths generally were found to be between 1.0D and 3.0D for the pile, while CPT had a fairly constant 10D influence depth below the cone, though still quantitatively small due to the much smaller diameter. Softer/looser materials demonstrated a larger influence length, especially above the pile tip compared to stronger soils. Pile embedment depth also played a large role in the mobilization behavior of the pile. The influence ranges indicated by the modeling results indicate that many of the empirical methods overestimate the zone of influence impacting end bearing. However, due to the limited scope and simplification of soil profiles, the constructed models may not cover full behavior. If weak layers are fairly thin and surrounded by stronger material, this could lead to over prediction by the CPT methods. Overly large influence depths up to 8D suggested by some methods could dampen the local weak/strong layers recorded by the CPT.

CHAPTER 7 CPT CAPACITY CALIBRATION

7.1 Introduction

Once prediction accuracy and statistical evaluation was completed, the next phase of this project was to adjust empirical factors for the predictive methods. By doing so, the goal is to increase accuracy of the CPT capacity methods, thus providing confidence in the CPT method of pile analysis compared to traditional methods. An attempt was made to calibrate all eight methods, while realizing not all methods may prove to be viable for accurate prediction. However, from a design perspective, having results from multiple methods will form a capacity envelope. With experience and engineering judgment, certain methods may offer optimal performance in varying conditions, or perhaps give a consistent more or less conservative prediction.

The basis for the CPT calibration was the CPT/PDA prediction ratio graphs extensively analyzed in the prior chapter. By adjusting empirical factors of the base equations, predicted capacities were modified to more closely match dynamic load test data. These adjustments represent multiple factors related to final determination of bearing capacity. First, and maybe most significantly, by scaling the point resistance (q_c) and sleeve friction (f_s) obtained from the cone penetration, Nebraska specific soil conditions are accounted for which is necessary because predictive methods explored in this project were not originally derived for the region. As an example, prediction quality explored by Abu Farsakh & Titi (2004) was conducted in Louisianan alluvial delta materials. In contrast, generally over consolidated windblown loesses, glacial tills, and some IGM's were encountered in this investigation. Similarly, NDOR uses

predominantly a few sizes and type of pile for bridge foundations, so empirical adjustments may account for properties unique to said pile. Driving systems and losses are also a factor in accuracy since the load response is measured to determine bearing capacity of soils, and a partially accounted for since similar diesel hammers are used.

7.2 Methodology

New factors were introduced to end bearing and skin friction capacity components of the CPT methods. Based on the results of the sorted evaluation, the empirical adjustments were made separately for end bearing and skin friction controlled pile based on the criteria discussed earlier. Improvement in accuracy was assessed by moving the CPT/PDA ration closer to 1:1, reduction in standard deviation, and finally improvement in linear fit quality. Rather than attempting to directly calibrate the total capacity prediction data, the new total capacity was determined from the adjusted end and skin bearing components. The objective was to obtain component accuracy as this holds more value compared to accurate total capacity that may be disproportioned compared to the load test results.

Linear regression slope information gave indication of relative scaling factors needed to improve the CPT predictions. By comparing the regression slope to the 45°-line, indication was given to increase or decrease the CPT parameter. For a baseline factor, equation 28 was used to determine an adjustment parameter, φ.

$$\varphi = \left[\left(1 + P_{reg}\right) * s\right] / P_{reg} \tag{28}$$

Where P_{reg} = slope of the regression line, s = scaling factor. The scaling factor was defaulted to .5 (50%), representing the midpoint between the 1:1 line and the current

regression line. The factor was subsequently modified to optimized the criteria outlined above. The final calibration factors are presented in tables 7.1 below.

Table 7.1 CPT calibration factors for end bearing pile

CPT calibration factors [φ] End Bearing Pile		
Method	**End Bearing Capacity**	**Skin Friction Capacity**
Penpile	*2.057*	*0.763*
Philipponnat	*1.115*	*0.331*
P&W	*1.074*	*0.475*
LCPC	*1.643*	*1.490*
Aoki	*0.688*	*0.685*
Schmertmann	*0.592*	*0.756*
European	*0.805*	*0.690*
Tumay	*0.544*	*0.938*

Table 7.2 CPT calibration factors for skin friction pile

CPT calibration factors [φ] Skin Friction Pile		
Method	**End Bearing Capacity**	**Skin Friction Capacity**
Penpile	*2.383*	*0.588*
Philipponnat	*1.075*	*0.762*
P&W	*1.155*	*1.027*
LCPC	*1.387*	*0.822*
Aoki	*0.864*	*0.393*
Schmertmann	*0.969*	*0.618*
European	*1.266*	*0.579*
Tumay	*0.766*	*0.651*

Statistical evaluation was also used to optimize the calibration factors presented above. Factors were modified based on p-value results from the test, increasing the statistical accuracy of the prediction methods. This evaluation was performed on the piles sorted by bearing criteria for both end bearing capacity and skin friction capacity. A bar graph was created for each of the four categories, indicating the relative quality of each prediction method. Furthermore, categorized approach indicates what particular pile type and bearing portion the method may or may not excel at in prediction. The following figures are the calibrated CPT methods t-test results for the two bearing conditions and two pile types.

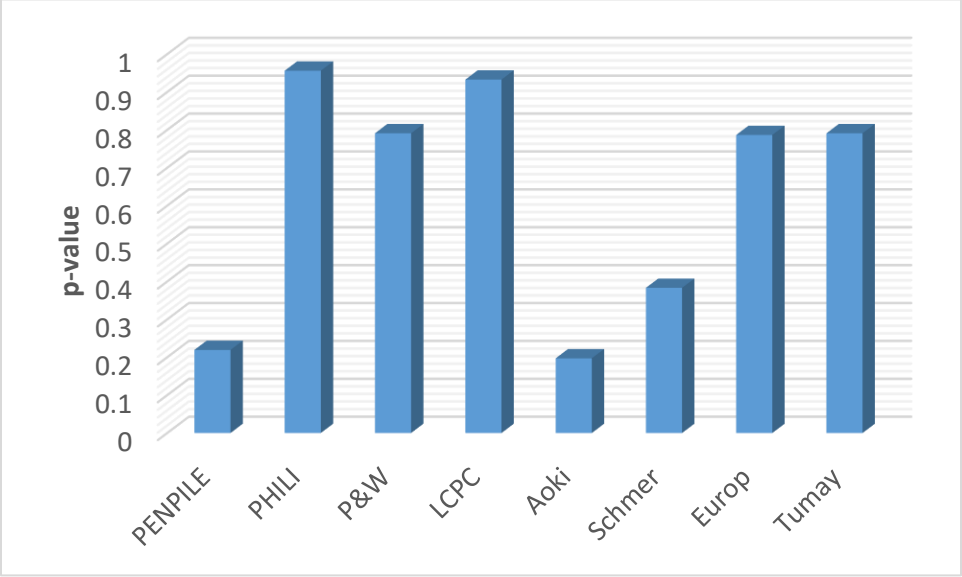

Fig. 7.1 CPT Accuracy Level – End Bearing Capacity-End Bearing Pile

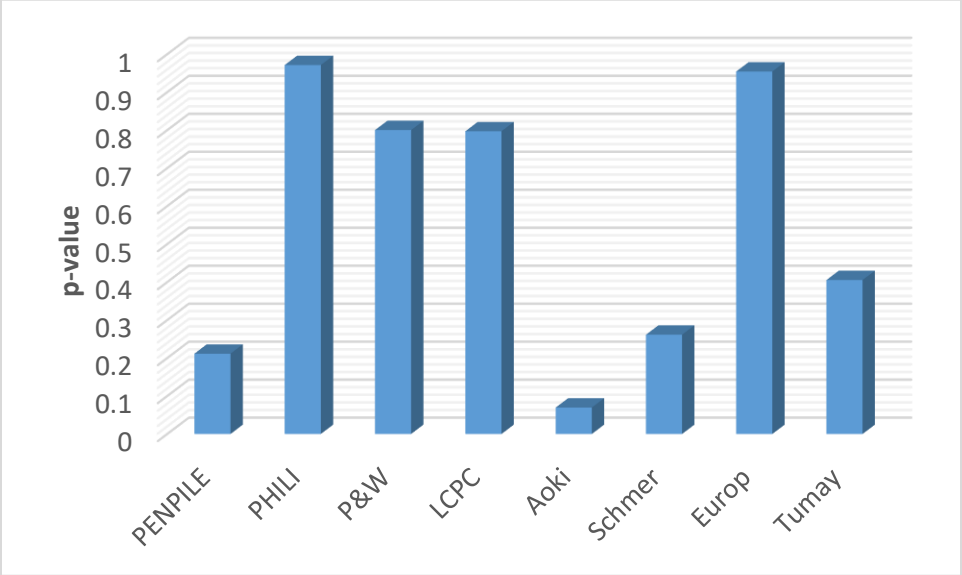

Fig. 7.2 CPT Accuracy Level – End Bearing Capacity-Skin Friction Pile

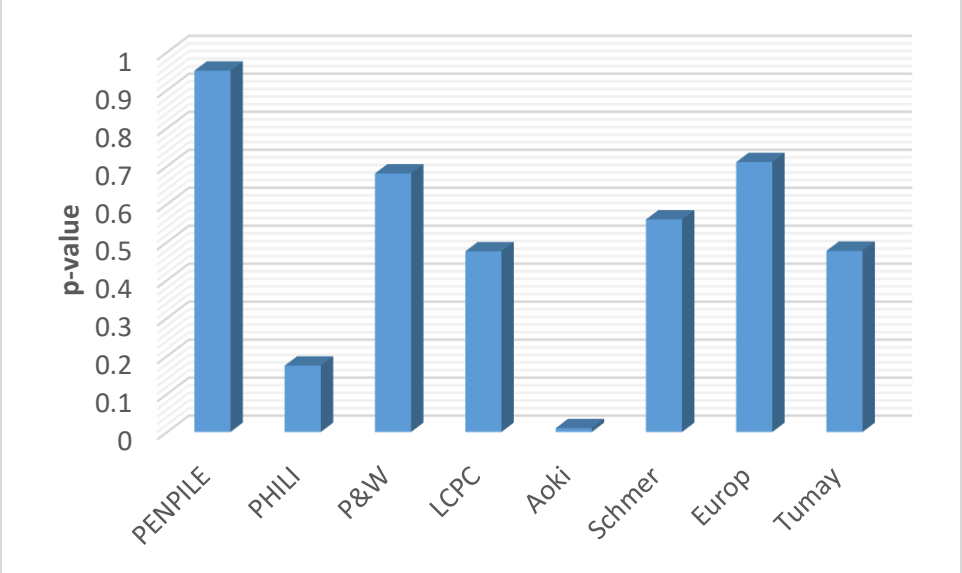

Fig. 7.3 CPT Accuracy Level – Skin Friction Capacity-End Bearing Pile

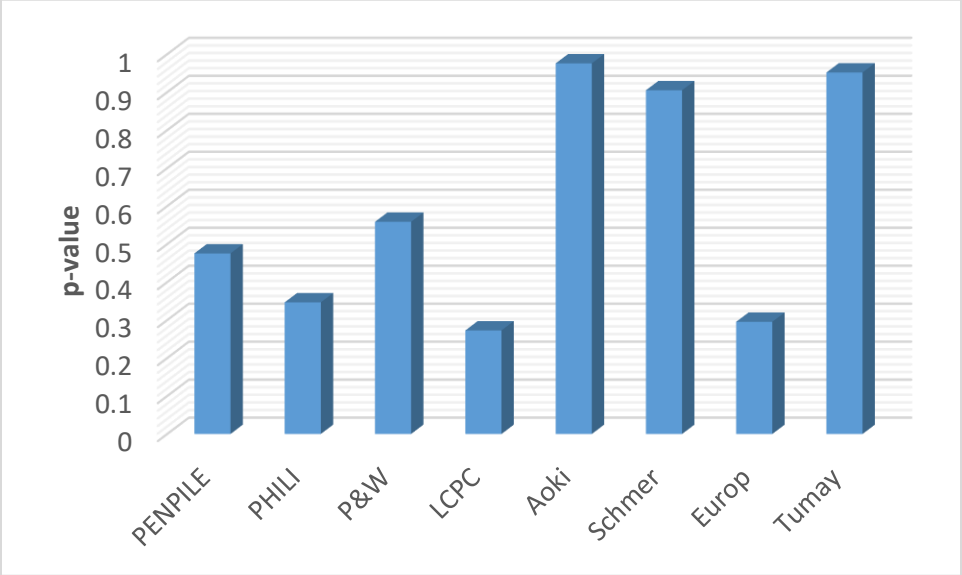

Fig. 7.4 CPT Accuracy Level – Skin Friction Capacity-Skin Friction Pile

The post calibration statistical analysis indicates significant improvement in prediction accuracy compared to the base CPT equations. The end bearing pile charts show that five of eight methods have p-values greater than 70% for end bearing capacity, and four methods exceeding the 60% threshold for skin friction capacity prediction. Similarly, for the case of side friction pile end bearing capacity results finished with two methods just under 80% and two methods exceeding p-values of 0.90. Skin friction capacity prediction also improved, with three methods indicating accuracy levels near 90%. These results are encouraging not only because the p-values increase post calibration, but more so because multiple methods indicate improved prediction performance compared to base results. Agreement in prediction by more than one methods speaks to higher reliability in CPT based bearing capacity prediction for pile. Additionally, multiple methods showing quality prediction for the individual bearing capacity components (end and skin capacity), increase the likelihood that total capacity will be accurate.

Accurate total capacity prediction is the ultimate goal of the calibration adjustments conducted above. Final CPT/PDA prediction charts and subsequent statistical evaluations were prepared for all eight CPT methods from the aggregated component capacities. Based on the positive results of the sorting process, it was deemed beneficial to measure the performance separately for end bearing (HP pile) and skin friction (steel pipe & concrete) piles. CPT/PDA charts for total calibrated capacity are shown in Figures 7.5 & 7.6.

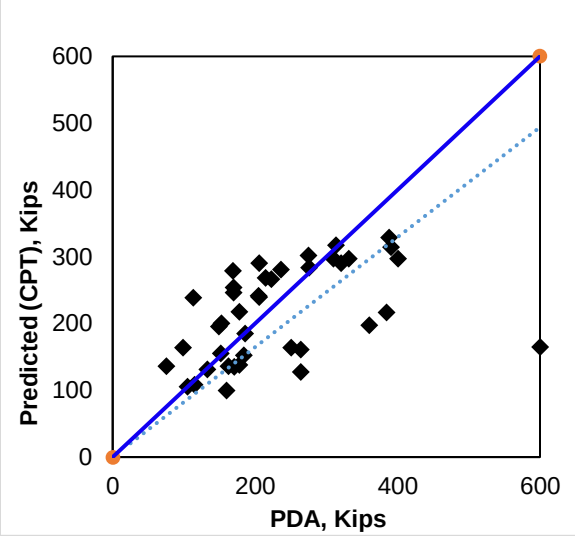

(a) Penpile

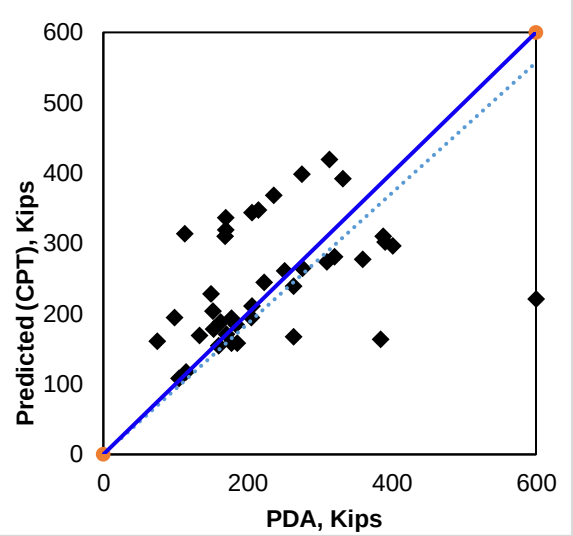

(b) Philipponnat

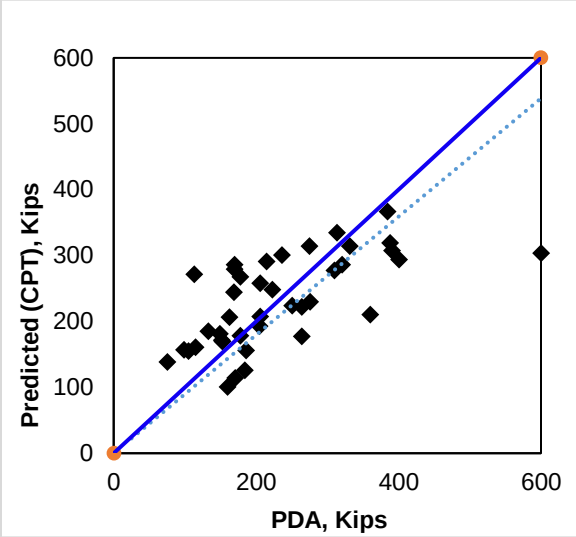

(c) Prince & Wardle

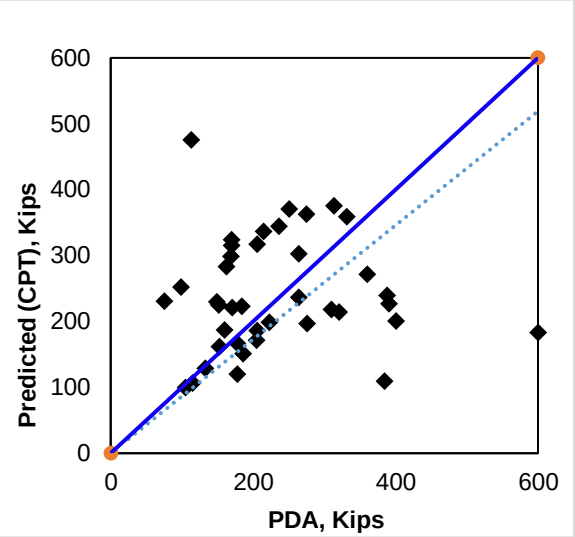

(d) LCPC

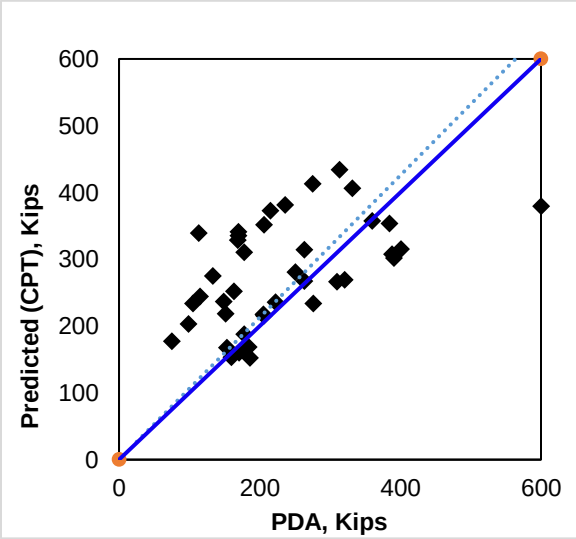

(e) Aoki

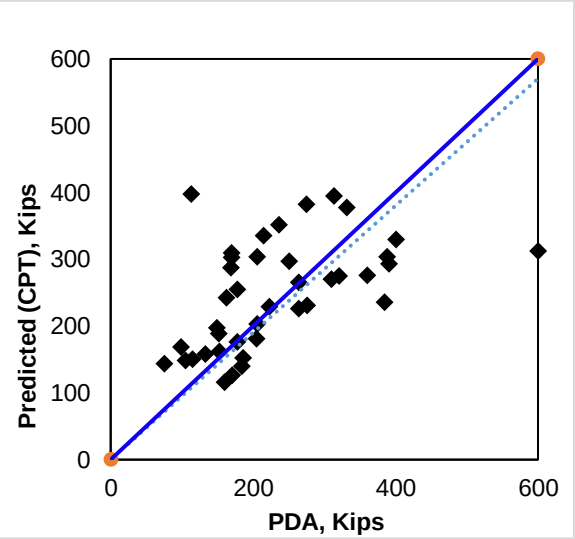

(f) Schmertmann

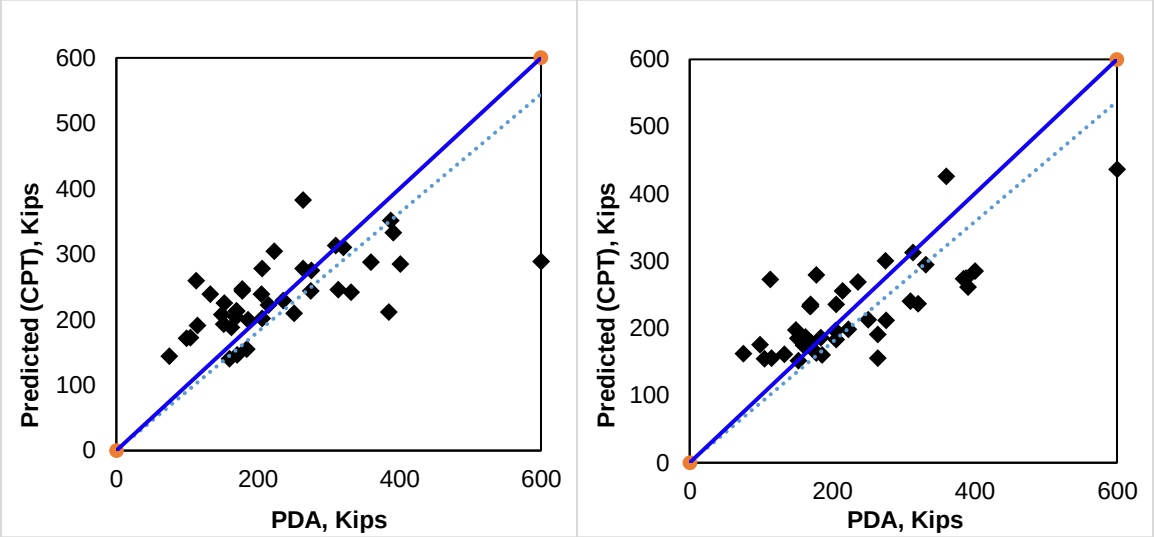

(g) European (h) Tumay & Fakhroo

Fig. 7.5 End Bearing Pile – Total Calibrated Capacity - PDA vs CPT methods

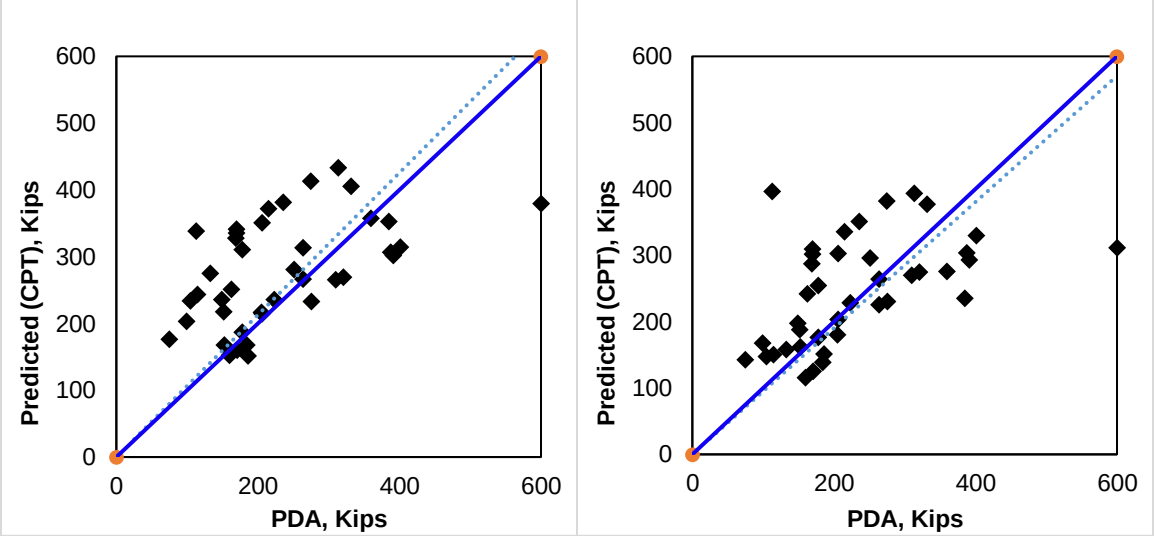

(a) Penpile (b) Philipponnat

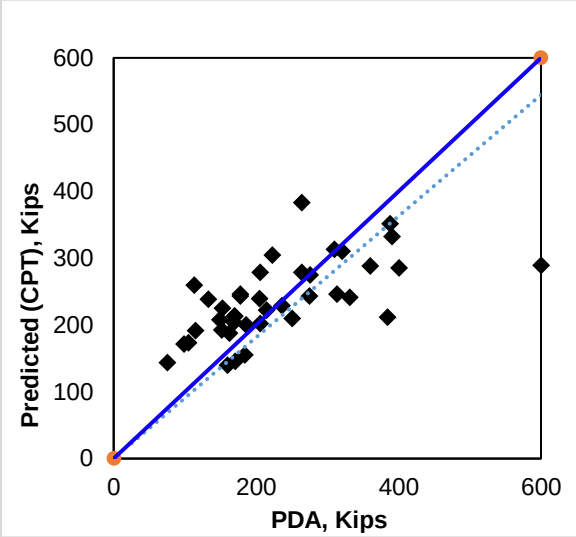

(c) Prince & Wardle

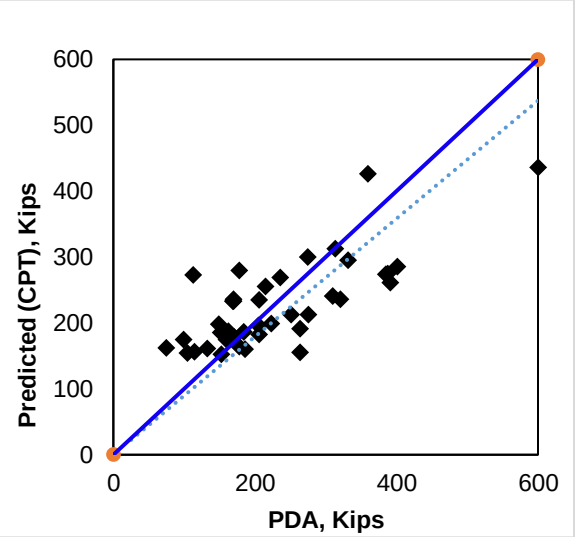

(d) LCPC

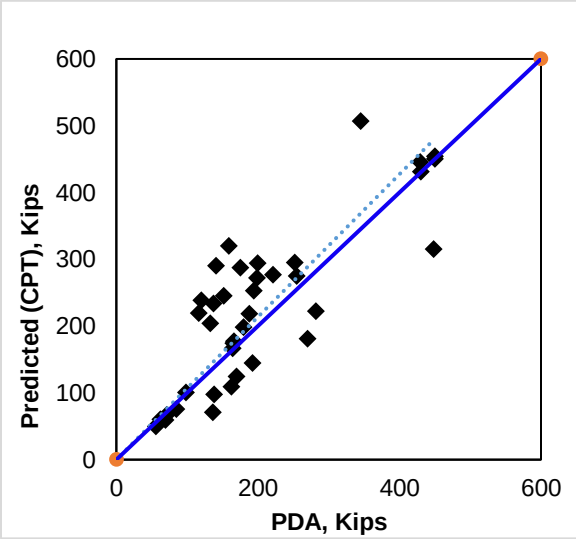

(e) Aoki

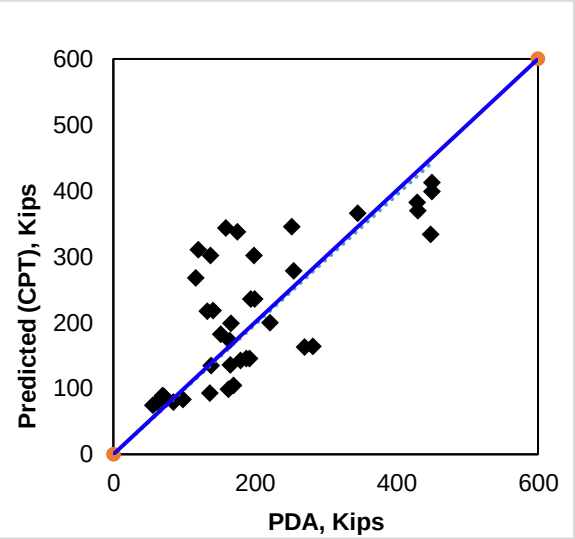

(f) Schmertmann

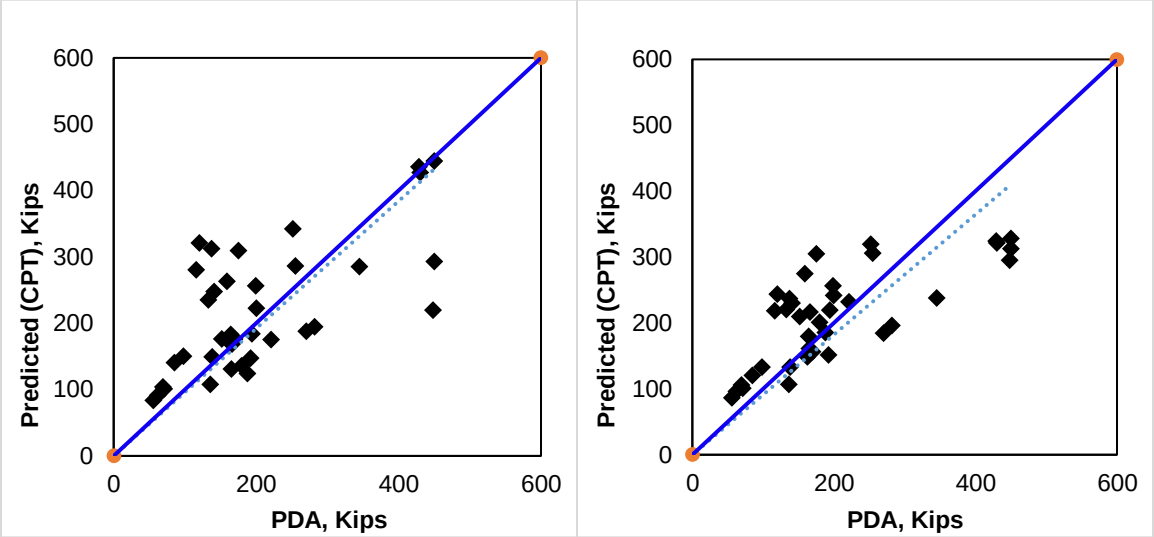

(g) European (h) Tumay & Fakhroo

Fig. 7.6 Skin Friction Pile – Total Calibrated Capacity - PDA vs CPT methods

Statistical performance measured by the t-test demonstrated significant improvement from the baseline CPT equations. Four of eight methods had p-values exceeding 0.60 after calibration, with Prince & Wardle's p-value in excess of 90%. Skin friction pile prediction also improved, and three of the methods had p-values at or over 0.50. Based on the t-test the calibrated Penpile method was the most accurate at 90% p-value. In general, statistical evaluation indicated higher p-values for end bearing piles compared to skin friction reliant piles. Refer to Figures 7.7 & 7.8 for the t-test outcomes. This trend is in agreement with the results of the individual bearing component analysis, where statistical accuracy was higher for the HP piles compared to pipe & prestressed concrete piles.

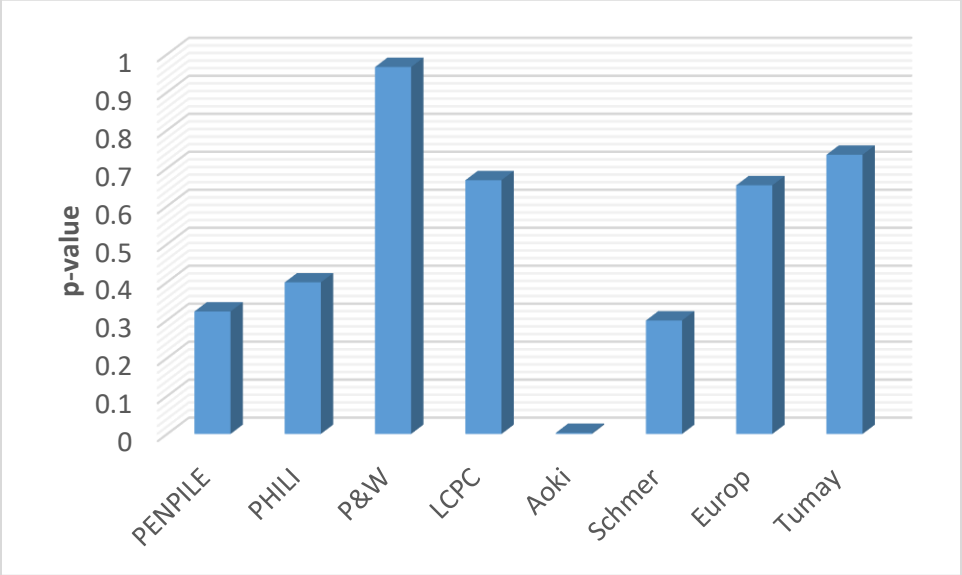

Fig. 7.7 Calibrated CPT Accuracy Level – Total Capacity – End Bearing Pile

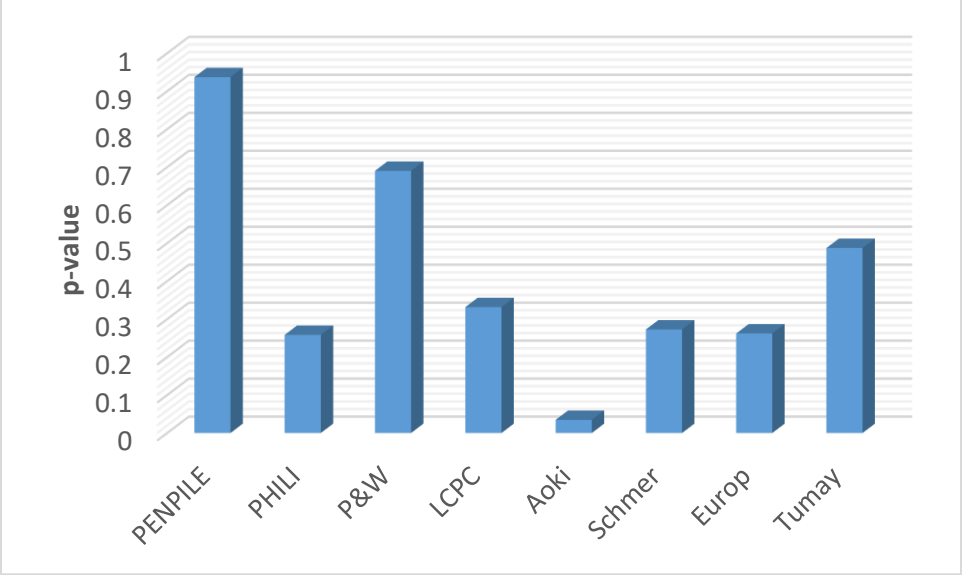

Fig. 7.8 Calibrated CPT Accuracy Level – Total Capacity – Skin Friction Pile

7.4 Validation Test Cases

While the calibrations presented above are based on the entire data population, further study was conducted to verify the modified CPT equations and gauge confidence of predictive methods. To this end, two bridge sites were set aside from the previous analysis phases conducted in this project. These projects were selected for two primary reasons. First, both sites have quality CPT data conducted in close proximity to the substructure, and well documented consistent PDA dynamic load test data existed. In conjunction, complete driving records and boring logs were available for complete analysis and verification. The second rational came from discussion with NDOR engineers regarding the soil conditions observed at each site. Both project 80-9(830) and 15-3(115) have primarily soft fine grained material with low SPT counts to depth. Underneath, firmer glacial till formations are present. Advisory committee members felt that these conditions represented optimal conditions where CPT geotechnical investigation could be deployed for bridge foundations with successful results. This is quantified by reaching necessary scour depths with the probe and offering time savings versus traditional mud rotary drilling methods conducted by department staff.

Both pile bearing mechanisms were represented by these projects with S080 41856 using HP12x53 piles while S015 13411 was constructed with steel pipe piles. This allowed for both sets of CPT method calibration factors to be tested. Tables 7.3 & 7.4 give a summary of PDA/CAPWAP load test results and calibrated CPT capacity predictions. Complete tabulated results can be found in Appendix A. 15 comparisons were made for these two projects, nine for pipe pile and six for HP pile.

Table 7.3 Summary of load test results for validation dataset

Log ID	SN	Subst	Pile Type	Length in Place [ft]	Driving Eqn Ultimate [kips]	CW-total [kips]	CW-skin [kips]	CW-end [kips]
1c	S015 13411	A1	pipe	66	143	185	76	109
2c	S015 13411	A1	pipe	69	165	232	179	53
3c	S015 13411	A1	pipe	72	182	249	178	71
4c	S015 13411	B1	pipe	52	240	197	113	84
5c	S015 13411	B1	pipe	55	298	204	148	56
6c	S015 13411	B1	pipe	59	246	223	152	71
7c	S015 13412	B2	pipe	57	202	185	116	69
8c	S015 13412	B2	pipe	60	212	201	154	47
9c	S015 13412	B2	pipe	62	216	217	160	57
10c	S080 41856	A1	HP12x53	64	122	171	147	24
11c	S080 41856	A1	HP12x53	67	171	160	133	27
12c	S080 41856	A1	HP12x53	70	210	198	166	32
13c	S080 41856	A2	HP12x53	62	188	276	194	82
14c	S080 41856	A2	HP12x53	65	231	302	232	70
15c	S080 41856	A2	HP12x53	68	268	342	255	87

Table 7.4 Summary of CPT capacity prediction for validation dataset

Log ID	CPT Depth [ft]	CW-total [kips]	CPT Method -Total Capacity [kips]							
			1	2	3	4	5	6	7	8
1c	69	**185**	183.6	138.4	169.0	124.7	151.8	186.8	208.0	175.6
2c	72.0	**232**	202.1	151.1	186.6	132.3	167.8	195.9	224.6	189.4
3c	75.0	**249**	215.5	163.6	210.4	139.7	176.9	213.2	245.4	197.8
4c	68.0	**197**	179.5	134.0	151.5	122.1	148.3	183.5	201.8	173.3
5c	71.0	**204**	195.0	146.5	180.5	129.6	162.6	191.5	217.5	184.5
6c	75.0	**223**	215.5	163.6	210.4	139.7	176.9	213.2	245.4	197.8
7c	77.2	**185**	178.9	115.3	150.7	101.7	129.1	173.4	224.9	178.6
8c	80.2	**201**	192.9	127.1	170.5	108.2	142.3	180.7	240.6	190.0
9c	82.2	**217**	203.6	134.1	185.8	112.7	151.4	192.2	256.5	194.6
10c	66.0	**171**	185.0	175.7	145.0	181.3	163.7	165.2	164.5	170.6
11c	69.0	**160**	184.1	177.3	143.5	186.5	172.0	167.3	169.4	176.9
12c	72.0	**198**	206.0	183.8	147.9	196.6	201.9	174.2	178.5	196.4
13c	61.1	**276**	286.0	302.5	278.5	276.1	304.7	307.0	259.2	246.9
14c	64.1	**302**	302.3	320.0	295.8	290.0	324.2	313.4	261.3	247.9
15c	67.1	**342**	315.8	338.9	312.4	302.4	342.5	337.0	271.2	263.6

The same forms of performance evaluation conducted for the main dataset was used again to evaluate these final two projects. CPT/PDA prediction ratio plots were compiled; however, all eight methods were combined into one figure for each capacity measure to gage a relative performance of each method. Additionally, total capacity results from the NDOR pile driving equation 25 was overlain (driving equation/PDA) as another comparison. This information if of value because there is often times small discrepancy between the driving equation and CAPWAP results, with the driving typically giving more conservative capacities. Figure 7.9 is the results from project 15-3(115) evaluating skin friction pile.

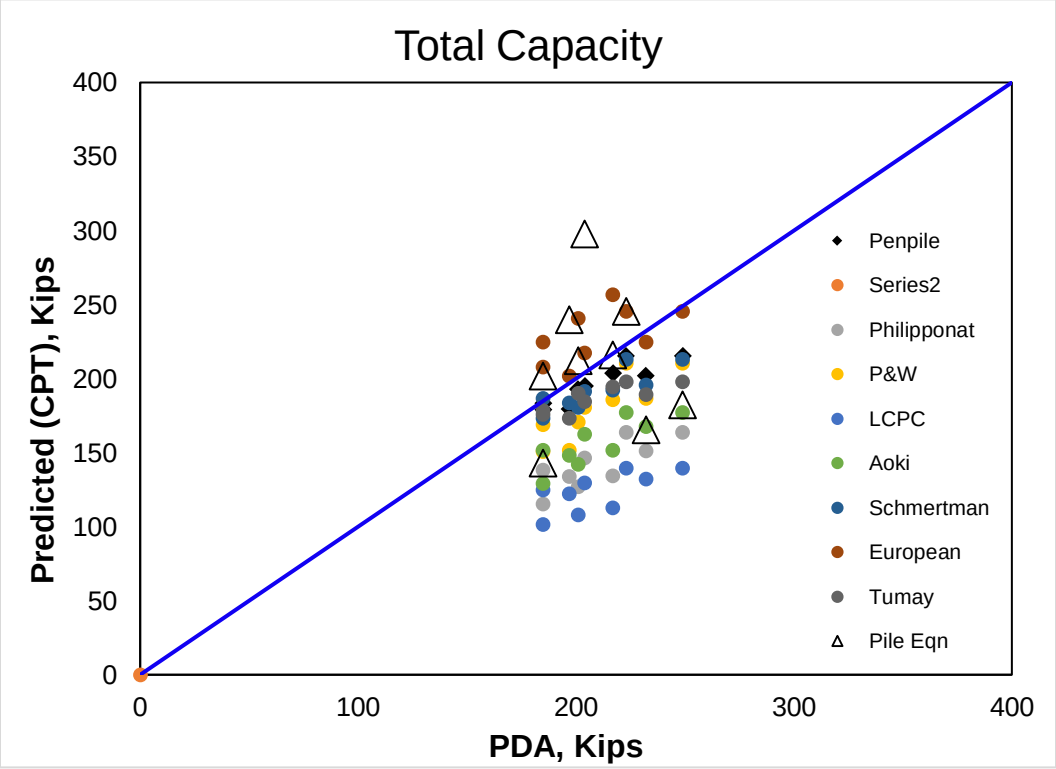

(a) Total Capacity

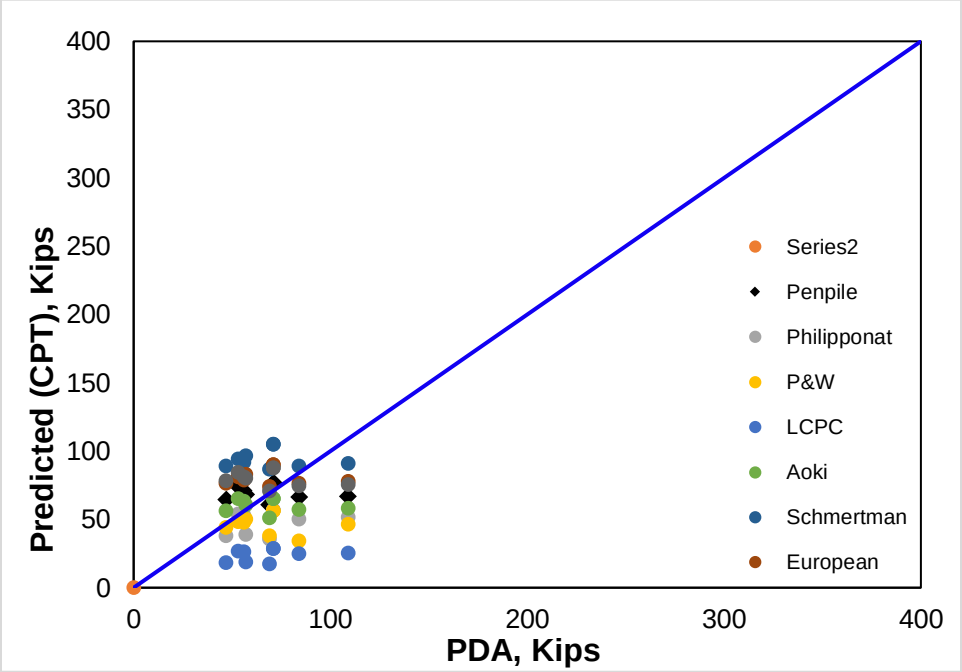

(b) End Bearing Capacity

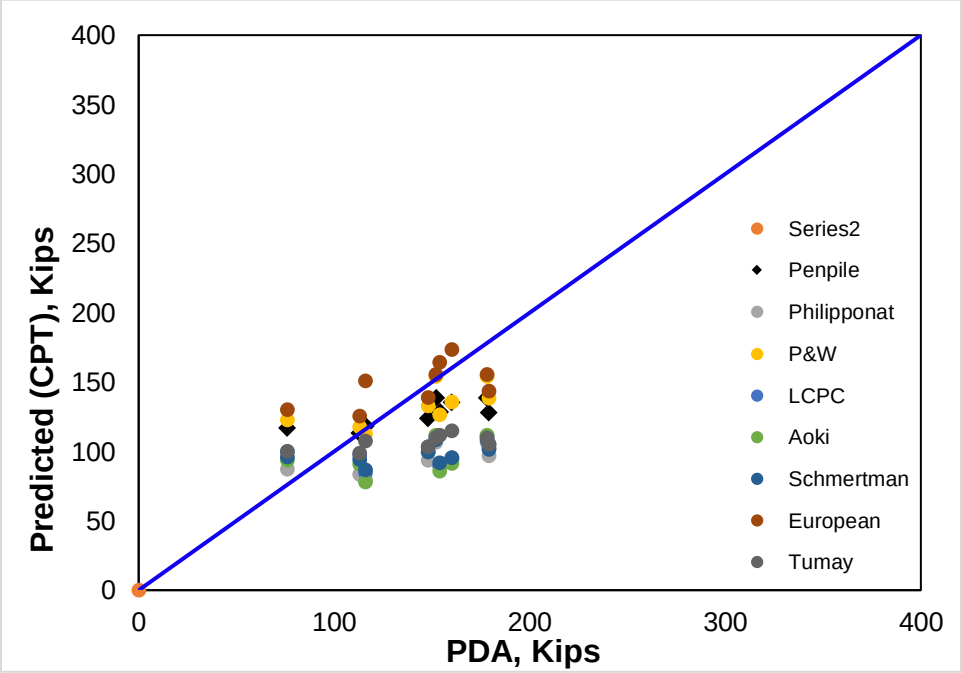

(c) Skin Friction Capacity

Fig. 7.9 Calibrated Bearing Capacity – PDA vs. CPT methods – Skin Friction Pile

The pipe pile studied to test the calibration factors showed generally accurate prediction by the adjusted CPT methods. End bearing capacity ranged from approximately 50 to 110 kips measured by the dynamic load test. The methods formed an envelope above and below the measured capacities. Penpile, Schmertmann, European, and Tumay & Fakhroo appeared to be the most accurate for the end bearing capacity. Graphical observation suggests the most of the CPT methods predicted higher for lower measured capacities and decreased slightly for the higher PDA values. End capacity appears to be slightly underpredicted by most methods. Figure 7.9c plots the skin friction capacity. Penpile, Prince & Wardle, and European methods indicate the most accurate prediction. The comparisons have a fairly consistent slope of increasing CPT capacity relating to pile embedment depth.

Total capacity prediction formed a very close relationship between predicted and measured capacities. Most accurate methods based on this analysis include the European method, with slight overprediction, and Penpile, Prince & Wardle, Schmertmann, and Tumay & Fakhroo methods giving nearly identical predicted capacities slightly below the measured values. The remaining methods under predicted total capacity, however still had a consistent increasing linear trend. These underpredicted capacities may hold value in a more conservative design capacity for pile design. Comparison of the CAPWAP values and predicted CPT capacities to the NDOR pile bearing equation (seen as triangles) confirms reasonably accurate values. The equation capacities indicate some comparisons above and below the dynamic load test data, comparing favorably with the range of values plotted by the eight predictive methods. Considering the soil conditions encountered at the 15-3(115) site the results from these comparisons indicate quality

prediction capability of the CPT methods. The till materials encountered in the lower portion of the pile embedment often gives low hammer fall (small rebound force) and the highly plastic nature yields easily under driving conditions. This behavior was confirmed by the driving logs for this structure. Subsequently, measuring/mobilizing the full capacity in the soil structure is often difficult. There is some spread among the methods, however statistical analysis of the skin friction piles indicated slightly less accurate prediction compared to end bearing pile.

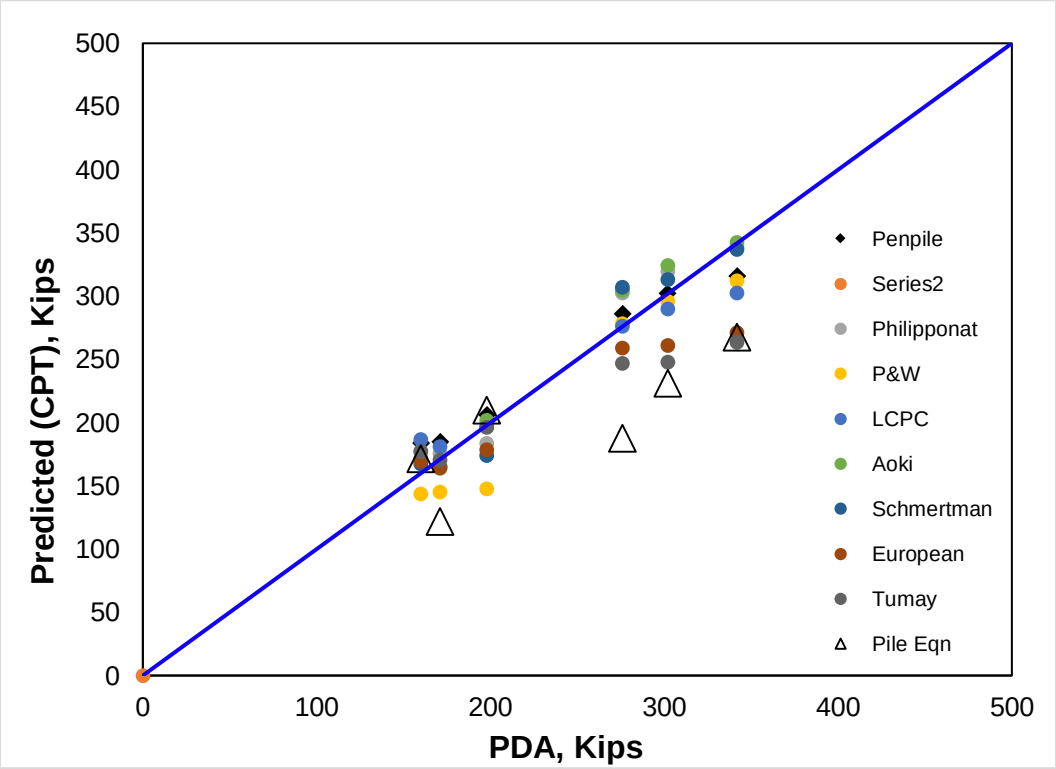

(a) Total Capacity

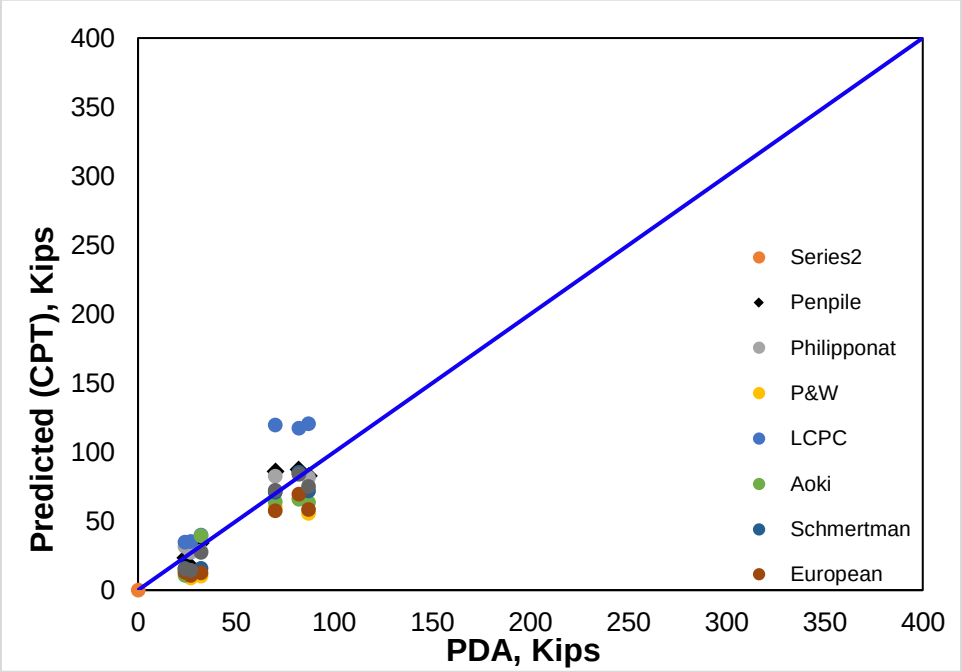

(b) End Bearing Capacity

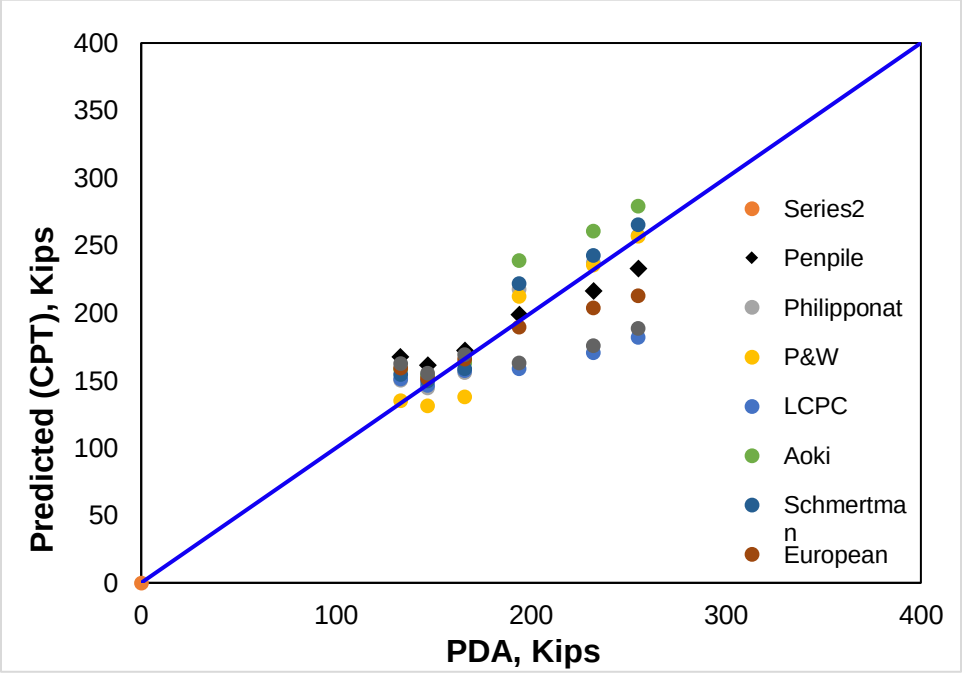

(c) Skin Friction Capacity

Fig. 7.10 Calibrated Bearing Capacity – PDA vs. CPT methods – End Bearing Pile

Figure 7.10 is the results from project 80-9(830) evaluating end bearing pile. Comparison between calibrated CPT empirical methods and dynamic load tests obtained at structure S080 41856 correlated very closely. End bearing capacity seen in Figure 7.10b was very closely grouped to the 1:1 CPT/PDA line for all methods. LCPC slightly overpredicted capacity for the higher PDA capacities, but still error was almost negligible. Results for skin friction capacity also had very good CPT/PDA prediction rations. All eight methods were within a close envelope, with Penpile, European, and Prince & Wardle appearing to be the most accurate for this site. CPT predictions were nearly in total agreement with load test results for the lower three skin frictions, with small variation developing for the comparisons in the 200-250 kip range.

Accuracy for total bearing capacity prediction of the HP12x53 pile in this project demonstrated excellent agreement. Philipponnat and Penpile methods gave the best predictions compared to the PDA measurements. All eight methods showed a strong increasing linear relationship with the load test results. This enhanced accuracy is supported by the higher p-values found for the calibrated methods in end bearing piles compared to skin friction piles. Pile driving equation capacities seen in Figure 7.10a are generally below the dark blue 1:1 line, meaning more conservative axial capacities. This was expected at this site because pile driving records indicated fairly high pile set (movement in/blow) with lower capacities at the end of initial driving. Additionally, fairly high setup factors were recorded at this project. This information suggests the CPT predictions as calibrated may point closer to long term capacities and those that CAPWAP analysis recognizes as higher resistance mobilization. Regardless of the more

conservative capacities, the driving equation supports evidence that the CPT methods demonstrated accurate capacity prediction at this test site.

CHAPTER 8 DISCUSSION & CONCLUSIONS

8.1 Ranking Evaluation

The primary objective of this study was to identify CPT method(s) that most reliably predict bearing capacity of pile, specifically for Nebraska. This task is complicated and from a design prospective carries safety implication. Evaluation conducted in previous sections analyzed three pile types: steel HP pile, steel pipe pile, and square prestressed concrete pile. Some size variation was also considered in the studied projects. With these considerations, it is understandable that a single method may not preform best for all scenarios. A key finding of the CPT prediction evaluation with PDA results was the impact of bearing mechanism, which is related to the pile type. Hence, further analysis of CPT methods was conducted on the categorized basis of end bearing and skin friction pile. Of course, actual piles derive bearing capacity from a combination of resistances, as reflected by the CAPWAP analysis. Optimizations of the prediction methods was based on accurate determination of end and skin portions of the bearing, leading to reliable total capacity prediction. Following this logic, evaluation and ranking of the CPT methods should not only consider total capacity, but accuracy of the components, and moreover for both categories of pile.

Performance ranking introduces subjectivity into the analysis. Prediction accuracy can be defined by statistical means, over/under prediction, and repeatability among other user defined outcomes. Thorough analysis should attempt to consider multiple measures and provide a global view of the evaluation. To this end, a set criterion consisting of four

components was established to measure and ultimately rank the CPT methods effectiveness. These measures are outlined below.

1) CPT/PDA prediction ratio (Q_p/Q_m). This measure provides a sense of inclination for over or under prediction. The value is an average from the entire comparison dataset.
2) Standard deviation. Defined by equation 29, where X is the individual sample, $\bar{X}$ is the sample mean, and n is the population size. This measures the variation in the predicted values away from the expected or mean value.

$$\sigma = \sqrt{\frac{\sum(X-\bar{X})^2}{n-1}} \tag{29}$$

3) P-value from the paired t-test. Refer to section 5.2 for details on this parameter. A statistical approach is an important component of accuracy evaluation.
4) R^2 value. The quality of linear regression fit indicates the quality of the prediction comparisons and also has applicability beyond discrete measurements. This measure was primarily used as a tool to modify CPT equations, improving fit. Intercepts were fixed, affecting the absolute values of the measure.

The criteria listed above was compiled for end bearing capacity, skin friction capacity, and total capacity. A ranking one through eight was assigned to the CPT methods for each of the criteria, then a four-component aggregated ranking score was assigned. The lowest aggregate score indicated the best overall ranking. This procedure is similar with the Abu-Farsakh & Titi 2004 study for Louisiana DOT.

First, methods were evaluated on a component basis; specifically end bearing and skin friction capacity. Assessment was conducted for end and skin friction pile separately. Next, rankings determined for both components were added together to find the best method for end bearing or side friction pile categories. Refer to tables 8.1 - 8.6 for these results.

Table 8.1 Component rankings-End bearing pile-end capacity

	avg		std-dev		t-test-pa		R2	
PENPILE	1.42	1	1.32	1	0.22	7	-1.87	8
PHILI	1.93	5	2.41	4	0.96	1	-1.50	7
P&W	1.82	3	2.42	5	0.79	3	-0.03	2
LCPC	2.25	8	3.96	8	0.93	2	-0.87	6
Aoki	2.00	6	2.59	7	0.20	8	0.01	1
Schmer	2.00	7	2.47	6	0.38	6	-0.58	5
Europ	1.79	2	2.23	3	0.79	5	-0.15	3
Tumay	1.88	4	2.21	2	0.79	4	-0.52	4

Table 8.2 Component rankings-End bearing pile-skin capacity

	avg		std-dev		t-test-pa		R2	
PENPILE	1.24	2	1.34	1	0.95	1	0.50	2
PHILI	1.42	6	1.72	4	0.17	7	0.36	4
P&W	1.20	1	1.35	2	0.68	3	0.54	1
LCPC	1.50	7	1.91	7	0.48	6	-0.18	8
Aoki	1.69	8	2.23	8	0.01	8	0.12	6
Schmer	1.35	4	1.58	3	0.56	4	0.23	5
Europ	1.38	5	1.73	5	0.71	2	0.43	3
Tumay	1.33	3	1.86	6	0.48	5	0.05	7

Table 8.3 End bearing pile component method rank

End bearing		Skin friction		Combined		Rank
13	P&W	6	PENPILE	20	**P&W**	**1**
13	Europ	7	P&W	23	**PENPILE**	**2**
14	Tumay	15	Europ	28	**Europ**	**3**
17	PENPILE	16	Schmer	35	**Tumay**	**4**
17	PHILI	21	PHILI	38	**PHILI**	**5**
22	Aoki	21	Tumay	40	**Schmer**	**6**
24	LCPC	28	LCPC	52	**LCPC**	**7**
24	Schmer	30	Aoki	52	**Aoki**	**8**

Table 8.4 Component rankings-Skin friction pile-end capacity

	avg		std-dev		t-test-pa		R2	
PENPILE	0.98	2	0.57	1	0.97	1	0.36	1
PHILI	1.03	3	0.75	4	0.21	7	0.31	2
P&W	1.05	4	1.01	7	0.80	3	0.31	3
LCPC	0.94	1	1.05	8	0.80	4	0.27	4
Aoki	1.32	8	0.98	6	0.07	8	0.26	5
Schmer	1.23	7	0.83	5	0.26	6	0.23	6
Europ	1.07	5	0.73	3	0.95	2	0.19	7
Tumay	1.19	6	0.70	2	0.41	5	0.14	8

Table 8.5 Component rankings-Skin friction pile-skin capacity

	avg		std-dev		t-test-pa		R2	
PENPILE	1.75	7	1.31	7	0.48	5	-5.69	8
PHILI	1.30	1	0.80	1	0.35	6	-2.45	7
P&W	1.67	4	1.26	6	0.56	4	-2.36	6
LCPC	1.70	6	1.08	3	0.27	8	-1.69	4
Aoki	1.45	2	0.91	2	0.98	1	-1.49	1
Schmer	1.60	3	1.17	4	0.90	3	-1.59	3
Europ	1.89	8	1.41	8	0.30	7	-1.53	2
Tumay	1.68	5	1.26	5	0.95	2	-1.98	5

Table 8.6 Skin friction pile component method rank

End bearing		Skin friction		Combined		Rank
5	PENPILE	6	Aoki	31	**PHILI**	**1**
16	PHILI	13	Schmer	32	**PENPILE**	**2**
17	P&W	15	PHILI	33	**Aoki**	**3**
17	LCPC	17	Tumay	37	**P&W**	**4**
17	Europ	20	P&W	37	**Schmer**	**4**
21	Tumay	21	LCPC	38	**LCPC**	**6**
24	Schmer	25	Europ	38	**Tumay**	**6**
27	Aoki	27	PENPILE	42	**Europ**	**8**

Component based performance measurement shows that for end bearing pile, Prince & Wardle, Penpile, and European methods are most accurate. The top three methods for friction pile are Philipponnat, Penpile, and Aoki & De Alencar. Performance scores were quantitively lower for end pile compared to friction pile, however the range of scores from 1st to 8th is substantially large for the end pile. Lower score values suggest that methods ranked more consistently among each of the four criteria, meaning end bearing pile prediction may be slightly more accurate of the two categories. Higher variation in compiled scores means more differentiation between the best and poorest ranking methods. Low score spread for friction pile suggests that difference between methods quality is less significant.

Next, the calibrated total capacity prediction accuracy was evaluated. Total capacity accuracy is ultimately the most important measure, but accuracy of end and frictional components is once again being measured due to the calibration process outlined in the previous section. Two purposes will be served, true total capacity analysis

and indirect assessment of end and frictional components to be compared to the previous rankings. The following tables outline total capacity performance scores and rankings.

Table 8.7 Total capacity rankings-End bearing pile

	avg		std-dev		t-test-pa		R2	
PENPILE	1.04	1	0.38	1	0.32	6	-0.58	4
PHILI	1.20	6	0.49	5	0.40	5	-0.73	5
P&W	1.11	3	0.39	4	0.97	1	-0.26	2
LCPC	1.24	7	0.73	8	0.67	3	-1.31	8
Aoki	1.37	8	0.54	7	0.00	8	-0.77	6
Schmer	1.20	5	0.52	6	0.30	7	-0.43	3
Europ	1.16	4	0.38	2	0.65	4	-0.96	7
Tumay	1.10	2	0.38	3	0.74	2	0.02	1

Table 8.8 Total capacity rankings-Skin friction pile

	avg		std-dev		t-test-pa		R2	
PENPILE	1.15	4	0.52	8	0.94	1	-0.38	8
PHILI	0.98	1	0.34	1	0.26	7	0.55	3
P&W	1.10	3	0.48	5	0.69	2	0.45	4
LCPC	1.09	2	0.38	2	0.33	4	0.63	2
Aoki	1.16	5	0.40	4	0.03	8	0.65	1
Schmer	1.17	6	0.50	6	0.27	5	0.41	5
Europ	1.23	8	0.50	7	0.26	6	0.19	6
Tumay	1.19	7	0.38	3	0.49	3	-0.03	7

Table 8.9 Total capacity ranking summary

End Piles		Rank	Friction Piles		Rank
8	Tumay	1	10	LCPC	1
10	P&W	2	12	PHILI	2
12	PENPILE	3	14	P&W	3
17	Europ	4	18	Aoki	4
21	PHILI	5	20	Tumay	5
21	Schmer	5	21	PENPILE	6
26	LCPC	7	22	Schmer	7
29	Aoki	8	27	Europ	8

Tumay & Fakhroo, Prince & Wardle, and Penpile methods ranked the highest for end bearing piles. LCPC, Philipponnat, and Prince & Wardle are the top three methods for friction pile. Scores were fairly close between both pile types. With the exception of Prince & Wardle, the rankings were quite different between the categories, providing further evidence that there is value in the separated evaluation conducted in the study. With that said, Prince & Wardle may prove to be fairly effective as a single method approach. The final step of the evaluation and ranking process was to combine the component approach with the total capacity evaluation. The goal being to compare reliability measures and give the most global view of method performance.

Table 8.10 CPT modified methods final ranking-End bearing pile

Component Rank		Total Rank		Combined		Rank
20	P&W	8	Tumay	30	**P&W**	**1**
23	PENPILE	10	P&W	35	**PENPILE**	**2**
28	Europ	12	PENPILE	43	**Tumay**	**3**
35	Tumay	17	Europ	45	**Europ**	**4**
38	PHILI	21	PHILI	59	**PHILI**	**5**
40	Schmer	21	Schmer	61	**Schmer**	**6**
52	LCPC	26	LCPC	78	**LCPC**	**7**
52	Aoki	29	Aoki	81	**Aoki**	**8**

Table 8.11 CPT modified methods final ranking-Skin friction pile

Component Rank		Total Rank		Combined		Rank
31	PHILI	10	LCPC	43	**PHILI**	**1**
32	PENPILE	12	PHILI	48	**LCPC**	**2**
33	Aoki	14	P&W	51	**P&W**	**3**
37	P&W	18	Aoki	51	**Aoki**	**3**
37	Schmer	20	Tumay	53	**PENPILE**	**5**
38	LCPC	21	PENPILE	58	**Tumay**	**6**
38	Tumay	22	Schmer	59	**Schmer**	**7**
42	Europ	27	Europ	69	**Europ**	**8**

Table 8.10 presents the final ranking of the CPT prediction methods for end bearing pile. This ranking is for the modified (calibrated) methods, which were adapted based on Nebraska specific conditions and load tests. The most accurate method for HP pile bearing capacity prediction is the modified Prince & Wardle method, followed by Penpile and Tumay & Fakhroo. Combined scores show a breakpoint in the rankings scores occurring between the 4th and 5th ranked methods. The two previous rankings had generally close agreement. Table 8.11 gives the final ranking for skin friction pile. Philipponnat's modified method shows the best performance. LCPC ranked 2nd followed by a tie for 3rd between Prince & Wardle and Aoki & De Alencar. The scores for friction pile were higher, but again had less variation than the end bearing pile.

8.2 Discussion of Potential Shortcomings

Determination of pile bearing capacity is not simply determined due to the complex mechanisms at work ranging from installation to soil pile interface interaction behavior. The empirical methods investigated relate q_c and f_s measurements from the CPT to q_b and unit q_s from the pile. The relationship between these resistance values is defined with a scaling factor to account for differences such as size. Numerical modeling of the mechanics also presents difficulty due to the extreme variability, and vulnerability to instability occurring at rigid (CPT probe or pile) and soft (soil) large deformation boundaries.

Dynamic vs static considerations play a large role in the quality of capacity predictions. Piles studied are driven into the ground by a dynamic, but intermittent inertial system. The CPT test is also a dynamic process; however, the probe is advanced at an intentionally slow, continuous rate. The process attempts to gain static strength

parameters by limiting dynamic influences such as induced excess pore pressure response. Furthermore, driving system losses and system damping parameters also affect the measured capacities, and cannot be easily accounted for by CPT results. Axial capacity in this study was determined by dynamic load testing (PDA) representing current capacity of the pile. The pile's capacity however will continue to increase do to "set up" phenomenon for a period of time. The effective bond between the soil and pile increases as the soil tightens back around the pile's surface. Further study is needed to compare the CPT method predictions to the long-term strength of the pile determined post set up.

End bearing vs skin friction proportioning of capacity is another factor that may have played a role in error from the CPT prediction methods. While the CAPWAP analysis gives a close estimate of the values, these proportions are highly sensitive to changes in the soil strata encountered and driving response of each soil. The values for each bearing component can change in only a few hammer blows. PDA/CAPWAP analysis is also sensitive to low hammer blow/high set (large penetration per blow) conditions. The behavior is indicated by some of the comparisons where the CAPWAP values are lower than the NDOR driving equation, which is typically the more conservative capacity. Due to CPT refusal and incomplete PDA records for some of the projects these conditions were unavoidable.

Finally, soil plugging behavior and effective area considerations should be mentioned. For displacement piles such as concrete pile, and closed end pipe pile which are used by NDOR maintain a constant toe area. Non-displacement pile such as open-end

pipe pile or HP piles, do not always maintain a constant cross-sectional area during driving. Figure 8.1 diagrams the zone on a HP pile that acts as variable area.

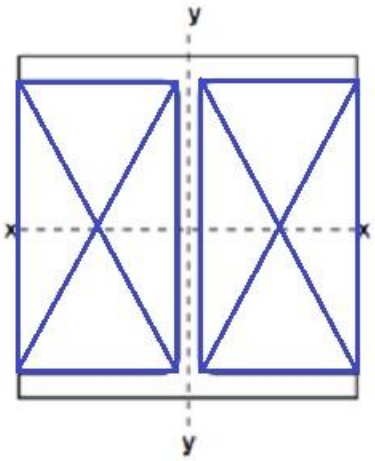

Fig. 8.1 HP pile soil plugging diagram

The blue area will initially not contribute to the pile's toe bearing area, but at some time during installation, typically cohesive stiff soils will form a soil plug which remains adjoined to the pile inside the HP channel. The soil plug increases the effective toe bearing area and the pile will act as a square displacement pile. It is extremely difficult to know when and if this plugging action takes place, and furthermore the behavior can revert pending encountered soil conditions. As a result, it is impractical to incorporate the variable effective toe area consideration in to the CPT prediction analysis code. The variability associated with this behavior is likely a large contributor to prediction error by the CPT methods.

8.3 Conclusion

Eight CPT methods were evaluated for pile capacity prediction performance of driven pile in Nebraska. Initial findings indicated reasonable end bearing capacity prediction, while the skin friction component was in most cases significantly over predicted compared to dynamic load test CAPWAP analysis. Performance trends indicated pile type was influencing individual method accuracy, and piles were classified as end bearing or frictional piles for further analysis. Due to the high variability in soils, regional considerations are often beneficial in design. Nebraska soils are generally overconsolidated, a factor that was not encountered in previous work found in the literature review. All CPT methods were calibrated for q_c and f_s values to optimize pile capacity prediction. Rankings criteria consisted of prediction accuracy, statistical performance, linear fit, and standard deviation. Summarized findings and recommendations are bulleted below.

- For "end bearing pile" considered to be steel HP piles the preferred method is the modified Prince & Wardle equation shown below.
    - $q_b = k_b q_c * 1.074$
    - $f = k_s f_s * 0.475$
- For "skin friction pile" considered to be steel pipe piles and square PPC piles the preferred method is the modified Philipponnat equation shown below.
    - $q_b = k_b q_{ca} * 1.075$
    - $f = \frac{\alpha_s}{F_s} q_{cs} * 0.762$

Numerical modeling further investigated cone and pile tip resistance behavior. Empirical methods suggest q_b/q_c ratios for reduction of CPT tip resistance translated to pile end bearing capacities. These factors were confirmed to be applicable to the Nebraska conditions studied. Influence depths above and below the pile toe affecting capacity were evaluated. Computational findings indicate that some of the empirical methods may have larger than needed influence zones for end bearing prediction, though additional study is suggested.

The cone penetration test offers a high resolution soil investigation tool, providing information often missed by traditional exploration methods. Traditional pile design methods used by NDOR are reliant on these traditional methods, primarily SPT results. Findings from the study suggest that multiple modified CPT empirical methods can offer quality pile specific prediction of axial bearing capacity. Further study may evaluate the potential use of hybridized methods, taking end bearing and skin friction components from various methods to further refine capacity prediction. Effectiveness of CPT based investigation and pile design is reliant primarily on the capability to advance the cone to necessary deep foundation depths. These depths and very stiff or dense gravels can pose challenges in Nebraska. With that in mind however, transition to higher data resolution based designed such as CPT technology could offer NDOR cost savings in pile, and the ability to conduct more informed deep foundation designs.

CHAPTER 9 REFERENCES

Abu-Farsakh, M., and Titi, H. (2004). "Assessment of Direct Cone Penetration Test Methods for Predicting the Ultimate Capacity of Friction Driven Piles". Journal of Geotechnical and Geoenvironmental Engineering, 130(9), 935-944.

Aoki, N. and de Alencar, D. (1975). An Approximate Method to Estimate the Bearing Capacity of Piles, *Proceedings, the 5th Pan-American Conference of Soil Mechanics and Foundation Engineering*, Buenos Aires, Vol. 1, pp. 367-376.

Bustamante, M., and L. Gianeeselli (1982). Pile Bearing Capacity Predictions by Means of Static Penetrometer CPT. *Proceedings of the 2nd European Symposium on Penetration Testing*, ESOPT-II, Amsterdam, Vol. 2, pp. 493-500.

Bolton, M.D., and White, D.J. (2005) Comparing CPT and pile base resistance in sand. *Journal of Geotechnical Engineering.* January 2005 issue, pp. 3-14.

Cabal, K. L., and Robertson, P. K. (2010). "*Guide to Cone Penetration Testing for Geotechnical Engineering*." Gregg Drilling & Testing, Inc., Signal Hill, CA.

Clisby, M.B., Scholtes, R.M., Corey, M.W., Cole, H.A., Teng, P., and Webb, J.D (1978). An Evaluation of Pile Bearing Capacities, Volume I, *Final Report, Mississippi State Highway Department*.

de Ruiter, J., and F.L. Beringen (1979). "Pile Foundations for Large North Sea Structures." *Marine Geotechnology*, Vol. 3, No. 3, pp. 267-314.

Heumann, C., Schomaker, M., and Shalabh. (2016). Introduction to Statistics and Data Analysis. Springer International Publishing Switzerland, Cape Town, SA.

Lunne, T., Robertson, P. K., and Powell, J. J. M. (1997). *Cone penetration testing in geotechnical practice*, Blackie Academic & Professional, London, 48–71.

Nebraska Department of Roads, Bridge Division. (2014). *Bridge Office Policies and Procedures.*

Nebraska Department of Roads, Materials & Research Division. (2012). *Geotechnical Policies and Procedure Manual.*

Price, G. and Wardle, I.F (1982). A Comparison Between Cone Penetration Test Results and the Performance of Small Diameter Instrumented Piles in Stiff Clay, *Proceedings, the 2nd European Symposium on Penetration Testing*, Amsterdam, Vol. 2, pp. 775-780.

Philipponnat, G. (1980). Methode Pratique de Calcul d'un Pieu Isole a l'aide du Penetrometre Statique. *Revue Francaise de Geotechnique*, 10, pp. 55-64.

Randolph, M. F., Dolwin, J. & Beck, R. (1994). Geotechnique 44, No. 3, 427-448

Robertson, P. (1990). "Soil classification using the cone penetration test". Canadian Geotechnical Journal, 27(1), 151-158.

Schmertmann, J.H. (1978). Guidelines for Cone Penetration Test, Performance and Design. U.S. Department of Transportation, Report No. FHWA-TS-78-209, Washington, D.C., 1978, p.145.

APPENDIX A PILE DRIVING AND LOAD TEST DATA

Table A-1 Project and in-place capacity data

PN	CN	SN	Substct	Pile Type	Pile #	Length in Place [ft]	Hammer	Ram [lbs]	STK [ft]	Set [in]	Driving Eqn Ultimate [kips]	PDA BN	CW-total [kips]	CW-skin [kips]	CW-end [kips]	CPT Depth [ft]
34-6(133)	12425	C05501305P	A1	HP12x53	1	45	APE 19-42	4190	7.52	0.95	124	169	163	151	12	29.9
		S034 31644	A1	HP12x53	10	55	APE 19-42	4190	7.41	0.65	154	169	160	132	28	46.1
		S034 31644	A1	HP12x53	10	57	APE 19-42	4190	7.34	0.50	176	204	171	147	24	47.8
		S034 31644	A1	HP12x53	10	60	APE 19-42	4190	7.67	0.44	196	260	184	129	55	50.3
		S034 31644	A2	HP12x53	6	45	APE 19-42	4190	5.19	1.45	64	104	75	9	66	40.1
		S034 31644	A2	HP12x53	6	50	APE 19-42	4190	5.72	1.20	81	162	99	35	64	44.6
		S034 31644	A2	HP12x53	6	55	APE 19-42	4190	6.57	0.70	131	227	152	132	20	49.1
		S034 31644	A2	HP12x53	6	58	APE 19-42	4190	6.50	0.70	130	256	149	122	27	51.7
		S034 31752	A1	HP12x53	5	34	APE 19-42	4190	7.44	0.30	223	106	251	101	150	29.2
		S034 31752	A2	HP12x53	24	35	APE 19-42	4190	6.03	0.83	109	77	113	97	16	34.0
		S034 31752	B1	HP12x53	26	40	APE 19-42	4190	7.83	0.23	259	261	313	3	311	31.0
		S034 31752	B2	HP12x53	5	35	APE 19-42	4190	7.18	0.50	172	117	233	104	129	33.8
77-2(1025)	11801	S077 09368	A1	pipe	15	80	Delmag 30-32	6615	7.28	0.20	393	40	448	273	175	78.5
		S077 09368	A2	pipe	6	90	Delmag 30-32	6615	7.28	0.30	344	205	429	372	57	84.0
		S077 09368	A2	pipe	6	92	Delmag 30-32	6615	7.35	0.20	397	264	450	96	354	86.0
		S077 09368	B1	pipe	3	87	Delmag 30-32	6615	8.07	0.28	394	112	450	326	124	81.7
		S077 09368	B2	pipe	27	87	Delmag 30-32	6615	7.32	0.23	382	71	430	269	161	82.0
80-2(106)	51459B	S080 08295L	A1	pipe	9	32	Delmag 30-32	6615	7.49	0.45	298	202	452	429	23	18.0
80-9(865)	12492	S080 40436	P1	Type I	10	34	APE 19-42	4190	5.39	0.40	143	837	166	30	136	66.3
81-2(1035)	42050A	S081 08578	A1	pipe	5	74	ICE 30S	3000	6.05	0.10	173	1021	163	134	29	69.8
		S081 08578	A1	pipe	5	65	ICE 30S	3000	5.07	0.10	145	402	85	61	24	65.8
		S081 08578	A1	pipe	5	70	ICE 30S	3000	5.72	0.10	163	684	98	76	22	69.5
		S081 08578	A1	pipe	5	75	ICE 30S	3000	5.92	0.05	185	1030	170	40	130	70.8

		S081 08578	B2	pipe	7	75	ICE 30S	3000	5.72	0.58	91	1408	137	89	48	81.0
		S081 08578	B2	pipe	7	68	ICE 30S	3000	5.82	0.63	88	1225	141	61	80	85.0
		S081 08578	B2	pipe	7	72	ICE 30S	3000	5.77	0.50	99	1346	116	37	79	86.0
		S081 08578	B2	pipe	7	75	ICE 30S	3000	5.84	0.50	100	1413	120	61	59	86.5
80-9(865)	12492	S080 40436	A1	pipe	12	55	APE 19-42	4190	6.00	0.65	125	119	192	141	51	63.3
		S080 40436	A1	pipe	12	65	APE 19-42	4190	6.26	0.60	136	240	164	59	105	73.3
		S080 40436	A1	pipe	12	75	APE 19-42	4190	6.31	0.55	144	456	133	47	86	83.3
80-9(838)	12465	S080 41341	A1	HP12x53	8	36	Delmag 19-42	4000	9.08	0.20	296	290	385	156	229	36.0
		S080 41341	A1	HP12x53	8	40	Delmag 19-42	4000	10.90	0.12	402	527	401	118	283	40.0
		S080 41341	A2	HP12x53	8	35	Delmag 19-42	4000	7.39	0.25	225	12	178	140	38	34.0
159-7(106)		S159 01373	N3 (P3)	HP14x89	16	85	APE 30-32	6615	8.40	0.30	397	8	360	155	205	83.0
		S159 01373	N2 (P2)	HP14x89	4	74	APE 30-32	6615	8.70	0.13	526	8	600	145	455	74.0
85-2(111)	22203	S085 0042	P1	pipe	39	37	Pileco 19-42	4010	5.27	1.20	71	27	56	13	43	46.1
		S085 0042	P1	pipe	39	40	Pileco 19-42	4010	6.06	1.00	93	76	62	12	50	49.1
		S085 0042	P1	pipe	39	42	Pileco 19-42	4010	6.34	0.90	104	103	71	21	50	51.1
		S085 0042	P2	pipe	39	43	Pileco 19-42	4010	7.25	0.50	166	85	136	81	55	52.5
		S085 0042	P2	pipe	39	46.5	Pileco 19-42	4010	6.42	0.50	147	132	138	70	68	56.0
		S085 0042	P3	pipe	39	39	Delmag 19-42	4000	6.20	1.00	94	9	69	51	18	55.0
7066(43)		C006602905	A2	HP10x42	5	44.5	SPI 19-42	4185	5.90	1.15	86	10	105	30	75	45.0
		C006602905	A2	HP10x42	5	44	SPI 19-42	4185	5.50	1.25	75	5	115	35	80	45.5
		C006602905	A2	HP10x42	5	47	SPI 19-42	4185	5.90	1.05	91	26	133	112	21	47.5
80-9(811)	21929	S080 43555	A1	HP12x53	6	45	Link Belt 520	5080	2.84	0.43	89	224	153	107	46	56.7
		S080 43555	A1	HP12x53	6	48	Link Belt 520	5080	3.60	0.33	126	319	178	133	45	59.7
		S080 43555	A1	HP12x53	6	52	Link Belt 520	5080	3.90	0.28	145	491	206	130	76	62.7
		S080 43555	A1	HP12x53	6	55	Link Belt 520	5080	4.10	0.24	161	637	223	177	46	65.7
		S080 43555	A2	HP12x53	6	40	MKT DE30	2800	7.00	0.15	172	312	186	133	53	51.0
		S080 43555	A2	HP12x53	6	45	MKT DE30	2800	7.80	0.14	195	805	205	150	55	56.0
		S080 43555	A2	HP12x53	6	50	MKT DE30	2800	8.30	0.12	214	1283	276	227	49	61.0
		S080 43555	A2	HP12x53	6	55	MKT DE30	2800	8.40	0.09	228	1823	310	270	40	66.0
		S080 43555	A2	HP12x53	6	60	MKT DE30	2800	9.10	0.02	280	2849	388	305	83	71.0

		S080 43555	P1	HP12x53	14	50	Link Belt 520	5080	5.70	0.10	276	1479	321	282	39	69.1
		S080 43555	P1	HP12x53	14	53	Link Belt 520	5080	6.20	0.05	327	1849	391	317	74	72.1
80-9(828)	12455	S080 42094	A1	Pipe	6	42	Delmag 25-32	5514	6.60	0.63	184	38	180	145	35	46.0
		S080 42094	A1	Pipe	6	45	Delmag 25-32	5514	5.90	0.57	174	95	165	99	66	49.0
		S080 42094	A1	Pipe	6	50	Delmag 25-32	5514	6.10	0.80	148	181	152	70	82	54.0
		S080 42094	A1	Pipe	6	55	Delmag 25-32	5514	6.50	0.50	205	285	221	109	112	59.0
		S080 42094	A1	Pipe	6	60	Delmag 25-32	5514	6.70	0.60	192	372	199	125	74	64.0
		S080 42094	A2	Pipe	15	47	Delmag 25-32	5514	6.40	0.38	230	171	252	136	116	50.4
		S080 42094	A2	Pipe	15	50	Delmag 25-32	5514	6.50	0.43	220	288	255	140	115	53.4
		S080 42094	A2	Pipe	15	55	Delmag 25-32	5514	6.60	0.38	238	425	270	188	82	58.4
		S080 42094	A2	Pipe	15	60	Delmag 25-32	5514	6.70	0.33	256	576	282	124	158	63.4
		S080 42094	P1	Type I	40	40	Delmag 25-32	5514	7.10	0.80	172	352	175	43	132	48.5
		S080 42094	P1	Type I	40	45	Delmag 25-32	5514	7.00	0.57	206	428	188	71	117	52.5
		S080 42094	P1	Type I	40	50	Delmag 25-32	5514	6.30	0.30	248	570	194	81	113	57.5
		S080 42094	P1	Type I	40	55	Delmag 25-32	5514	6.50	0.57	191	751	159	93	66	62.5
		S080 42094	P1	Type I	40	60	Delmag 25-32	5514	6.30	0.32	242	912	200	107	93	68.5
80-9(801)	21867	S080 44207	P4	HP12x53	35	55	Delmag 25-32	5514	7.00	0.75	176	91	170	138	32	62.5
		S080 44207	P4	HP12x53	35	60	Delmag 25-32	5514	7.60	0.60	218	181	206	160	46	67.5
		S080 44207	P4	HP12x53	35	65	Delmag 25-32	5514	7.70	0.52	238	270	236	149	87	72.5
		S080 44207	P4	HP12x53	35	70	Delmag 25-32	5514	7.80	0.46	256	379	275	206	69	77.5
		S080 44207	P4	HP12x53	35	73	Delmag 25-32	5514	8.00	0.55	240	450	314	241	73	80.5
		S080 44207	P4	HP12x53	57	52	Delmag 25-32	5514	7.00	0.85	163	30	169	94	75	59.5
		S080 44207	P4	HP12x53	57	57	Delmag 25-32	5514	6.70	0.80	162	104	170	147	23	64.5
		S080 44207	P4	HP12x53	57	63	Delmag 25-32	5514	7.30	0.63	204	198	215	175	40	70.5
		S080 44207	P4	HP12x53	57	69	Delmag 25-32	5514	8.00	0.46	263	356	332	237	95	76.5
15-3(115)	32132	S015 13411	A1	pipe	9	66	MKT 33-30-20	3300	5.30	0.20	143	868	185	76	109	69.0
		S015 13411	A1	pipe	9	69	MKT 33-30-20	3300	5.70	0.15	165	1112	232	179	53	72.0
		S015 13411	A1	pipe	9	72	MKT 33-30-20	3300	5.80	0.10	182	1337	249	178	71	75.0
		S015 13411	B1	pipe	3	52	Pileco 19-42	4010	6.80	0.15	240	909	197	113	84	68.0

		S015 13411	B1	pipe	3	55	Pileco 19-42	4010	7.80	0.10	298	1133	204	148	56	71.0
		S015 13411	B1	pipe	3	59	Pileco 19-42	4010	6.00	0.06	246	2018	223	152	71	75.0
		S015 13412	B2	pipe	7	57	MVE M-12	2822	7.50	0.10	202	991	185	116	69	77.2
		S015 13412	B2	pipe	7	60	MVE M-12	2822	7.90	0.10	212	1410	201	154	47	80.2
		S015 13412	B2	pipe	7	62	MVE M-12	2822	7.70	0.08	216	1825	217	160	57	82.2
80-9(830)	12457	S080 41856	A1	HP12x53	3	64	Delmag 19-42	4000	6.40	0.70	122	603	171	147	24	66.0
		S080 41856	A1	HP12x53	3	67	Delmag 19-42	4000	7.50	0.50	171	661	160	133	27	69.0
		S080 41856	A1	HP12x53	3	70	Delmag 19-42	4000	7.80	0.35	210	742	198	166	32	72.0
		S080 41856	A2	HP12x53	9	62	Delmag 19-42	4000	7.80	0.45	188	759	276	194	82	61.1
		S080 41856	A2	HP12x53	9	65	Delmag 19-42	4000	8.10	0.30	231	848	302	232	70	64.1
		S080 41856	A2	HP12x53	9	68	Delmag 19-42	4000	8.20	0.20	268	1022	342	255	87	67.1

APPENDIX B CPT CAPACITIES

Table B-1 Complete CPT prediction data Part I

									Penpile			Philipponat			Prince & Wardle			LCPC		
SN	Sub	Pile type	pile #	LIP [ft]	**CW-total [kips]**	CW-skin [kips]	CW-end [kips]	CPT Depth [ft]	End [kips]	Skin [kips]	**Total [kips]**	End [kips]	Skin [kips]	**Total [kips]**	End [kips]	Skin [kips]	**Total [kips]**	End [kips]	Skin [kips]	**Total [kips]**
C05501305P	A1	HP12x53	1	45	**163**	151	12	29.9	29.2	100.1	**129.3**	112.1	190.7	**302.8**	131.7	147.9	**279.5**	127.0	49.7	**176.7**
S034 31644	A1	HP12x53	10	55	**160**	132	28	46.1	14.3	92.5	**106.7**	37.6	339.6	**377.1**	36.9	138.3	**175.2**	51.3	68.8	**120.1**
S034 31644	A1	HP12x53	10	57	**171**	147	24	47.8	27.9	102.2	**130.1**	43.4	371.4	**414.8**	42.9	154.3	**197.2**	68.8	72.1	**140.9**
S034 31644	A1	HP12x53	10	60	**184**	129	55	50.3	30.0	119.1	**149.1**	40.2	422.7	**462.9**	41.5	186.2	**227.7**	64.9	78.1	**143.0**
S034 31644	A2	HP12x53	6	45	**75**	9	66	40.1	26.2	107.5	**133.6**	51.3	314.3	**365.5**	52.9	185.7	**238.6**	71.0	76.8	**147.8**
S034 31644	A2	HP12x53	6	50	**99**	35	64	44.6	28.7	137.4	**166.1**	57.1	395.1	**452.2**	45.5	246.3	**291.8**	74.5	87.3	**161.8**
S034 31644	A2	HP12x53	6	55	**152**	132	20	49.1	13.4	167.9	**181.3**	42.6	472.8	**515.4**	33.7	309.6	**343.3**	47.6	98.2	**145.8**
S034 31644	A2	HP12x53	6	58	**149**	122	27	51.7	26.9	183.8	**210.7**	51.6	516.3	**567.9**	31.3	336.7	**368.0**	45.2	104.4	**149.5**
S034 31752	A1	HP12x53	5	34	**251**	101	150	29.2	50.0	80.3	**130.3**	171.9	208.6	**380.4**	151.0	141.3	**292.4**	172.6	58.4	**231.0**
S034 31752	A2	HP12x53	24	35	**113**	97	16	34.0	55.2	164.0	**219.2**	178.8	344.6	**523.4**	142.7	269.8	**412.5**	197.3	101.3	**298.6**
S034 31752	B1	HP12x53	26	40	**264**	65	199	31.0	41.5	54.9	**96.4**	103.5	156.8	**260.3**	130.9	84.7	**215.5**	105.3	42.7	**148.0**
S034 31752	A1	HP12x53	5	35	**264**	84	180	33.8	49.1	79.3	**128.3**	152.2	209.4	**361.6**	151.0	137.3	**288.3**	128.7	61.0	**189.7**
S077 09368	A1	pipe	15	80	**448**	273	175	78.5	23.7	227.7	**251.4**	101.9	572.5	**674.4**	77.7	325.1	**402.8**	130.5	151.0	**281.5**
S077 09368	A2	pipe	6	90	**429**	372	57	84.0	70.9	257.6	**328.5**	238.7	645.6	**884.3**	270.7	413.8	**684.5**	249.3	194.0	**443.4**
S077 09368	A2	pipe	6	92	**450**	96	354	86.0	77.1	271.8	**348.9**	247.7	679.6	**927.3**	214.6	447.7	**662.2**	244.5	210.7	**455.3**
S077 09368	B1	pipe	3	87	**450**	326	124	81.7	28.9	236.2	**265.0**	146.7	593.9	**740.6**	232.8	343.8	**576.6**	146.6	160.2	**306.7**
S077 09368	B2	pipe	27	87	**430**	269	161	82.0	55.1	245.0	**300.1**	188.5	612.6	**801.1**	191.6	384.0	**575.6**	208.5	177.8	**386.4**
S080 08295L	A1	pipe	9	32	**345**	214	131	18.0	106.8	83.0	**189.8**	326.5	221.0	**547.5**	278.0	168.3	**446.3**	348.2	104.3	**452.5**
S080 40436	P1	Type I	10	34	**166**	30	136	66.3	40.8	153.8	**194.6**	162.6	262.2	**424.8**	117.5	274.2	**391.7**	183.4	71.4	**254.8**
S081 08578	A1	pipe	5	74	**85**	61	24	69.8	13.3	104.5	**117.7**	19.0	304.2	**323.2**	14.1	130.9	**145.1**	14.1	76.1	**90.2**
S081 08578	A1	pipe	5	65	**98**	76	22	65.8	15.0	124.4	**139.4**	19.4	338.4	**357.8**	18.7	158.7	**177.4**	14.5	85.6	**100.1**
S081 08578	A1	pipe	5	70	**163**	134	29	69.5	9.6	142.5	**152.2**	26.3	378.4	**404.7**	57.1	188.8	**245.9**	14.9	94.4	**109.3**
S081 08578	A1	pipe	5	75	**170**	40	130	70.8	21.5	148.7	**170.1**	30.9	392.8	**423.8**	29.0	198.9	**227.9**	18.3	97.5	**115.8**

S081 08578	B2	pipe	7	75	**141**	61	80	81.0	49.5	299.1	**348.5**	27.8	589.8	**617.6**	31.8	500.1	**532.0**	23.9	168.8	**192.7**
S081 08578	B2	pipe	7	68	**116**	37	79	85.0	58.2	326.5	**384.7**	103.6	654.0	**757.6**	51.3	565.2	**616.5**	34.2	191.1	**225.3**
S081 08578	B2	pipe	7	72	**137**	89	48	86.0	37.2	349.9	**387.1**	51.2	703.4	**754.6**	46.5	614.6	**661.1**	34.9	198.2	**233.1**
S081 08578	B2	pipe	7	75	**120**	61	59	86.5	32.6	357.6	**390.2**	52.2	719.9	**772.1**	46.5	631.0	**677.6**	35.1	200.5	**235.6**
S080 40436	A1	pipe	12	55	**192**	141	51	63.3	8.8	219.2	**228.0**	51.4	534.7	**586.1**	12.9	339.0	**352.0**	31.3	161.1	**192.5**
S080 40436	A1	pipe	12	65	**164**	59	105	73.3	17.6	251.1	**268.7**	57.5	619.8	**677.2**	20.2	379.7	**399.9**	31.9	182.1	**214.0**
S080 40436	A1	pipe	12	75	**133**	47	86	83.3	21.3	290.8	**312.2**	48.3	720.7	**769.0**	29.0	435.9	**464.9**	32.2	206.0	**238.2**
S080 41341	A1	HP12x53	8	36	**385**	156	229	36.0	57.1	129.9	**186.9**	86.8	201.6	**288.4**	260.7	198.5	**459.2**	12.5	59.8	**72.2**
S080 41341	A1	HP12x53	8	40	**401**	118	283	40.0	84.4	161.5	**245.9**	184.7	272.7	**457.3**	164.4	268.6	**433.0**	35.6	95.5	**131.1**
S080 41341	A2	HP12x53	8	35	**178**	140	38	34.0	27.7	106.4	**134.1**	84.5	193.8	**278.2**	186.2	153.5	**339.7**	21.9	56.7	**78.5**
S159 01373	N3 (P3)	HP14x89	16	85	**360**	155	205	83.0	24.6	192.3	**216.9**	64.1	623.4	**687.6**	91.9	253.8	**345.8**	39.7	138.2	**177.9**
S159 01373	N2 (P2)	HP14x89	4	74	**600**	145	455	74.0	26.0	146.1	**172.1**	57.8	472.2	**530.0**	188.3	231.9	**420.2**	20.0	100.6	**120.6**
S085 0042	P1	pipe	39	37	**56**	13	43	46.1	7.8	102.1	**109.8**	12.6	154.5	**167.1**	8.7	116.8	**125.4**	9.6	53.6	**63.2**
S085 0042	P1	pipe	39	40	**62**	12	50	49.1	10.6	110.1	**120.7**	15.2	170.9	**186.2**	12.4	125.7	**138.1**	9.8	58.5	**68.3**
S085 0042	P1	pipe	39	42	**71**	21	50	51.1	12.1	115.9	**128.0**	15.2	181.7	**196.9**	11.0	132.4	**143.3**	10.0	61.8	**71.8**
S085 0042	P2	pipe	39	43	**136**	81	55	52.5	6.6	121.3	**127.9**	15.6	193.7	**209.3**	42.5	140.3	**182.8**	10.1	65.2	**75.3**
S085 0042	P2	pipe	39	46.5	**138**	70	68	56.0	16.6	136.7	**153.3**	20.9	226.1	**247.0**	20.6	163.9	**184.6**	15.1	73.1	**88.2**
S085 0042	P3	pipe	39	39	**69**	51	18	55.0	9.3	105.9	**115.2**	15.0	178.8	**193.8**	14.6	117.5	**132.1**	12.7	64.6	**77.3**
C006602905	A2	HP10x42		44.5	**105**	30	75	45.0	38.0	35.3	**73.3**	57.3	134.7	**192.0**	126.4	44.7	**171.1**	7.9	57.9	**65.7**
C006602905	A2	HP10x42		44	**115**	35	80	45.5	38.7	38.0	**76.7**	62.8	143.5	**206.3**	129.5	49.2	**178.7**	8.2	62.2	**70.4**
C006602905	A2	HP10x42		47	**133**	112	21	47.5	46.3	47.0	**93.3**	98.9	177.5	**276.4**	146.6	62.9	**209.4**	9.4	75.7	**85.1**
S080 43555	A1	HP12x53	6	45	**153**	107	46	56.7	27.4	188.6	**216.0**	43.2	393.0	**436.1**	43.4	280.0	**323.4**	25.3	81.0	**106.2**
S080 43555	A1	HP12x53	6	48	**178**	133	45	59.7	27.9	209.9	**237.8**	41.5	446.2	**487.7**	33.7	324.3	**358.0**	21.3	88.2	**109.5**
S080 43555	A1	HP12x53	6	52	**206**	130	76	62.7	31.2	230.0	**261.2**	41.8	498.0	**539.8**	44.5	364.0	**408.5**	26.7	95.3	**122.0**
S080 43555	A1	HP12x53	6	55	**223**	177	46	65.7	35.5	252.9	**288.4**	53.5	558.5	**612.0**	60.5	417.4	**478.0**	27.6	102.6	**130.2**
S080 43555	A2	HP12x53	6	40	**186**	133	53	51.0	25.3	174.7	**200.0**	37.9	351.4	**389.4**	34.3	270.8	**305.1**	26.4	72.4	**98.8**
S080 43555	A2	HP12x53	6	45	**205**	150	55	56.0	39.8	209.8	**249.6**	43.3	441.6	**485.0**	39.4	343.4	**382.7**	27.7	84.3	**112.0**
S080 43555	A2	HP12x53	6	50	**276**	227	49	61.0	45.2	249.3	**294.6**	78.5	536.1	**614.6**	39.6	427.6	**467.2**	29.4	99.5	**128.9**
S080 43555	A2	HP12x53	6	55	**310**	270	40	66.0	38.4	285.9	**324.3**	57.9	633.2	**691.1**	51.6	507.1	**558.7**	31.2	112.2	**143.4**
S080 43555	A2	HP12x53	6	60	**388**	305	83	71.0	39.5	324.7	**364.2**	60.5	734.5	**795.0**	52.7	599.3	**652.0**	33.0	124.3	**157.3**

S080 43555	P1	HP12x53	14	50	**321**	282	39	69.1	37.3	280.4	**317.7**	60.1	645.5	**705.6**	53.0	522.1	**575.1**	32.3	107.8	**140.1**
S080 43555	P1	HP12x53	14	53	**391**	317	74	72.1	40.1	303.8	**343.9**	60.9	706.0	**767.0**	50.5	578.8	**629.3**	33.5	115.1	**148.6**
S080 42094	A1	Pipe	6	42	**180**	145	35	46.0	21.9	162.1	**184.0**	58.2	401.8	**460.0**	60.5	237.0	**297.5**	37.0	116.0	**153.0**
S080 42094	A1	Pipe	6	45	**165**	99	66	49.0	20.0	172.2	**192.3**	60.4	439.2	**499.7**	99.6	250.1	**349.7**	34.5	127.8	**162.3**
S080 42094	A1	Pipe	6	50	**152**	70	82	54.0	45.0	187.2	**232.1**	41.8	489.0	**530.8**	23.7	268.2	**291.9**	35.3	141.6	**176.9**
S080 42094	A1	Pipe	6	55	**221**	109	112	59.0	70.8	220.7	**291.6**	103.6	568.5	**672.1**	20.6	345.9	**366.5**	37.3	165.6	**202.9**
S080 42094	A1	Pipe	6	60	**199**	125	74	64.0	33.5	251.2	**284.7**	113.8	645.5	**759.3**	80.9	413.4	**494.3**	50.1	193.7	**243.8**
S080 42094	A2	Pipe	15	47	**252**	136	116	50.4	42.4	199.9	**242.3**	104.6	494.0	**598.6**	109.5	322.5	**432.0**	31.8	146.7	**178.5**
S080 42094	A2	Pipe	15	50	**255**	140	115	53.4	41.7	211.3	**253.0**	119.1	544.5	**663.6**	123.4	337.9	**461.3**	34.1	167.4	**201.5**
S080 42094	A2	Pipe	15	55	**270**	188	82	58.4	19.9	229.4	**249.3**	89.7	621.8	**711.5**	48.7	361.7	**410.4**	45.2	190.8	**236.0**
S080 42094	A2	Pipe	15	60	**282**	124	158	63.4	25.5	242.4	**267.9**	64.9	667.4	**732.3**	31.7	377.7	**409.4**	46.5	201.9	**248.4**
S080 42094	P1	Type I	40	40	**175**	43	132	48.5	42.5	174.1	**216.7**	112.6	475.6	**588.1**	139.7	258.2	**397.9**	26.9	191.7	**218.6**
S080 42094	P1	Type I	40	45	**188**	71	117	52.5	52.2	179.2	**231.5**	77.5	520.1	**597.5**	14.6	237.5	**252.1**	43.8	211.0	**254.8**
S080 42094	P1	Type I	40	50	**194**	81	113	57.5	32.6	212.4	**245.0**	111.1	599.7	**710.8**	98.8	307.4	**406.2**	41.5	244.1	**285.6**
S080 42094	P1	Type I	40	55	**159**	93	66	62.5	37.3	249.7	**287.0**	102.5	691.0	**793.4**	176.9	391.8	**568.7**	44.3	281.7	**326.0**
S080 42094	P1	Type I	40	60	**200**	107	93	68.5	48.4	267.3	**315.7**	85.1	829.8	**914.9**	39.2	391.1	**430.3**	43.0	324.4	**367.5**
S080 44207	P4	HP12x53	35	55	**170**	138	32	62.5	21.8	264.6	**286.4**	89.1	663.8	**753.0**	75.8	467.7	**543.4**	54.2	152.1	**206.3**
S080 44207	P4	HP12x53	35	60	**206**	160	46	67.5	31.2	296.1	**327.3**	82.6	760.1	**842.7**	24.5	527.6	**552.1**	45.0	163.3	**208.3**
S080 44207	P4	HP12x53	35	65	**236**	149	87	72.5	17.0	322.4	**339.4**	76.9	854.3	**931.2**	48.2	566.9	**615.1**	51.3	174.4	**225.7**
S080 44207	P4	HP12x53	35	70	**275**	206	69	77.5	18.1	347.3	**365.3**	74.2	954.3	**1028.4**	47.0	602.0	**649.0**	52.5	185.5	**238.0**
S080 44207	P4	HP12x53	35	73	**314**	241	73	80.5	19.3	363.7	**383.1**	75.6	1013.5	**1089.1**	55.5	627.6	**683.2**	53.4	193.0	**246.4**
S080 44207	P4	HP12x53	57	52	**169**	94	75	59.5	45.8	241.4	**287.3**	98.3	604.7	**703.0**	57.9	414.8	**472.6**	51.9	143.4	**195.3**
S080 44207	P4	HP12x53	57	57	**170**	147	23	64.5	19.4	280.4	**299.8**	92.8	704.6	**797.4**	55.0	503.3	**558.3**	54.7	157.1	**211.9**
S080 44207	P4	HP12x53	57	63	**215**	175	40	70.5	15.4	310.5	**325.9**	70.3	813.5	**883.8**	47.9	547.5	**595.4**	50.9	169.5	**220.4**
S080 44207	P4	HP12x53	57	69	**332**	237	95	76.5	17.6	342.2	**359.8**	74.0	934.6	**1008.5**	50.2	594.7	**644.8**	52.2	183.4	**235.5**
S015 13411	A1	pipe	9	66	**185**	76	109	69.0	66.6	117.0	**183.6**	51.4	87.0	**138.4**	46.4	122.6	**169.0**	25.3	99.4	**124.7**
S015 13411	A1	pipe	9	69	**232**	179	53	72.0	74.2	127.9	**202.1**	54.1	97.0	**151.1**	48.3	138.3	**186.6**	26.9	105.4	**132.3**
S015 13411	A1	pipe	9	72	**249**	178	71	75.0	76.8	138.6	**215.5**	56.9	106.7	**163.6**	56.3	154.1	**210.4**	28.4	111.2	**139.7**
S015 13411	B1	pipe	3	52	**197**	113	84	68.0	66.3	113.2	**179.5**	50.4	83.6	**134.0**	34.0	117.5	**151.5**	24.7	97.3	**122.1**

S015 13411	B1	pipe	3	55	**204**	148	56	71.0	70.9	124.0	**195.0**	52.9	93.5	**146.5**	47.7	132.8	**180.5**	26.3	103.3	**129.6**
S015 13411	B1	pipe	3	59	**223**	152	71	75.0	76.8	138.6	**215.5**	56.9	106.7	**163.6**	56.3	154.1	**210.4**	28.4	111.2	**139.7**
S015 13412	B2	pipe	7	57	**185**	116	69	77.2	60.7	118.2	**178.9**	35.8	79.4	**115.3**	38.0	112.7	**150.7**	17.4	84.2	**101.7**
S015 13412	B2	pipe	7	60	**201**	154	47	80.2	64.5	128.5	**192.9**	38.2	89.0	**127.1**	44.0	126.5	**170.5**	18.1	90.0	**108.2**
S015 13412	B2	pipe	7	62	**217**	160	57	82.2	68.2	135.4	**203.6**	38.7	95.4	**134.1**	50.4	135.4	**185.8**	18.6	94.1	**112.7**
S080 41856	A1	HP12x53	3	64	**171**	147	24	66.0	23.5	161.5	**185.0**	31.4	144.3	**175.7**	13.8	131.3	**145.0**	34.9	146.4	**181.3**
S080 41856	A1	HP12x53	3	67	**160**	133	27	69.0	16.7	167.4	**184.1**	27.5	149.9	**177.3**	8.6	134.9	**143.5**	35.3	151.2	**186.5**
S080 41856	A1	HP12x53	3	70	**198**	166	32	72.0	33.8	172.2	**206.0**	28.1	155.7	**183.8**	10.3	137.6	**147.9**	39.6	157.0	**196.6**
S080 41856	A2	HP12x53	9	62	**276**	194	82	61.1	87.2	198.8	**286.0**	85.0	217.5	**302.5**	66.2	212.3	**278.5**	117.3	158.8	**276.1**
S080 41856	A2	HP12x53	9	65	**302**	232	70	64.1	85.8	216.4	**302.3**	82.5	237.6	**320.0**	60.4	235.4	**295.8**	119.7	170.3	**290.0**
S080 41856	A2	HP12x53	9	68	**342**	255	87	67.1	82.8	233.1	**315.8**	81.7	257.1	**338.9**	55.7	256.7	**312.4**	120.7	181.7	**302.4**

Table B-2 Complete CPT prediction data Part II

									Aoki			Schmertmann			European			Tumay		
SN	Sub	Pile type	pile #	LIP [ft]	**CW-total [kips]**	CW-skin [kips]	CW-end [kips]	CPT Depth [ft]	End [kips]	Skin [kips]	**Total [kips]**	End [kips]	Skin [kips]	**Total [kips]**	End [kips]	Skin [kips]	**Total [kips]**	End [kips]	Skin [kips]	**Total [kips]**
C05501305P	A1	HP12x53	1	45	**163**	151	12	29.9	222.0	144.6	**366.5**	251.1	123.1	**374.2**	150.7	96.3	**247.0**	211.7	76.6	**288.3**
S034 31644	A1	HP12x53	10	55	**160**	132	28	46.1	70.9	152.1	**223.0**	96.9	77.1	**173.9**	57.4	136.0	**193.3**	101.8	127.3	**229.1**
S034 31644	A1	HP12x53	10	57	**171**	147	24	47.8	69.7	163.2	**232.9**	99.7	88.4	**188.1**	59.8	141.4	**201.2**	101.3	131.6	**232.9**
S034 31644	A1	HP12x53	10	60	**184**	129	55	50.3	63.0	182.1	**245.0**	99.8	106.2	**206.0**	59.9	154.6	**214.4**	104.2	137.6	**241.9**
S034 31644	A2	HP12x53	6	45	**75**	9	66	40.1	63.4	194.7	**258.1**	81.3	125.5	**206.8**	48.8	151.8	**200.5**	90.3	120.0	**210.3**
S034 31644	A2	HP12x53	6	50	**99**	35	64	44.6	68.9	227.0	**296.0**	89.8	152.1	**241.9**	53.9	185.3	**239.2**	94.0	132.2	**226.1**
S034 31644	A2	HP12x53	6	55	**152**	132	20	49.1	57.1	260.6	**317.6**	87.0	180.9	**267.9**	52.2	218.7	**270.9**	89.4	145.8	**235.2**
S034 31644	A2	HP12x53	6	58	**149**	122	27	51.7	67.6	277.1	**344.7**	86.5	193.3	**279.8**	51.9	240.1	**292.0**	97.3	154.1	**251.4**
S034 31752	A1	HP12x53	5	34	**251**	101	150	29.2	246.6	162.1	**408.7**	300.0	157.2	**457.2**	188.0	84.3	**272.2**	221.8	98.3	**320.1**
S034 31752	A2	HP12x53	24	35	**113**	97	16	34.0	232.9	260.3	**493.2**	300.0	290.2	**590.2**	188.0	156.8	**344.8**	334.2	96.4	**430.6**
S034 31752	B1	HP12x53	26	40	**264**	65	199	31.0	285.1	103.5	**388.5**	245.4	106.7	**352.1**	281.9	74.5	**356.4**	169.2	67.8	**237.0**
S034 31752	A1	HP12x53	5	35	**264**	84	180	33.8	346.2	110.2	**456.4**	246.6	157.1	**403.6**	346.2	150.9	**497.1**	207.7	82.9	**290.6**
S077 09368	A1	pipe	15	80	**448**	273	175	78.5	233.4	288.7	**522.0**	193.8	236.6	**430.3**	116.3	100.2	**216.5**	245.1	164.5	**409.6**

S077 09368	A2	pipe	6	90	**429**	372	57	84.0	354.7	354.0	**708.7**	266.0	200.9	**466.8**	166.7	353.4	**520.0**	266.0	185.1	**451.1**
S077 09368	A2	pipe	6	92	**450**	96	354	86.0	350.0	386.5	**736.5**	266.0	228.4	**494.3**	166.7	369.0	**535.6**	266.0	190.3	**456.2**
S077 09368	B1	pipe	3	87	**450**	326	124	81.7	379.8	310.7	**690.5**	266.0	249.2	**515.2**	166.7	107.2	**273.9**	266.0	167.5	**433.5**
S077 09368	B2	pipe	27	87	**430**	269	161	82.0	351.6	322.5	**674.1**	266.0	180.8	**446.8**	166.7	338.7	**505.4**	266.0	180.3	**446.3**
S080 08295L	A1	pipe	9	32	**345**	214	131	18.0	497.0	197.8	**694.8**	266.0	174.4	**440.4**	166.7	93.1	**259.7**	266.0	52.4	**318.4**
S080 40436	P1	Type I	10	34	**166**	30	136	66.3	120.3	184.8	**305.1**	93.6	174.6	**268.2**	56.2	156.1	**212.3**	165.1	137.7	**302.8**
S081 08578	A1	pipe	5	74	**85**	61	24	69.8	23.0	142.0	**165.0**	29.7	80.8	**110.5**	17.8	199.3	**217.1**	32.7	146.8	**179.5**
S081 08578	A1	pipe	5	65	**98**	76	22	65.8	44.5	157.9	**202.5**	25.9	93.1	**119.0**	15.6	222.5	**238.0**	39.3	157.6	**196.9**
S081 08578	A1	pipe	5	70	**163**	134	29	69.5	45.2	178.5	**223.6**	35.7	103.8	**139.5**	21.4	245.0	**266.4**	52.7	165.3	**218.0**
S081 08578	A1	pipe	5	75	**170**	40	130	70.8	59.5	184.6	**244.1**	38.2	108.6	**146.8**	22.9	249.2	**272.2**	61.1	168.0	**229.1**
S081 08578	B2	pipe	7	75	**141**	61	80	81.0	180.9	340.5	**521.3**	69.5	243.9	**313.5**	41.7	327.1	**368.8**	126.5	204.3	**330.7**
S081 08578	B2	pipe	7	68	**116**	37	79	85.0	74.8	394.1	**468.9**	94.2	285.4	**379.7**	56.5	348.7	**405.3**	101.1	217.0	**318.0**
S081 08578	B2	pipe	7	72	**137**	89	48	86.0	76.0	427.8	**503.8**	116.4	305.6	**422.0**	69.9	372.4	**442.2**	116.4	227.4	**343.8**
S081 08578	B2	pipe	7	75	**120**	61	59	86.5	76.0	439.4	**515.3**	121.2	311.8	**433.0**	72.7	380.3	**453.0**	121.2	231.2	**352.4**
S080 40436	A1	pipe	12	55	**192**	141	51	63.3	22.5	319.1	**341.5**	28.9	188.9	**217.8**	17.3	213.1	**230.4**	30.8	196.3	**227.1**
S080 40436	A1	pipe	12	65	**164**	59	105	73.3	32.2	353.7	**385.9**	42.9	211.9	**254.8**	25.7	255.2	**280.9**	45.1	222.5	**267.6**
S080 40436	A1	pipe	12	75	**133**	47	86	83.3	57.9	391.9	**449.7**	72.2	237.9	**310.1**	43.3	302.2	**345.5**	76.2	248.7	**325.0**
S080 41341	A1	HP12x53	8	36	**385**	156	229	36.0	385.2	128.4	**513.6**	255.0	111.8	**366.8**	153.0	128.5	**281.5**	300.0	117.7	**417.7**
S080 41341	A1	HP12x53	8	40	**401**	118	283	40.0	266.9	191.5	**458.4**	300.0	201.1	**501.1**	219.1	157.5	**376.6**	300.0	129.8	**429.8**
S080 41341	A2	HP12x53	8	35	**178**	140	38	34.0	334.1	118.0	**452.1**	300.0	102.1	**402.1**	206.3	112.0	**318.4**	300.0	123.8	**423.8**
S159 01373	N3 (P3)	HP14x89	16	85	**360**	155	205	83.0	213.2	307.8	**521.0**	249.9	169.0	**419.0**	150.0	242.6	**392.5**	249.9	309.2	**559.1**
S159 01373	N2 (P2)	HP14x89	4	74	**600**	145	455	74.0	328.3	224.2	**552.5**	345.0	142.5	**487.5**	207.0	177.4	**384.3**	345.0	265.0	**610.0**
S085 0042	P1	pipe	39	37	**56**	13	43	46.1	20.0	81.4	**101.3**	25.6	80.3	**106.0**	15.4	107.2	**122.6**	27.2	99.8	**127.1**
S085 0042	P1	pipe	39	40	**62**	12	50	49.1	29.9	88.3	**118.1**	26.1	86.8	**112.9**	15.7	119.4	**135.0**	34.9	106.0	**140.9**
S085 0042	P1	pipe	39	42	**71**	21	50	51.1	34.8	92.9	**127.7**	32.7	91.5	**124.1**	19.6	127.3	**146.9**	37.5	110.2	**147.7**
S085 0042	P2	pipe	39	43	**136**	81	55	52.5	37.7	98.0	**135.7**	35.2	95.0	**130.2**	21.1	135.4	**156.5**	42.9	113.1	**156.0**
S085 0042	P2	pipe	39	46.5	**138**	70	68	56.0	61.7	112.6	**174.3**	71.7	104.4	**176.0**	43.0	155.5	**198.5**	71.7	120.0	**191.7**
S085 0042	P3	pipe	39	39	**69**	51	18	55.0	24.2	96.9	**121.0**	35.8	87.2	**123.1**	21.5	127.9	**149.5**	35.8	120.3	**156.2**
C006602905	A2	HP10x42		44.5	**105**	30	75	45.0	235.2	105.2	**340.4**	208.3	32.4	**240.7**	139.7	87.6	**227.2**	300.0	51.5	**351.5**
C006602905	A2	HP10x42		44	**115**	35	80	45.5	242.3	112.4	**354.7**	208.3	35.8	**244.1**	159.7	90.6	**250.2**	300.0	53.3	**353.3**

C006602905	A2	HP10x42		47	**133**	112	21	47.5	256.1	144.4	**400.5**	208.3	46.1	**254.4**	208.3	102.5	**310.9**	300.0	60.4	**360.4**
S080 43555	A1	HP12x53	6	45	**153**	107	46	56.7	60.1	184.3	**244.5**	82.7	149.4	**232.1**	49.6	268.1	**317.7**	90.1	109.8	**200.0**
S080 43555	A1	HP12x53	6	48	**178**	133	45	59.7	64.9	208.0	**272.9**	85.6	166.2	**251.8**	51.3	297.0	**348.4**	96.2	118.5	**214.6**
S080 43555	A1	HP12x53	6	52	**206**	130	76	62.7	84.6	229.0	**313.5**	111.6	181.5	**293.1**	67.0	325.4	**392.3**	116.2	127.4	**243.6**
S080 43555	A1	HP12x53	6	55	**223**	177	46	65.7	85.7	257.8	**343.5**	126.4	203.1	**329.5**	75.8	352.5	**428.3**	129.1	137.0	**266.1**
S080 43555	A2	HP12x53	6	40	**186**	133	53	51.0	61.7	159.4	**221.1**	85.1	134.3	**219.4**	51.1	230.3	**281.4**	88.1	119.3	**207.4**
S080 43555	A2	HP12x53	6	45	**205**	150	55	56.0	118.2	197.8	**316.0**	98.1	161.9	**260.0**	58.9	278.2	**337.1**	124.5	136.7	**261.3**
S080 43555	A2	HP12x53	6	50	**276**	227	49	61.0	85.6	254.8	**340.4**	109.6	219.6	**329.1**	65.7	321.4	**387.1**	119.8	156.6	**276.4**
S080 43555	A2	HP12x53	6	55	**310**	270	40	66.0	85.9	301.7	**387.6**	130.4	255.4	**385.7**	78.2	363.2	**441.5**	133.1	179.0	**312.1**
S080 43555	A2	HP12x53	6	60	**388**	305	83	71.0	96.7	351.3	**447.9**	141.6	290.8	**432.3**	84.9	410.3	**495.2**	154.0	203.3	**357.2**
S080 43555	P1	HP12x53	14	50	**321**	282	39	69.1	85.1	307.7	**392.8**	137.8	255.8	**393.6**	82.7	353.8	**436.5**	139.8	170.5	**310.3**
S080 43555	P1	HP12x53	14	53	**391**	317	74	72.1	102.9	337.5	**440.4**	141.2	276.8	**418.0**	84.7	382.8	**467.5**	160.1	185.4	**345.4**
S080 42094	A1	Pipe	6	42	**180**	145	35	46.0	121.3	236.5	**357.8**	62.3	131.7	**193.9**	37.4	144.5	**181.8**	140.1	143.8	**284.0**
S080 42094	A1	Pipe	6	45	**165**	99	66	49.0	85.1	256.6	**341.6**	50.8	140.0	**190.8**	30.5	152.9	**183.3**	81.1	151.6	**232.7**
S080 42094	A1	Pipe	6	50	**152**	70	82	54.0	155.2	281.2	**436.5**	90.4	152.0	**242.4**	54.2	174.8	**229.1**	133.6	164.2	**297.9**
S080 42094	A1	Pipe	6	55	**221**	109	112	59.0	164.3	341.7	**506.0**	73.8	206.4	**280.2**	44.3	196.7	**241.0**	150.9	178.0	**328.9**
S080 42094	A1	Pipe	6	60	**199**	125	74	64.0	133.8	398.8	**532.6**	155.0	245.1	**400.2**	93.0	220.6	**313.7**	169.8	193.7	**363.5**
S080 42094	A2	Pipe	15	47	**252**	136	116	50.4	211.9	285.2	**497.1**	260.5	150.2	**410.7**	156.3	216.8	**373.1**	266.0	177.0	**443.0**
S080 42094	A2	Pipe	15	50	**255**	140	115	53.4	173.1	318.2	**491.3**	184.5	160.4	**344.9**	110.7	229.1	**339.8**	241.1	186.3	**427.4**
S080 42094	A2	Pipe	15	55	**270**	188	82	58.4	44.3	363.1	**407.4**	55.5	176.1	**231.7**	33.3	245.0	**278.3**	69.2	201.5	**270.7**
S080 42094	A2	Pipe	15	60	**282**	124	158	63.4	83.3	382.8	**466.0**	50.2	186.2	**236.4**	30.1	263.4	**293.5**	71.7	216.2	**287.9**
S080 42094	P1	Type I	40	40	**175**	43	132	48.5	215.7	257.2	**473.0**	241.1	167.9	**409.0**	144.7	187.1	**331.8**	264.7	157.2	**421.9**
S080 42094	P1	Type I	40	45	**188**	71	117	52.5	121.4	288.8	**410.2**	38.7	173.5	**212.2**	23.2	158.4	**181.6**	110.9	154.5	**265.4**
S080 42094	P1	Type I	40	50	**194**	81	113	57.5	135.5	345.2	**480.8**	92.6	235.4	**328.0**	55.5	185.0	**240.6**	141.9	170.2	**312.1**
S080 42094	P1	Type I	40	55	**159**	93	66	62.5	182.6	413.0	**595.5**	167.6	292.2	**459.8**	100.5	214.0	**314.5**	198.9	188.4	**387.4**
S080 42094	P1	Type I	40	60	**200**	107	93	68.5	137.9	445.2	**583.1**	75.8	262.7	**338.5**	45.5	275.0	**320.5**	118.0	232.9	**350.9**
S080 44207	P4	HP12x53	35	55	**170**	138	32	62.5	95.3	402.5	**497.7**	119.1	306.8	**425.9**	71.5	226.2	**297.6**	131.6	174.7	**306.2**
S080 44207	P4	HP12x53	35	60	**206**	160	46	67.5	67.1	445.6	**512.7**	69.1	347.0	**416.1**	41.5	244.4	**285.8**	93.3	196.5	**289.8**
S080 44207	P4	HP12x53	35	65	**236**	149	87	72.5	77.2	479.4	**556.6**	112.9	376.7	**489.5**	67.7	252.8	**320.5**	116.9	218.4	**335.3**
S080 44207	P4	HP12x53	35	70	**275**	206	69	77.5	86.7	515.5	**602.2**	130.0	403.2	**533.1**	78.0	261.8	**339.8**	137.5	239.8	**377.3**

S080 44207	P4	HP12x53	35	73	**314**	241	73	80.5	93.5	539.2	**632.6**	126.1	422.5	**548.6**	75.7	267.7	**343.4**	140.0	252.4	**392.4**
S080 44207	P4	HP12x53	57	52	**169**	94	75	59.5	110.3	368.4	**478.8**	130.8	277.9	**408.7**	78.5	204.4	**282.8**	147.9	162.5	**310.4**
S080 44207	P4	HP12x53	57	57	**170**	147	23	64.5	62.5	426.6	**489.1**	101.2	330.3	**431.5**	60.7	237.2	**297.9**	111.8	183.5	**295.2**
S080 44207	P4	HP12x53	57	63	**215**	175	40	70.5	79.7	463.2	**542.8**	104.1	362.0	**466.2**	62.5	248.8	**311.3**	107.7	209.6	**317.3**
S080 44207	P4	HP12x53	57	69	**332**	237	95	76.5	83.7	508.3	**592.1**	129.1	397.6	**526.7**	77.5	260.0	**337.5**	135.5	235.6	**371.0**
S015 13411	A1	pipe	9	66	**185**	76	109	69.0	58.0	93.8	**151.8**	90.8	96.1	**186.8**	77.9	130.1	**208.0**	75.4	100.2	**175.6**
S015 13411	A1	pipe	9	69	**232**	179	53	72.0	65.0	102.7	**167.8**	94.3	101.6	**195.9**	80.9	143.7	**224.6**	84.4	105.0	**189.4**
S015 13411	A1	pipe	9	72	**249**	178	71	75.0	65.1	111.8	**176.9**	104.8	108.4	**213.2**	89.9	155.4	**245.4**	87.8	110.0	**197.8**
S015 13411	B1	pipe	3	52	**197**	113	84	68.0	57.3	91.0	**148.3**	89.2	94.3	**183.5**	76.6	125.3	**201.8**	74.6	98.6	**173.3**
S015 13411	B1	pipe	3	55	**204**	148	56	71.0	63.1	99.5	**162.6**	91.7	99.8	**191.5**	78.7	138.8	**217.5**	81.2	103.3	**184.5**
S015 13411	B1	pipe	3	59	**223**	152	71	75.0	65.1	111.8	**176.9**	104.8	108.4	**213.2**	89.9	155.4	**245.4**	87.8	110.0	**197.8**
S015 13412	B2	pipe	7	57	**185**	116	69	77.2	51.1	78.1	**129.1**	86.5	86.9	**173.4**	74.2	150.7	**224.9**	70.9	107.7	**178.6**
S015 13412	B2	pipe	7	60	**201**	154	47	80.2	56.4	85.9	**142.3**	88.8	91.9	**180.7**	76.2	164.3	**240.6**	78.3	111.7	**190.0**
S015 13412	B2	pipe	7	62	**217**	160	57	82.2	60.2	91.2	**151.4**	96.7	95.5	**192.2**	83.0	173.5	**256.5**	80.0	114.6	**194.6**
S080 41856	A1	HP12x53	3	64	**171**	147	24	66.0	10.5	153.2	**163.7**	15.8	149.4	**165.2**	12.9	151.6	**164.5**	15.3	155.4	**170.6**
S080 41856	A1	HP12x53	3	67	**160**	133	27	69.0	14.0	158.0	**172.0**	12.8	154.4	**167.3**	10.5	158.9	**169.4**	14.5	162.4	**176.9**
S080 41856	A1	HP12x53	3	70	**198**	166	32	72.0	39.2	162.7	**201.9**	15.5	158.6	**174.2**	12.7	165.8	**178.5**	27.2	169.2	**196.4**
S080 41856	A2	HP12x53	9	62	**276**	194	82	61.1	65.8	238.9	**304.7**	85.3	221.7	**307.0**	69.6	189.6	**259.2**	83.8	163.1	**246.9**
S080 41856	A2	HP12x53	9	65	**302**	232	70	64.1	63.7	260.5	**324.2**	70.7	242.7	**313.4**	57.7	203.7	**261.3**	72.1	175.8	**247.9**
S080 41856	A2	HP12x53	9	68	**342**	255	87	67.1	63.3	279.2	**342.5**	71.6	265.4	**337.0**	58.4	212.8	**271.2**	74.9	188.7	**263.6**